Systemic regulation of *Drosophila* innate immune response

A Thesis

Submitted in partial fulfillment of the requirements

Of the degree of

Doctor of Philosophy

By

Bhagyashree Kaduskar

20113120

INDIAN INSTITUTE OF SCIENCE EDUCATION AND RESEARCH, PUNE

2017

CERTIFICATE

Certified that the work incorporated in the thesis entitled **"Systemic regulation of *Drosophila* innate immune response"**, submitted by **Bhagyashree Kaduskar** was carried out by the candidate, under my supervision. The work presented here or any part of it has not been included in any other thesis submitted previously for the award of any degree or diploma from any other University or Institution.

Dr. G.S. Ratnaparkhi

Supervisor

Date:

DECLARATION

I declare that this written submission represents my ideas in my own words and where others‟ ideas have been included; I have adequately cited and referenced the original sources. I also declare that I have adhered to all principles of academic honesty and integrity and have not misrepresented or fabricated or falsified any idea/data/fact/source in my submission. I understand that violation of the above will be cause for disciplinary action by the Institute and can also evoke penal action from the sources that have not been properly cited or from whom proper permission has not been taken when needed.

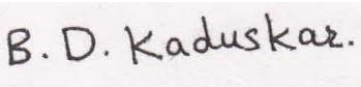

Bhagyashree Kaduskar
20113120
Date:

Acknowledgements

Where do I start? I can't thank my guide and 'boss' (as we named him!), Dr. Girish Ratnaparkhi enough for everything he has done for me over the last 7 years. Be it giving me the opportunity to work in his lab or with barely 2 months of looking at flies under the scope, giving me the opportunity to do a genetic screen in Japan, he has always looked for ways to make my PhD an enjoyable (as much as Phd can be!) experience. He has backed me when data was scarce and at the same time encouraged me (occasionally with gifts like pendrive) at moments of exciting piece of data. I really thank him for never saying "NO" to any experiment, however crazy it sounded (though, he would try to pursue why certain ideas are likely to fail!).

I thank my RAC members, Dr. Jomon Joseph and Dr. Vasudevan Seshadri for their constant inputs and suggestions which kept my PhD moving forward. Special thanks to Jomon for pestering me for generating the Caspar-specific antibody. I would like to sincerely thank Prof. L. S. Shashidhara for setting up common lab system in Biology, which ensured that I was exposed to many different aspects of research ranging from drosophila genetics to plant ecology. I would also like to thank all faculties of IISER Biology for a fantastic, interactive and approachable inter-lab relations. I take this opportunity to thank Richa and Girish for common lab meetings. I also thank Dr. Girish Deshpande for the periodic scientific inputs and discussions.

A very special thank you to my lab 'seniors' Mithila, 'His highness' Senthil and Vallari, my best friends in IISER, for setting up healthy lab environment. A special thanks to Senthil for all the tea-time and labmeet backbench discussions. My labmates Kriti, Shweta, Amarendranath (Bahubali), Prajna, Sushmita, Aparna, Neena deserve a big thanks their immense support, help but above all for a fantastic lab atmosphere, something I will miss and cherish for life.

Life outside lab is equally important while doing a PhD. I was lucky to have friends like Ameya (and his bike rides), Shraddha, Sneha, and Anirudha, who not only helped me with discussions form across disciplines but also for introducing me to many facets of scientific thinking. The "Round table' discussions and debates were a memorable treat!

I would also like to thank Prof. Ryu UEDA and his lab members for wonderful three months in Japan within and outside the lab. I would also like to thank Neha and Pradeep, my Indian friends in Japan, with whom, I visited exciting beautiful places in Japan.

I would like to thank Prof. Sanjeev Galande and his lab members for their help with setting up TaqMan system. I also thank Dr. Harinath and his lab for help with TLC experiments.

My sincere thanks to Dr. Siddhesh and his lab for their immense help which made working with lipids a reality. I would also like to thank Varada Abhyankar for our excellent collaboration and above all, our decade old friendship.

My special thanks to Dr. Shashikant Acharya for his support and encouragement throughout my PhD. I would really like to thank Dr. Anuradha Ratnaparkhi for all the teatime discussions, encouragements at the low times and for constantly sharing the scientific excitement.

I would like to thank the Biology dept. staff, Mrinalini, Piyush, Kalpesh, Shabnam, Rupali and Vijay for managing all our lab needs well. I would also like to thank IISER fly facility for hassle-free fly food supply and stock maintenance. I would also like to thank the academic and admin sections of IISER for taking care of all paper work. Special thanks to Suraj's gingner tea.

My sincere thanks to Flybase, Bloomington stock center, NCBS fly facility, DSHB for fly stocks and antibodies.

I thank CSIR for funding my funding during PhD and JASSA-Sokendai for funding my Japan trip.

Above all, I am grateful to my parents and especially my brother for their love, support, understanding and always believing in me and finally a special thank you to my cat, Snowee (for just being a cat, that's enough!!).

Dedicated to all the flies I have sent to 'fly Heaven' during this work.....

Table of Contents

List of Figures

List Of Tables

List of Publications

The work done in my Ph.D should lead to the following papers/reviews. The list includes papers that are under revision or still being written.

1. *SUMO-Enriched Proteome for Drosophila Innate Immune Response*. Handu M, **Kaduskar B**, Ravindranathan R, Soory A, Giri R, Elango VB, Gowda H, Ratnaparkhi GS. G3 (Bethesda). 2015 Aug 18;5(10):2137-54. doi: 10.1534/g3.115.020958.
2. *Drosophila DNA/RNA methyltransferase contributes to robust host defense in ageing animals by regulating lipid homeostasis*. Abhyankar V, **Kaduskar B**, Kamat SS, Deobagkar DD, Ratnaparkhi GS. Under Submission, Journal of Biological Chemistry, 2017
3. *FlySUMObase: A database of predicted SUMOylated Drosophila proteins*. **Kaduskar B** & Ratnaparkhi GS.
4. *SUMOylation of Caspar/dFAF1 regulates Immune Deficient signaling in Drosophila*. **Kaduskar B** & Ratnaparkhi GS.

Chapter 1

Innate Immunity: A universal system for host defense

Drosophila melanogaster's natural environment consists of heavy load of micro-organisms from decaying food matter. Despite this, flies and other insects are not susceptible to infection. This fact intrigued Hans Boman and his colleagues, and led to the discovery of inducible immune response in insects, specifically in the silk moth (Boman, Nilsson et al. 1972). Soon after, *Drosophila* became a model organism of choice for research on immunity, with various components of immune pathways identified by genetic and molecular studies (Engstrom, Kadalayil et al. 1993, Lemaitre, Nicolas et al. 1996). Innate immune response pathways in flies are evolutionary well conserved with vertebrates. This conservation of pathways (Medzhitov, Preston-Hurlburt et al. 1997) and ease of doing genetics and molecular studies along with absence of adaptive immune pathways in flies has led to an explosive increase in the number of discoveries made in flies in the last five decades (reviewed in (Khush and Lemaitre 2000, Williams 2001, Hoffmann and Reichhart 2002, Tzou, De Gregorio et al. 2002, Brennan and Anderson 2004, Lemaitre and Hoffmann 2007, Govind 2008, Buchon, Broderick et al. 2009, Buchon, Silverman et al. 2014)

The Innate immune system is more generic than the adaptive immune system. The components of the system recognize conserved features of pathogens and become quickly activated to help destroy invaders. The innate immune system is ancestral and found in all multicellular organisms including plants and animals. The basic mechanisms governing innate host defense are conserved allowing invertebrate models to be used to understand vertebrate innate responses. Vertebrates have an additional layer of immunity, namely adaptive immunity which arose in evolution less than 500 million years ago and is integrated with existing innate systems. The innate responses are immediate post-infection and in fact lead to triggering of many aspects of the adaptive immune response which is activated later in time, when counted post-infection. The innate immune system includes Physical barriers, cellular and humoral response, each of which is described in detail in subsequent sections.

1.1 Physical barriers

Like vertebrates, in flies, the first line of defense against invading pathogens is the presence of physical barriers such as external cuticle, gut, and trachea. Cuticle is a layer covering the external surface and the surfaces of foregut and hindgut surfaces. It acts as a support for muscle attachment as well as functions as a protective barrier against environmental factors (Svend, 2009). In *Drosophila*, stiffness and strength of the cuticle is regulated by barsicon, a neuropeptide hormone (Qisheng Song, 2012), along with a couple of more factors. Particularly, the genes *black* and *ebony* regulate the synthesis of N-β-ananyldopamine (NBAD), a compound that confers stiffness to the cuticle. Mutants of these genes have lower stiffness and puncture resistance, making the flies susceptible to physical injuries and infection (Svend, 2012).

Analogous to vertebrate trachea, *Drosophila* trachea is a branched, tubular gas-filled organ. It consists of primary, secondary, and terminal branches. The tracheal lumen is covered by a cuticular lining, which blocks the exit of water, preventing dehydration. It also blocks the entry of microbes, offering protection. Epithelial cells of trachea, in response to pathogenic bacteria, express antimicrobial peptides (AMPs) and other stress response genes (Ferrandon, Jung et al. 1998, Tzou, Ohresser et al. 2000, Wagner, Holle et al. 2008). The expression of AMPs in surface tissues was identified using transgenic fluorescent AMP reporter constructs, which demonstrated enhanced AMP expression in response to local infection (Tzou, Ohresser et al. 2000, Davis and Engstrom 2012).

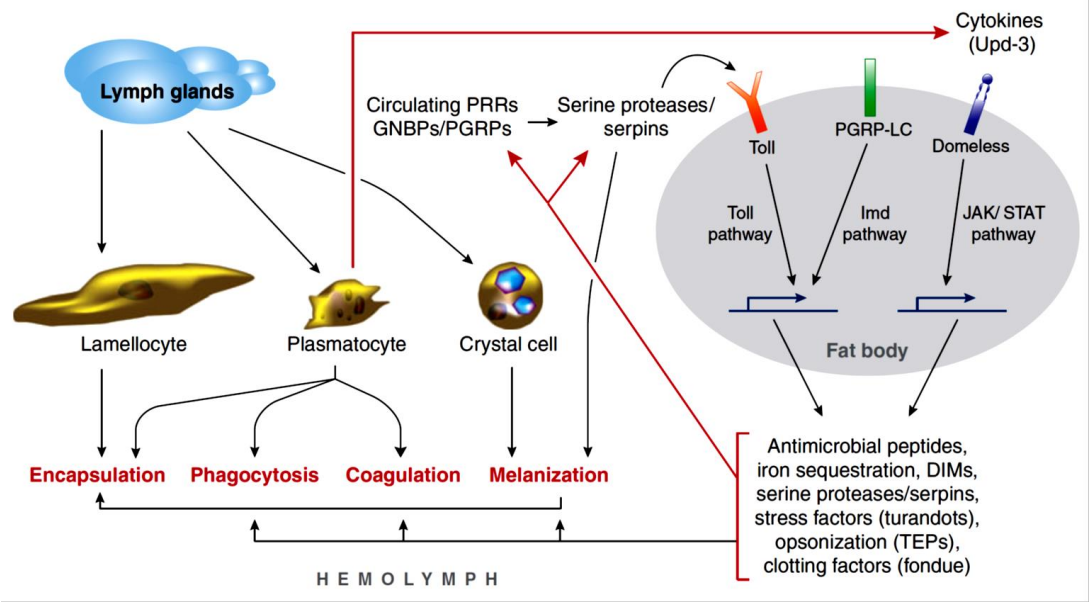

Figure 1-1: Schematics of defense mechanisms in *Drosophila* melanogaster. Lymph gland, hemocytes and fat body play critical role in *Drosophila* immunity. In case of infection, fat body secretes antimicrobial peptides into the hemolymph. Lymph gland regulates macrophages, lamellocytes, plasmatocytes and crystal cells. These different cell types are involved in different cellular responses like encapsulation, phagocytosis, coagulation and melanization. Both these responses help combat infection in flies. (Lemaitre and Hoffmann 2007)

If the physical barriers fail to combat infection, cellular processes like phagocytosis, encapsulation, and melanization fight with pathogens. Along with these cellular responses, systemic humoral response in the form of AMPs produced by the activation of Toll and IMD pathways (De Gregorio et al., 2002) and generation of highly microbicidal hypochlorus acid (HOCl) is employed. These two processes together help in mounting a robust immune response against pathogen invasion. These pathways are summarized in **Figure1.1**.

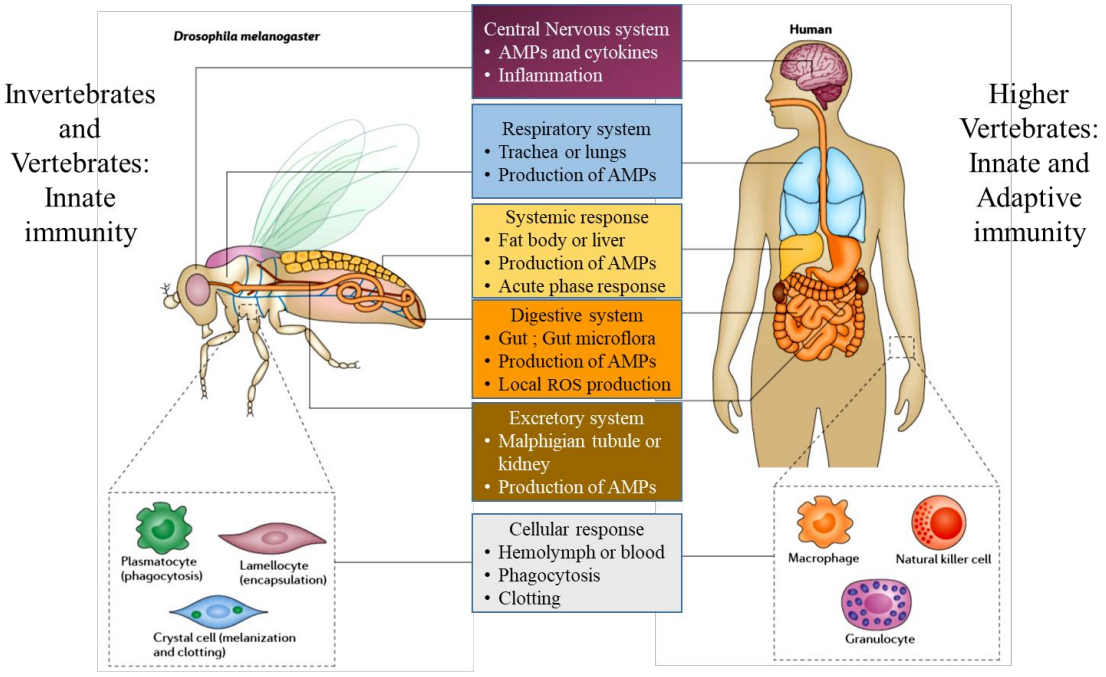

Figure 1-2: Components of innate immunity are similar in flies and humans. Organ system in *Drosophila* is analogous to that in humans. In *Drosophila*, like in vertebrates, brain or central nervous system control the physiology through the secretion of neuropeptides. The system also controls immune response by secreting hormones and AMPs. The respiratory organs, lungs in vertebrates and trachea in *Drosophila*, act as physical barriers against invading pathogens and mount immune response through macrophages and secretion of AMPs. The systemic regulation of energy homeostasis and immune response is achieved through vertebrate liver while in flies, this job is done by fat body. Although flies have an open circulatory system, they have various types of blood cells known as hemocytes. All three types of hemocytes have specialized functions in flies. For example, plasmatocytes function similar to macrophages, whereas crystal cells help in clotting. (Buchon, Silverman et al. 2014)

1.2 Cellular immunity

Flies have circulating hemolymph with many free flowing hemocytes. Flies contain three types of blood cells: plasmatocytes, lamellocytes, and crystal cells. These blood cells are regulated by different signaling pathways, have distinct structures, and have specialized functions. Plasmatocytes constitute 90–95% of total hemocytes. They are present in all developmental stages of the fly, from embryonic stage to adulthood. Plasmatocytes are small, round cells involved in phagocytosis. Lamellocytes are not found in embryos or adult flies but found only in the larval stage in very small numbers. The numbers, however, can be increased by infection with a parasitoid wasp. The third type of cells is crystal cells. They constitute the remaining 5% of hemocytes and are involved in melanization.

1.2.1 *Phagocytosis:* The term "phagocytosis" is derived from Greek words phagein = to eat quickly, kytos = cell, and osis = process. Phagocytosis is an evolutionarily well-conserved process of efficiently eliminating apoptotic cells and infectious agents. The phagocytic cells engulf microbes or apoptotic cells by triggering a series of cellular cascades: binding of bacteria or dead cells to cell surface receptor, change in cell shape by cytoskeleton reorganization, internalization of the bound particle, and destruction of the internalized particle in the phagosomes. This destruction within the phagosomes is a combined effect of lysosomal enzymes, reactive oxygen species (ROS), nitric oxide (NO), and intracellular AMPs. In flies, macrophage-like S2 cells are extensively studied using genetics and molecular approaches to identify scavenger receptors such as Croquemort, Peste (Philips, Rubin et al. 2005, Stuart and Ezekowitz 2005), and SR-CI (Ramet, Pearson et al. 2001); EGF-repeat proteins such as Draper, Eater, and Nimrod CI (Kocks, Cho et al. 2005, Kurucz, Markus et al. 2007); and pathogen-specific cell surface receptors such as PGPRP-LC and PGPRL-SC1a (Ramet, Manfruelli et al. 2002, Garver, Wu et al. 2006).

1.2.2 *Melanization:* In nature, flies are injured or infected by parasitoid wasp eggs. These eggs are big in size and cannot be tackled by phagocytosis. The injured region of the fly needs to be repaired. For such a situation, melanin is synthesized and deposited either at the site of injury or on the surface of the egg. *Drosophila* cells that function in this process are called Crystal cells. These cells synthesize prophenoloxidase crystals; cleaving of ehich form melanin and toxic intermediates (De Gregorio, Han et al. 2002). The wound repair by melanization is similar to the clotting process in vertebrates. The clot formed at the site of injury traps hemocytes that synthesize melanin to harden and close the clot (Bidla, Lindgren et al. 2005). The proteomic analysis of the clot has identified proteins such as Hemolectin, Fondue, and transglutaminase (TG) (Karlsson, Korayem et al. 2004, Scherfer, Karlsson et al. 2004, Scherfer, Qazi et al. 2006, Agianian, Lesch et al. 2007).

1.2.3 *Encapsulation:* Another mechanism to tackle parasitoid wasp eggs is to encapsulate the eggs completely using large, flat lamellocytes. The production of these hemocytes in larvae is induced by wasp eggs precursors (Rizki and Rizki 1984, Sorrentino, Carton et al. 2002). The encapsulated egg is then destroyed by ROS and toxins secreted by the lamellocytes.

1.3 Humoral response

In response to pathogenic attack, AMPs are released primarily from the fat body and hemocytes into the hemolymph. This release is critically controlled in normal, uninfected flies and expressed only when challenged with infection. This signal specific activation of AMPs is regulated by NF-kB and GATA-like transcription factors. The three NF-kB factors in *Drosophila* are Dorsal/Dif and Relish. Dorsal and Dif, protein products of two clustered genes, *dorsal and dif*, contain N-terminal Rel homology DNA binding domain (RHD) and C-terminal trans-activator domain. Both of these proteins function redundantly as part of Toll pathway. The third NK-kB, Relish, is a p105 homolog, with N-terminal Rel domian and C-terminal inhibitory ankyrin repeat domain. The C-terminal inhibitory domain is cleaved in response to infection, and N-terminal Rel domain transcribes AMPs downstream of the IMD pathway. These domains functions in regulation of humoral response.

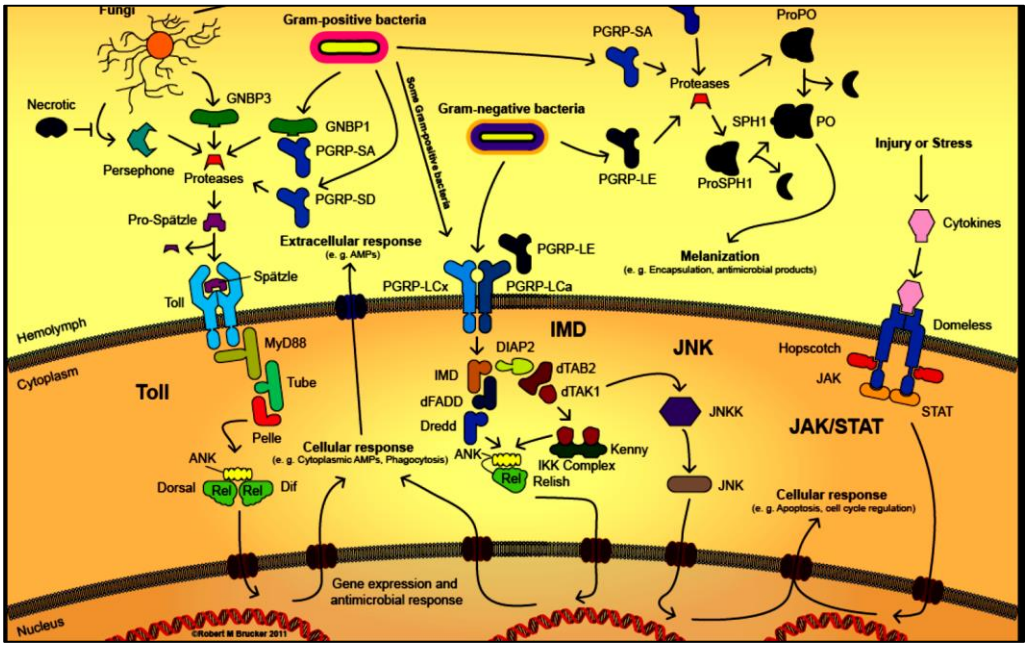

Figure 1-3: Humoral immune pathways in *Drosophila* melanogaster. Different humoral pathways are activated in response to different types of infections. Fungal and Gram positive bacterial infection infections activate Toll pathway while Gram negative bacterial infection activates IMD pathway. IMD pathway activation in turn regulates activity of JNK pathway. JAK/STAT pathway on the other hand is activated in response to stress or injury. These humoral pathways also communicate with cellular responses for a robust immune activation and regulation Uvell & Engstrom, 2007; ©Robert Brucker

.

1.3.1 *Toll pathway:* Dorsal is a part of the evolutionarily conserved signaling cascade (**Figure1.4**) which plays central role in dorso-ventral patterning in flies. The role of Toll pathway in fly immunity was first identified by Hultmark and colleagues in 1995 (Rosetto, Engstrom et al. 1995). The pathway includes ligand Spatzle, Toll-receptor, MyD88 adaptor protein, IkB homolog, Cactus, and NF-kB factors Dorsal and Dif. In response to fungal or gram positive infection, Spatzle is activated by proteolytic cleavage. Activated Spatzle binds to the transmembrane Toll receptor and leads to recruitment of MyD88, Tube and Pellino (Pelle) to the site of Toll receptors. This recruitment is essential for phosphorylation and degradation of fly IkB, Cactus (Sun, Bristow et al. 2002, Zhou, Silverman et al. 2005, Jang, Chosa et al. 2006, Arnot, Gay et al. 2010). Cactus binds to NF-kB factors, Dorsal and Dif, and retain them in the nucleus. When Cactus is degraded, these NF-kB factors are free to translocate to the nucleus to activate target genes including AMPs like *drosomycin* and *defensin* (Belvin, Jin and Anderson, 1995). Recent studies in *Drosophila* macrophage-like S2 cells identify GATA binding transcription factors, Pannier and u-shaped to regulate the Toll pathway.

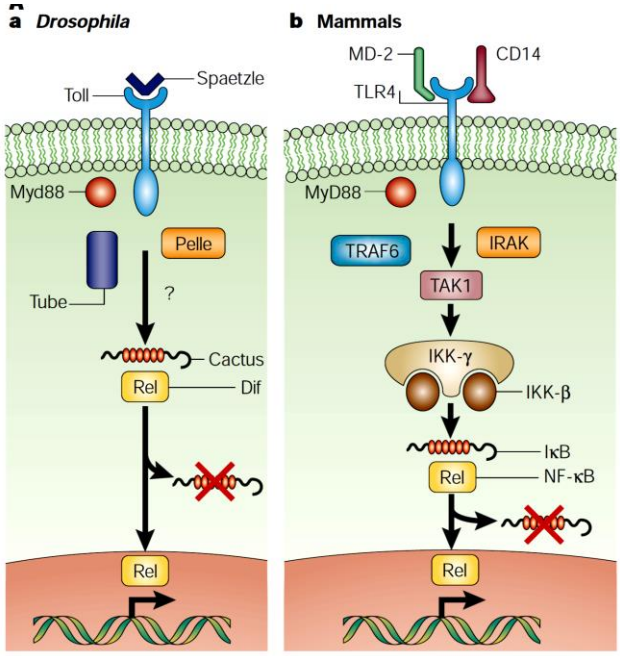

Figure 1-4: Schematic representation of conserved Toll pathway. Toll pathway components include transmembrane Toll receptor, adaptor proteins MyD88, Tube and pelle. Binding of Spatzle to Toll receptor activates Toll signaling cascade which leads to degradation of Cactus, and translocation of Rel-domian containing Dorsal/Dif into the nucleus. Similar pathway is employed in activation of TLR4 mediated signaling in cytokine production in mammals. Reprinted by permission from Macmillan Publishers Ltd: Nature Reviews Genetics, (Kurtz and EwBank), copyright (2003).

Along with regulation at level of transcription, Toll pathway components are regulated by multiple post-translational modifications. For example, a key component of the Toll pathway, Cactus is ubiquitinated in response to infection. This leads to degradation of Cactus and nuclear localization of NF-kB factors, Dorsal and Dif (Shelton CA and Wasserman SA., 1993). Another player in Toll pathway, β-arrestin binds to ERK to inhibit ERK phosphorylation. Phosphorylation of ERK is required for phosphorylation and thereby, nuclear translocation of Dorsal (Sun, Lan et al. 2016). Along with phosphorylation, Dorsal is also regulated by SUMOylation. SUMOylation of Dorsal makes it a potent transcriptional activator in S2 cells (Bhaskar, Smith et al. 2002).

1.3.2 *IMD Pathway*. *imd* pathway mutants showed impaired immune response against gram negative bacterial infection with very little effect on *drosomycin* production (Lemaitre, Kromer-Metzger et al. 1995). Genetic screens that followed, have identified various components of IMD pathway which show homology with components of mammalian TNFR1 signaling. For instance, *Drosophila* IMD pathway receptor, PGPRP is identified as homolog of TNFR1, the receptor involved in classical NF-kB signaling in vertebrates (**Figure1.5**). DREDD, homolog of mammalian Caspase-8, cleaves the NF-kB factor, Relish, and allows nuclear translocation of Relish (Stoven et al.2003). These similarities between innate immune signaling pathways in flies and vertebrates make the fly an important model for studying these pathways.

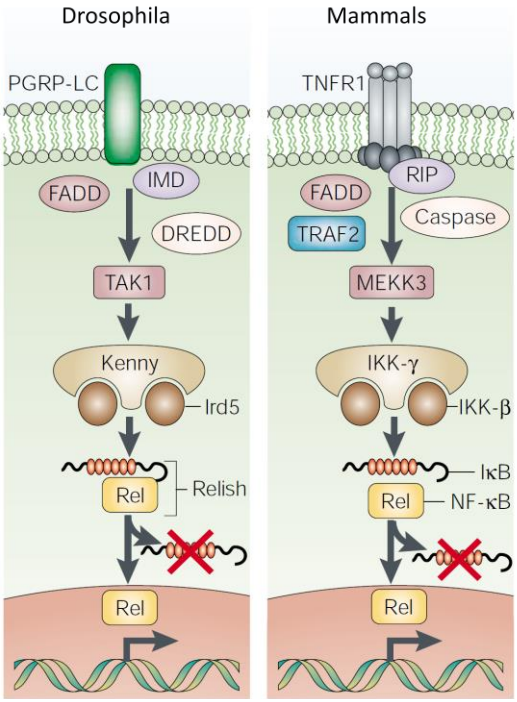

Figure 1-5: Conserved IMD pathway in *Drosophila* melanogaster and mammals. IMD pathway is activated in flies in response to gram negative bacterial infection. The pathway components are conserved in flies and mammals. Reprinted by permission from Macmillan Publishers Ltd: Nature Reviews Genetics, (Kurtz and EwBank), copyright (2003).

1.3.3 *JAK/STAT pathway*: Like other immune pathways, JAK/STAT pathway is also well conserved from flies to mammals. Similar to Toll pathway, JAK/STAT pathway is critical for early development in flies. It is a key signaling pathway that regulates embryonic segmentation. JAK/STAT pathway consists of three components: receptor Domeless, Janus kinase, Hopsctch (Hop) and transcription factor STAT.

Primarily, viral infection leads to binding of Unpaired (Upd) cytokines to transmembrane domeless (Dome) receptor. This in turn activates Hopscotch. Activation of the kinase leads to auto-phosphorylation of Hopscotch along with phosphorylation of Dome. Phosphorylated Dome recruits signal-transducer and activator of transcription at 92E (STAT92E). This recruitment brings Hop in close proximity to STAT92E and leads to phosphorylation of STAT92E. Phosphorylated STAT92E dimerize and translocate to the nucleus to transcribe stress genes, thioester-containing proteins (Teps) and Turandot (Tot) (**Figure1.6**)(Myllymaki and Ramet, 2014). JAK/STAT pathway mutants show normal immune response against bacteria and fungi but are susceptible to *Drosophila* C virus infection (Shuai and Liu 2003, Agaisse and Perrimon 2004) suggesting role for JAK/STAT pathway in viral immunity.

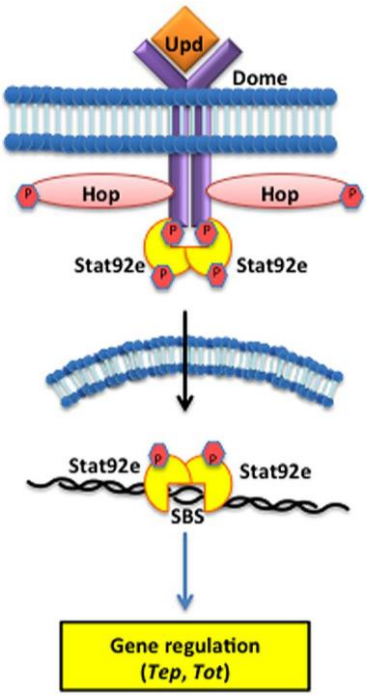

Figure 1-6: JAK/STAT pathway in *Drosophila* melanogaster. Three component system of JAK/STAT pathway include a transmembrane receptor, Domeless (Dome,purple), Janus kinase, Hopscotch (HOP, pink) and effector transcription factor, STAT92E (yellow). Pathway is activated in response to septic injury or viral infection when Unpaired cytokines (Upd, orange) bind to Domeless. This leads to binding of Hop to Dome and phosphorylation of Dome. STAT92E binds to phosphorylated Dome, is then phosphorylated by Hop. Phosphorylated STAT92E enters the nucleus and activates stress response genes Tep and Tot (Stokes et al. 2015)

JAK/STAT pathway is extensively regulated by phosphorylation as described. In addition, SUMOylation of STAT92E modulates its transcriptional activity (Gronholm, Ungureanu et al. 2010). Trigger and dynamics of STAT92E SUMOylation need further investigation.

1.4 Systemic regulation of innate immunity.

1.4.1 *'Gut feeling' in immunity:*

As described earlier, different signaling cascade components are regulated at transcription level or post-translationally by phosphorylation, ubiquitination or SUMOylation. Fat body and hemocytes are two important organs that play critical role in generating immune response against pathogenic invasion. Along with these two organs, fly gut also mounts a robust immune response against constant attack by pathogens and physical damage.

Drosophila gut has a very similar structure to that of vertebrate intestine, with highly compartmentalized monolayer tube of epithelial cells. These cells secrete mucin-like proteins

within the lumen to maintain a layer of mucus. This layer acts as first line of defense against engulfed micro-organisms (Eckmann and Kagnoff 2005, Syed, Hard et al. 2008, Buchon, Broderick et al. 2009). Like vertebrates, fly gut is also home to a variety of commensal bacteria. 1-30 different bacterial species belonging to genera *Lactobacillus* and *Acetobacter* make-up the fly gut microbiota These microbes induce secretion of insulin pathway which regulates larval development (Ridley, Wong et al. 2012). The microbiota also regulates stem-cell proliferation essential for normal gut physiology. Gut microbiota as well as pathogenic bacteria promote production of Unpaired 3 (Upd3), ligand for JAK/STAT pathway, promote homeostatic response to regulate intestinal stem cell (ISC) niche (Buchon, Broderick et.al. 2009). Loss of ISCs makes flies susceptible to infection and shortens fly life-span. The load and diversity of gut microbiota increases as the fly age and affects gut physiology which in turn affects immune response (Corby-Harris, Habel et al. 2007, Ren, Webster et al. 2007, Ryu, Anikin et al. 2008, Buchon, Broderick et al. 2009, Osman, Buchon et al. 2012).

Gut cells induce production of reactive oxygen species (ROS) and AMPs. ROS is produced by two NADPH enzymes conserved between flies and vertebrates. Dual oxidase (DUOX) generates microbicidal H_2O_2 and hypochlorous acid (HOCl) while NADPH oxidase (NOX) generates only H_2O_2. *Drosophila* mutants for DUOX activity show enhanced susceptibility to infection with enteric pathogens. Even in presence of dietary bacteria and yeast, the life-span of these mutants is reduced (Krause 2007, Ha, Lee et al. 2009, Ha, Lee et al. 2009).

Production of AMPs from gut is a conserved phenomenon across the animal kingdom (Mahida and Chan, 1997). Expression of AMPs in the fly gut is region specific. This spatial regulation of AMP production is thought to be a result of region-specific expression of transcription factors responsible for AMP production (Tzou, Ohresser et al. 2000, Eckmann 2005, Buchon, Osman et al. 2013). For example, Caudal, a negative regulator of AMPs, is expressed specifically in the midgut. Caudal mutants show cell death in the gut and have a shortened life-span (Ryu, Kim et al. 2008). Receptors of IMD pathway, PGPRP-LC is expressed in the anterior gut while PGPRP-LE is expressed in midgut and the posterior gut. This allows for fine-tuning of bacterial sensing within the fly gut (Bosco-Drayon, Poidevin et al. 2012, Buchon, Osman et al. 2013). Pirk (poor IMD response upon knock-in), negative regulator of IMD pathway, is expressed specifically in the gut. Pirk, itself is regulated by IMD pathway. This negative feedback loop allows

fine-tuning of immune response in the gut (Agarwal 2008, Kleino, Myllymaki et al. 2008, Lhocine, Ribeiro et al. 2008). FOXO (forkhead box subgroup O) is transcription factor involved in the regulation of the insulin signaling pathway. FOXO is chronically activated specifically in the gut of aging flies. This leads to down-regulation of PGPRP-SC2, a negative regulator of IMD pathway, which causes hyperactivation of IMD pathway in the aging fly gut (Becker, Loch et al. 2010, Guo, Karpac et al. 2014).

Another humoral response pathway, JAK/STAT regulates Drosomycin class AMPs specifically in the gut. The activation of the JAK/STAT pathway is not dependent on microbial infection but dependent on septic injury. This allows for sensing physical damage of the intestine along with bacterial infection (Boutros, Agaisse et al. 2002, Agaisse and Perrimon 2004).

1.4.2. *Metabolic and immune pathway cross-talk for robust immune response*.

In flies and mammals, systemic regulation is achieved by hormonal signals. Insulin, hormone central to metabolic regulation, is also critical for regulation of inflammatory signaling (Hotamisligil 2008). In flies, fat body stores excess fat as TAGs and regulate metabolism (Arrese and Soulages, 2010). Fat body is also a critical player in innate immune response in flies. Fat body, in response to dietary changes and microbial infections, releases signaling factors that regulate insulin secretion, growth, metabolism and immune response. In flies, systemic infection with *Mycobacterium* leads to metabolic shifts leading to decrease in TAGs levels. Hyperactivation of immune response leads to dysregulation of metabolic pathways, which in turn causes wasting. This phenomenon is seen in humans and flies (Fitzpatrick and Young 2013).

While infections regulate metabolism, metabolism, in turn, also regulates innate immune response. In flies, leptin family cytokines, Upd proteins, are secreted in fed state from the fat body. This activates JAK/STAT pathway which in turn regulates insulin secretion in the brain and regulates growth and metabolism (**Figure1.7**) (Rajan and Perrimon 2012).

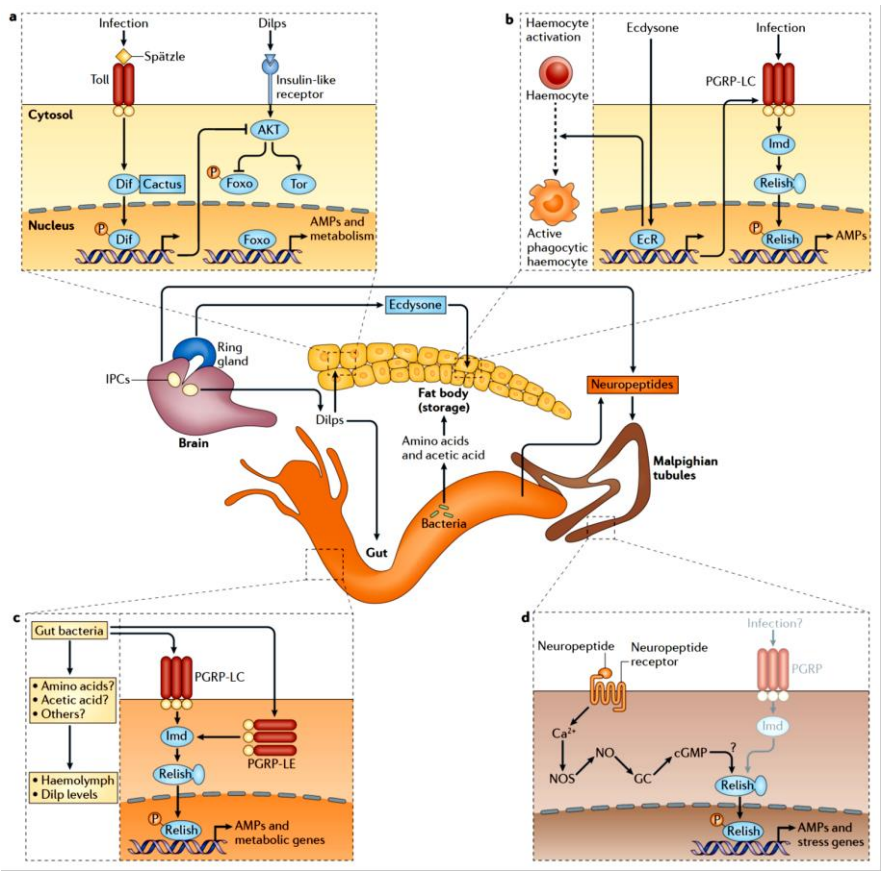

Figure 1-7: Multiple organs involved in immune response in the fly. There are multiple circuis that function between different organs in the fly. (A) In the fat body, humoral response Toll pathway inhibits insulin signaling through NF-kB factor Dif, affecting growth. Conversely, insulin pathway component, FOXO regulates AMP production. (B) In larval brain, and adult body, Ecdysone, hormone, a key regulator of development and life-cycle, also regulates IMD pathway through expression of PGPRP-LE and also via direct regulation of AMP production. Ecdysome (20E) also regulates phagocytic activity of pupal hemocytes. (C) Gut commensal bacteria produce acetic acid which in turn regulates production of Dilps in the brain. This regulates growth and development of the fly. (D) In Malphigian tubules, secretion of neuropeptides activates production of nitrous oxide dependent NF-kB response. Copyright (Buchon, Silverman et al. 2014).

Metabolic pathways and innate immune signaling pathways integrate through multiple points. For example, Mef2 (myocyte enhancer factor 2) is phosphorylated by AKT signaling under normal conditions. This phosphorylation of Mef2 promotes anabolism. Upon immune challenge, phosphorylated Mef2 levels decrease, enzymes involved in anabolism reduce and immune genes are activated (**Figure1.8**) (Clark, Tan et al. 2013).

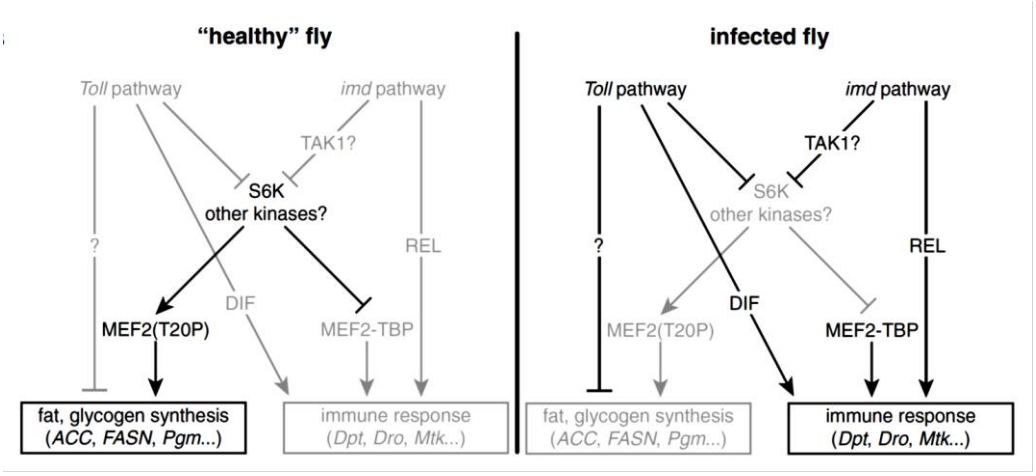

Figure 1-8: Mef2 dependent regulation of metabolism and immunity. In a healthy fly, the immune pathways are inactive. S6K are active, which in turn activate MEF2. MEF2 activates anabolic enzymes involved in fat and glycogen synthesis. When infected, the immune pathways, Toll and IMD are active. These pathways in turn inhibit S6 kinase. This inhibition leads to formation of MEF2-TBP complex which in turn activate immune response genes, antimicrobial peptides. (Clark et al., Cell, 2013)

In another example, the MAPK-ERK signaling plays important role in growth and development. Insulin and growth factors induce MAPK-ERK signaling on one hand and Pirk, a gut specific feedback inhibitor of IMD pathway, on the other. This negative feedback is crucial in protecting gut cells from hyperactive inflammatory response and extends fly life-span (Zhang, Thompson et al. 2011, Slack, Alic et al. 2015).

Insulin also controls Ecdysone, key hormone in *Drosophila* development and life-cycle. Ecdysone forms a heterodimer with USP and ecdysone receptor (EcR) that activates the transcription factor, 20E. The target genes of 20E have a direct effect on IMD pathway signaling. The target genes positively regulate PGPRP mediated IMD signaling. Some of the target genes of 20E, like *pnr* and *srp*, directly activate antimicrobial peptides, independent of signaling via IMD. IMD pathway activation is also controlled by 20E via transcription of nuclear hormone receptor, Eip75B (**Figure1.9**) (Rus, Flatt et al. 2013).

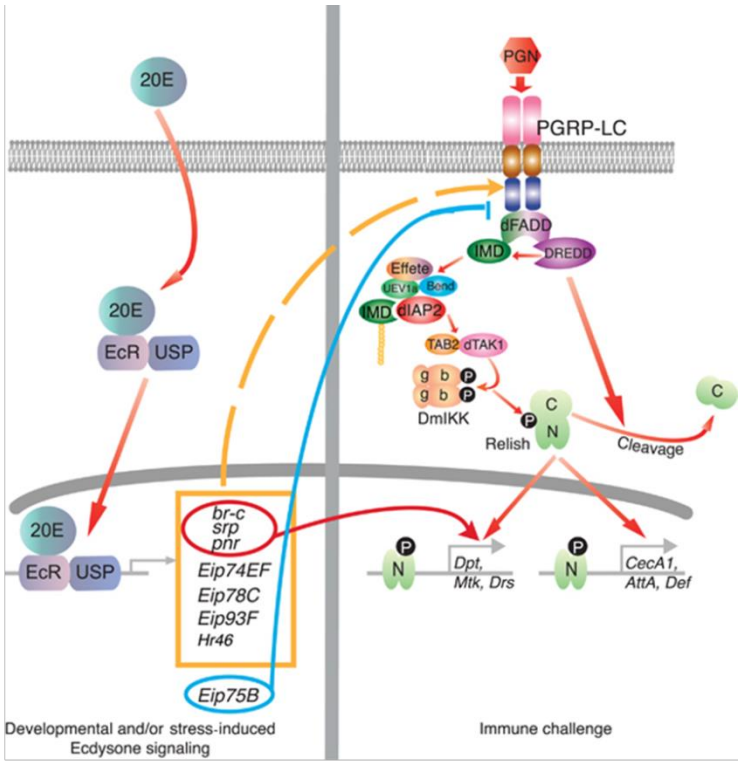

Figure 1-9: Ecdysone signaling in development and immunity. The canonical ecdysone(20E) pathway regulated IMD pathway at two different levels, first at the receptor level and second, at the level of antimicrobial peptides. 20E dimerizes with USP and ecdysone receptor (EcR). This protein complex then translocated to the nucleus for activation of target genes. These target genes positively regulate PGPRP receptors. A sub-set of these target genes, *br-c*, *srp and pnr* directly activate antimicrobial peptides, independent of the PGPRP- receptor mediated signaling. 20E induces expression of Eip75B, nuclear hormone receptor, which interferes with PGPRP-receptor signaling and negatively regulates IMD pathway. Reproduced from (Rus, Flatt et al. 2013).

1.5 Regulation of immunity using PTMs

Post-translational modifications like phosphorylation, ubiquitination and SUMOylation modulate immune pathways. As described earlier in the chapter, phosphorylation regulates the activity of many different targets in all humoral pathways. The role of ubiquitin is established in both *Drosophila* and mammalian immunity. For instance, in response to infection, IκB is ubiquitinated, which leads to its degradation. Degradation of IκB leads to nuclear translocation of NF-κB that up-regulates transcription of target genes. Regulation of stability and signaling by many other players like IMD and DREDD is achieved by ubiquitination. Another Ubiquitin-like modifier, SUMO, has been implicated in regulation of fly immunity. SUMO/Ubc9 mutant flies show impaired immune response. In case of humoral pathway regulation, activity of at least one

protein from each pathway is controlled by SUMOylation. For example, in Toll pathway, Dorsal is SUMOylated and this regulates its activity as a transcription factor (Bhaskar, Smith et al. 2002). IMD pathway component, IRD5 SUMOylation is essential for activation of antimicrobial peptide, *attacinA* (Fukuyama, Verdier et al. 2013). SUMOylation of STAT92E, transcription factor of JAK/STAT pathway, on the other hand, inhibits its transcription activity (Gronholm, Ungureanu et al. 2010). In ecdysone pathway component, USP is also a target for SUMOylation. SUMOylation of USP maintains stability of USP, which in turn, regulates 20E signaling (Wang, Wang et al. 2014). These examples highlight the importance of SUMOylation in immune regulation.

SUMO will be discussed in further detail in the next chapter.

1.6 PERMISSIONS

Figures reproduced from Annual Reviews of Immunology (Figure 1) allow free permission for reproducibility. For Figures reproduced in Nature Reviews of Immunology (Figure 2 and 7) and Nature Review of Genetics (Figure 4 and 5), permission from the concerned journal is officially obtained.

BIBLOGRAPHY

Agaisse, H. and N. Perrimon (2004). "The roles of JAK/STAT signaling in *Drosophila* immune responses." Immunol Rev **198**: 72-82.

Agarwal, R. K. (2008). "Probiotics--the health friendly gut bacteria." Indian Pediatr **45**(12): 953-954.

Agianian, B., C. Lesch, O. Loseva and M. S. Dushay (2007). "Preliminary characterization of hemolymph coagulation in Anopheles gambiae larvae." Dev Comp Immunol **31**(9): 879-888.

Arnot, C. J., N. J. Gay and M. Gangloff (2010). "Molecular mechanism that induces activation of Spatzle, the ligand for the *Drosophila* Toll receptor." J Biol Chem **285**(25): 19502-19509.

Becker, T., G. Loch, M. Beyer, I. Zinke, A. C. Aschenbrenner, P. Carrera, T. Inhester, J. L. Schultze and M. Hoch (2010). "FOXO-dependent regulation of innate immune homeostasis." Nature **463**(7279): 369-373.

Bhaskar, V., M. Smith and A. J. Courey (2002). "Conjugation of Smt3 to dorsal may potentiate the *Drosophila* immune response." Mol Cell Biol **22**(2): 492-504.

Bidla, G., M. Lindgren, U. Theopold and M. S. Dushay (2005). "Hemolymph coagulation and phenoloxidase in *Drosophila* larvae." Dev Comp Immunol **29**(8): 669-679.

Bosco-Drayon, V., M. Poidevin, I. G. Boneca, K. Narbonne-Reveau, J. Royet and B. Charroux (2012). "Peptidoglycan sensing by the receptor PGRP-LE in the *Drosophila* gut induces immune responses to infectious bacteria and tolerance to microbiota." Cell Host Microbe **12**(2): 153-165.

Boutros, M., H. Agaisse and N. Perrimon (2002). "Sequential activation of signaling pathways during innate immune responses in *Drosophila*." Dev Cell **3**(5): 711-722.

Boman, H. G., I. Nilsson and B. Rasmuson (1972). "Inducible Antibacterial Defence System in Drosophila." Nature **237**: 232.

Brennan, C. A. and K. V. Anderson (2004). "Drosophila: The Genetics of Innate Immune Recognition and Response." Annual Review of Immunology **22**(1): 457-483.

Buchon, N., N. A. Broderick, S. Chakrabarti and B. Lemaitre (2009). "Invasive and indigenous microbiota impact intestinal stem cell activity through multiple pathways in *Drosophila*." Genes Dev **23**(19): 2333-2344.

Buchon, N., D. Osman, F. P. David, H. Y. Fang, J. P. Boquete, B. Deplancke and B. Lemaitre (2013). "Morphological and molecular characterization of adult midgut compartmentalization in *Drosophila*." Cell Rep **3**(5): 1725-1738.

Buchon, N., N. Silverman and S. Cherry (2014). "Immunity in *Drosophila* melanogaster--from microbial recognition to whole-organism physiology." Nat Rev Immunol **14**(12): 796-810.

Clark, R. I., S. W. Tan, C. B. Pean, U. Roostalu, V. Vivancos, K. Bronda, M. Pilatova, J. Fu, D. W. Walker, R. Berdeaux, F. Geissmann and M. S. Dionne (2013). "MEF2 is an in vivo immune-metabolic switch." Cell **155**(2): 435-447.

Corby-Harris, V., K. E. Habel, F. G. Ali and D. E. Promislow (2007). "Alternative measures of response to Pseudomonas aeruginosa infection in *Drosophila* melanogaster." J Evol Biol **20**(2): 526-533.

Davis, M. M. and Y. Engstrom (2012). "Immune response in the barrier epithelia: lessons from the fruit fly *Drosophila* melanogaster." J Innate Immun **4**(3): 273-283.

De Gregorio, E., S. J. Han, W. J. Lee, M. J. Baek, T. Osaki, S. Kawabata, B. L. Lee, S. Iwanaga, B. Lemaitre and P. T. Brey (2002). "An immune-responsive Serpin regulates the melanization cascade in *Drosophila*." Dev Cell **3**(4): 581-592.

Eckmann, L. (2005). "Defence molecules in intestinal innate immunity against bacterial infections." Curr Opin Gastroenterol **21**(2): 147-151.

Eckmann, L. and M. F. Kagnoff (2005). "Intestinal mucosal responses to microbial infection." Springer Semin Immunopathol **27**(2): 181-196.

Engstrom, Y., L. Kadalayil, S. C. Sun, C. Samakovlis, D. Hultmark and I. Faye (1993). "kappa B-like motifs regulate the induction of immune genes in Drosophila." J Mol Biol **232**(2): 327-333.

Ferrandon, D., A. C. Jung, M. Criqui, B. Lemaitre, S. Uttenweiler-Joseph, L. Michaut, J. Reichhart and J. A. Hoffmann (1998). "A drosomycin-GFP reporter transgene reveals a local immune response in *Drosophila* that is not dependent on the Toll pathway." EMBO J **17**(5): 1217-1227.
Fitzpatrick, M. and S. P. Young (2013). "Metabolomics--a novel window into inflammatory disease." Swiss Med Wkly **143**: w13743.
Fukuyama, H., Y. Verdier, Y. Guan, C. Makino-Okamura, V. Shilova, X. Liu, E. Maksoud, J. Matsubayashi, I. Haddad, K. Spirohn, K. Ono, C. Hetru, J. Rossier, T. Ideker, M. Boutros, J. Vinh and J. A. Hoffmann (2013). "Landscape of protein-protein interactions in *Drosophila* immune deficiency signaling during bacterial challenge." Proc Natl Acad Sci U S A **110**(26): 10717-10722.
Garver, L. S., J. Wu and L. P. Wu (2006). "The peptidoglycan recognition protein PGRP-SC1a is essential for Toll signaling and phagocytosis of Staphylococcus aureus in *Drosophila*." Proc Natl Acad Sci U S A **103**(3): 660-665.
Govind, S. (2008). "Innate immunity in Drosophila: Pathogens and pathways." Insect science (Online) **15**(1): 29-43.
Gronholm, J., D. Ungureanu, S. Vanhatupa, M. Ramet and O. Silvennoinen (2010). "Sumoylation of *Drosophila* transcription factor STAT92E." J Innate Immun **2**(6): 618-624.
Guo, L., J. Karpac, S. L. Tran and H. Jasper (2014). "PGRP-SC2 promotes gut immune homeostasis to limit commensal dysbiosis and extend lifespan." Cell **156**(1-2): 109-122.
Ha, E. M., K. A. Lee, S. H. Park, S. H. Kim, H. J. Nam, H. Y. Lee, D. Kang and W. J. Lee (2009). "Regulation of DUOX by the Galphaq-phospholipase Cbeta-Ca2+ pathway in *Drosophila* gut immunity." Dev Cell **16**(3): 386-397.
Ha, E. M., K. A. Lee, Y. Y. Seo, S. H. Kim, J. H. Lim, B. H. Oh, J. Kim and W. J. Lee (2009). "Coordination of multiple dual oxidase-regulatory pathways in responses to commensal and infectious microbes in *Drosophila* gut." Nat Immunol **10**(9): 949-957
Hoffmann, J. A. and J. M. Reichhart (2002). "Drosophila innate immunity: an evolutionary perspective." Nat Immunol **3**(2): 121-126..
Hotamisligil, G. S. (2008). "Inflammation and endoplasmic reticulum stress in obesity and diabetes." Int J Obes (Lond) **32 Suppl 7**: S52-54.
Jang, I. H., N. Chosa, S. H. Kim, H. J. Nam, B. Lemaitre, M. Ochiai, Z. Kambris, S. Brun, C. Hashimoto, M. Ashida, P. T. Brey and W. J. Lee (2006). "A Spatzle-processing enzyme required for toll signaling activation in *Drosophila* innate immunity." Dev Cell **10**(1): 45-55.
Karlsson, C., A. M. Korayem, C. Scherfer, O. Loseva, M. S. Dushay and U. Theopold (2004). "Proteomic analysis of the *Drosophila* larval hemolymph clot." J Biol Chem **279**(50): 52033-52041.
Khush, R. S. and B. Lemaitre (2000). "Genes that fight infection: what the Drosophila genome says about animal immunity." Trends Genet **16**(10): 442-449.
Kleino, A., H. Myllymaki, J. Kallio, L. M. Vanha-aho, K. Oksanen, J. Ulvila, D. Hultmark, S. Valanne and M. Ramet (2008). "Pirk is a negative regulator of the *Drosophila* Imd pathway." J Immunol **180**(8): 5413-5422.
Kocks, C., J. H. Cho, N. Nehme, J. Ulvila, A. M. Pearson, M. Meister, C. Strom, S. L. Conto, C. Hetru, L. M. Stuart, T. Stehle, J. A. Hoffmann, J. M. Reichhart, D. Ferrandon, M. Ramet and R. A. Ezekowitz (2005). "Eater, a transmembrane protein mediating phagocytosis of bacterial pathogens in *Drosophila*." Cell **123**(2): 335-346.
Krause, K. H. (2007). "Aging: a revisited theory based on free radicals generated by NOX family NADPH oxidases." Exp Gerontol **42**(4): 256-262.
Kurucz, E., R. Markus, J. Zsamboki, K. Folkl-Medzihradszky, Z. Darula, P. Vilmos, A. Udvardy, I. Krausz, T. Lukacsovich, E. Gateff, C. J. Zettervall, D. Hultmark and I. Ando (2007). "Nimrod, a putative phagocytosis receptor with EGF repeats in *Drosophila* plasmatocytes." Curr Biol **17**(7): 649-654.
Lemaitre, B., E. Nicolas, L. Michaut, J. M. Reichhart and J. A. Hoffmann (1996). "The dorsoventral regulatory gene cassette spatzle/Toll/cactus controls the potent antifungal response in Drosophila adults." Cell **86**(6): 973-983.

Lemaitre, B. and J. Hoffmann (2007). "The host defense of *Drosophila* melanogaster." Annu Rev Immunol **25**: 697-743.
Lemaitre, B., E. Kromer-Metzger, L. Michaut, E. Nicolas, M. Meister, P. Georgel, J. M. Reichhart and J. A. Hoffmann (1995). "A recessive mutation, immune deficiency (imd), defines two distinct control pathways in the *Drosophila* host defense." Proc Natl Acad Sci U S A **92**(21): 9465-9469.
Lhocine, N., P. S. Ribeiro, N. Buchon, A. Wepf, R. Wilson, T. Tenev, B. Lemaitre, M. Gstaiger, P. Meier and F. Leulier (2008). "PIMS modulates immune tolerance by negatively regulating *Drosophila* innate immune signaling." Cell Host Microbe **4**(2): 147-158
Medzhitov, R., P. Preston-Hurlburt and C. A. Janeway, Jr. (1997). "A human homologue of the Drosophila Toll protein signals activation of adaptive immunity." Nature **388**(6640): 394-397..
Osman, D., N. Buchon, S. Chakrabarti, Y. T. Huang, W. C. Su, M. Poidevin, Y. C. Tsai and B. Lemaitre (2012). "Autocrine and paracrine unpaired signaling regulate intestinal stem cell maintenance and division." J Cell Sci **125**(Pt 24): 5944-5949.
Philips, J. A., E. J. Rubin and N. Perrimon (2005). "*Drosophila* RNAi screen reveals CD36 family member required for mycobacterial infection." Science **309**(5738): 1251-1253.
Rajan, A. and N. Perrimon (2012). "*Drosophila* cytokine unpaired 2 regulates physiological homeostasis by remotely controlling insulin secretion." Cell **151**(1): 123-137.
Ramet, M., P. Manfruelli, A. Pearson, B. Mathey-Prevot and R. A. Ezekowitz (2002). "Functional genomic analysis of phagocytosis and identification of a *Drosophila* receptor for E. coli." Nature **416**(6881): 644-648.
Ramet, M., A. Pearson, P. Manfruelli, X. Li, H. Koziel, V. Gobel, E. Chung, M. Krieger and R. A. Ezekowitz (2001). "*Drosophila* scavenger receptor CI is a pattern recognition receptor for bacteria." Immunity **15**(6): 1027-1038.
Ren, C., P. Webster, S. E. Finkel and J. Tower (2007). "Increased internal and external bacterial load during *Drosophila* aging without life-span trade-off." Cell Metab **6**(2): 144-152.
Ridley, E. V., A. C. Wong, S. Westmiller and A. E. Douglas (2012). "Impact of the resident microbiota on the nutritional phenotype of *Drosophila* melanogaster." PLoS One **7**(5): e36765.
Rizki, R. M. and T. M. Rizki (1984). "Selective destruction of a host blood cell type by a parasitoid wasp." Proc Natl Acad Sci U S A **81**(19): 6154-6158.
Rosetto, M., Y. Engstrom, C. T. Baldari, J. L. Telford and D. Hultmark (1995). "Signals from the IL-1 receptor homolog, Toll, can activate an immune response in a *Drosophila* hemocyte cell line." Biochem Biophys Res Commun **209**(1): 111-116.
Rus, F., T. Flatt, M. Tong, K. Aggarwal, K. Okuda, A. Kleino, E. Yates, M. Tatar and N. Silverman (2013). "Ecdysone triggered PGRP-LC expression controls *Drosophila* innate immunity." The EMBO Journal **32**(11): 1626-1638.
Ryu, J.-H., S.-H. Kim, H.-Y. Lee, J. Y. Bai, Y.-D. Nam, J.-W. Bae, D. G. Lee, S. C. Shin, E.-M. Ha and W.-J. Lee (2008). "Innate Immune Homeostasis by the Homeobox Gene Caudal and Commensal-Gut Mutualism in *Drosophila*." Science **319**: 777-782.
Ryu, M. J., V. Anikin, S. H. Hong, H. Jeon, Y. G. Yu, M. H. Yu, S. Chernysh and C. Lee (2008). "Activation of NF-kappaB by alloferon through down-regulation of antioxidant proteins and IkappaBalpha." Mol Cell Biochem **313**(1-2): 91-102.
Scherfer, C., C. Karlsson, O. Loseva, G. Bidla, A. Goto, J. Havemann, M. S. Dushay and U. Theopold (2004). "Isolation and characterization of hemolymph clotting factors in *Drosophila* melanogaster by a pullout method." Curr Biol **14**(7): 625-629.
Scherfer, C., M. R. Qazi, K. Takahashi, R. Ueda, M. S. Dushay, U. Theopold and B. Lemaitre (2006). "The Toll immune-regulated *Drosophila* protein Fondue is involved in hemolymph clotting and puparium formation." Dev Biol **295**(1): 156-163.
Shuai, K. and B. Liu (2003). "Regulation of JAK-STAT signalling in the immune system." Nat Rev Immunol **3**(11): 900-911.
Slack, C., N. Alic, A. Foley, M. Cabecinha, Matthew P. Hoddinott and L. Partridge (2015). "The Ras-Erk-ETS-Signaling Pathway Is a Drug Target for Longevity." Cell **162**(1): 72-83.

Sorrentino, R. P., Y. Carton and S. Govind (2002). "Cellular immune response to parasite infection in the *Drosophila* lymph gland is developmentally regulated." Dev Biol **243**(1): 65-80.
Stuart, L. M. and R. A. Ezekowitz (2005). "Phagocytosis: elegant complexity." Immunity **22**(5): 539-550.
Sun, H., B. N. Bristow, G. Qu and S. A. Wasserman (2002). "A heterotrimeric death domain complex in Toll signaling." Proc Natl Acad Sci U S A **99**(20): 12871-12876.
Sun, J. J., J. F. Lan, X. Z. Shi, M. C. Yang, G. J. Niu, D. Ding, X. F. Zhao, X. Q. Yu and J. X. Wang (2016). "beta-Arrestins Negatively Regulate the Toll Pathway in Shrimp by Preventing Dorsal Translocation and Inhibiting Dorsal Transcriptional Activity." J Biol Chem **291**(14): 7488-7504.
Syed, Z. A., T. Hard, A. Uv and I. F. van Dijk-Hard (2008). "A potential role for *Drosophila* mucins in development and physiology." PLoS One **3**(8): e3041.
Tzou, P., S. Ohresser, D. Ferrandon, M. Capovilla, J. M. Reichhart, B. Lemaitre, J. A. Hoffmann and J. L. Imler (2000). "Tissue-specific inducible expression of antimicrobial peptide genes in *Drosophila* surface epithelia." Immunity **13**(5): 737-748.
Tzou, P., E. De Gregorio and B. Lemaitre (2002). "How Drosophila combats microbial infection: a model to study innate immunity and host-pathogen interactions." Curr Opin Microbiol **5**(1): 102-110.
Wagner, A. Y., E. Holle, L. Holle, X. Yu and G. Schwamberger (2008). "Immunological tolerance and tumor rejection in embryo-aggregated chimeric mice - lessons for tumor immunity." BMC Cancer **8**: 370.
Wang, J., S. Wang and S. Li (2014). "Sumoylation modulates 20-hydroxyecdysone signaling by maintaining USP protein levels in *Drosophila*." Insect Biochem Mol Biol **54**: 80-88.
Williams, M. J. (2001). "Regulation of antibacterial and antifungal innate immunity in fruitflies and humans." Adv Immunol **79**: 225-259.

Zhang, W., B. J. Thompson, V. Hietakangas and S. M. Cohen (2011). "MAPK/ERK Signaling Regulates Insulin Sensitivity to Control Glucose Metabolism in *Drosophila*." PLOS Genetics **7**(12): e1002429.

Zhou, R., N. Silverman, M. Hong, D. S. Liao, Y. Chung, Z. J. Chen and T. Maniatis (2005). "The role of ubiquitination in *Drosophila* innate immunity." J Biol Chem **280**(40): 34048-34055.

Chapter 2

FlySUMObase: A database of SUMOylated proteins in *Drosophila melanogaster*

2.1 SUMMARY

Unlike mammalian cells, *Drosophila* is not a popular model system for SUMO proteome analysis. Only a few SUMO proteomes have been studied and they are limited to one or two developmental stages of *Drosophila*. This study aims to predict potential *Drosophila* SUMOylated proteins by identifying SUMOylated mammalian homologs and making a list of fly orthologs. The homology-based list is then combined with known SUMOylated species in *Drosophila* to generate a current database of SUMOylated species, christened FlySUMObase. The database was then analyzed to get a systemic view of SUMO modification in biological processes. Further, the database allows us to predict SUMO targets in flies. These targets can be prioritized and subject to experimental validation. Based on my analysis, I have identified potentially SUMOylated proteins in *Drosophila*, such as Pont, Nph2, Iswi, and members of the MARS complex. A subset of proteins in FlySUMObase are targets that relate to the immune response. For my Ph.D. I have chosen a few interesting targets and performed further experimental validation to uncover biological roles for SUMO modification for these targets.

2.2 ABBREVIATIONS

SUMO: Small Ub-like modifier; DIOPT: DRSC Integrative Ortholog Prediction Tool; MARS: Multiaminoacyl tRNA synthetase complex; CS: Confidence Score

2.3 INTRODUCTION

SUMO is a **S**mall **U**biquitin-like **MO**difier conserved from yeast to humans. The modification is carried out using a series of enzymes similar to the Ubiquitin cycle **(Figure 1)**. This modification occurs in a series of reactions mediated by Sae1/Sae2, Ubc9, and E3 ligases.

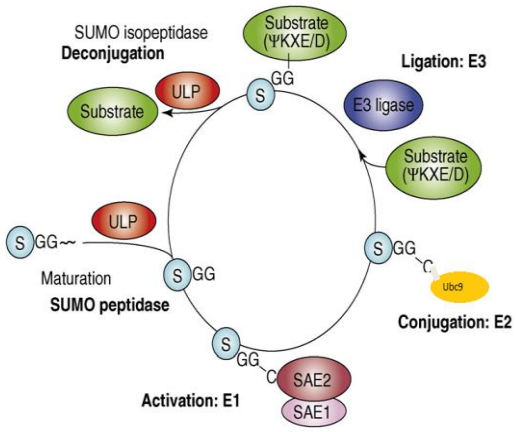

Figure 2-1: The SUMO Cycle. The SUMO congugation/decongugation cycle functions as follows. In an ATP-independent manner, Ulp1, the SUMO protease, cleaves off amino acids beyond GG residues. This exposes the C-terminal di-glycine residues for attachment to the cystein residue of SUMO activation enzymes E1/E2 in ATP-dependent way. The SUMO is then transferred to SUMO conjugase dUbc9 after which it is transferred to target protein via an isopeptide linkage with NH-group of lysine. *Drosophila* contains a single SUMO called Smt3 and a conjugase Ubc9. This modification is made reversible using Ulp1 as a deconjugase (Rodriguez, Dargemont, and Hay 2001; Sampson, Wang, and Matunis 2001) Adapted from (Miura, Jin, and Hasegawa 2007).

Like many other post-translational modifications, only a small percentage of target protein is SUMOylated and is sufficient to carry out its specified function. The various effects that SUMOylation can grant to a protein range from change in sub-cellular localization, switch between active/inactive states of the target, to, making/breaking of protein-protein interactions. The new protein interactions can occur through SIM (**S**UMO **i**nteraction **m**otifs) on one protein and SUMOylation on the other protein (Zhu et al. 2008; Kerscher 2007). A number of individual proteins involved in different cellular processes, specifically transcription and DNA damage response are identified as SUMOylation targets (Dantuma and van Attikum 2016). Many have observed global increase in SUMOylation in response to different stresses (Bruderer et al. 2011; Rodriguez, Dargemont, and Hay 2001; Golebiowski et al. 2009; Matic et al. 2010; Augustine et al. 2016) .To identify these global changes in response to stress due to SUMOylation, the most commonly used approach is analyzing SUMO-specific proteomes by mass spectrometry. Till date, seven such SUMO proteomes in response to heat stress and proteasomal inhibition from yeast and mammalian systems are available. These mammalian and yeast SUMO proteomes also identify the precise SUMOylation site on the target protein. This is possible due to the use of a modified SUMO which leaves behind a very short peptide tag post trypsin digestion.

Importance of SUMOylation is also uncovered by knockdown studies. Ubiquitous knockdown of SUMO and ubc9 causes embryonic lethality in mammals as well as *Drosophila* defining critical role for SUMOylation in development. The first *Drosophila* SUMO proteome was published on early embryogenesis stage (Nie et al. 2009). The proteome was obtained by two-step pulldown of SUMOylated species and identifying these using LC/MS. This list comprises of 124 SUMOylation target proteins. Tissue specific knockdown of Ubc9, on the other hand, in *Drosophila* leads to systemic inflammation, loss of fat body integrity and defective haematopoesis (Paddibhatla et al. 2010). Flies with single copy of Ubc9 show melanotic tumors, indicators of over-proliferation of hemocytes in the *Drosophila* larvae (Fukuyama et al. 2013). Handu et al has shown defective regulation of both Toll and IMD pathway when SUMO is down-regulated in *Drosophila* derived, macrophage-like S2 cells (Handu et al. 2015). These results suggest significant contribution of SUMO in mounting robust immune response in flies. Even though multiple reports corroborate both Toll and IMD pathway being regulated by SUMOylation, only one protein from each pathway is experimentally shown to be SUMOylated. Of note, SUMOylation of Dorsal, NFκ-B factor part of Toll pathway, regulates antimicrobial peptide response (Bhaskar, Smith, and Courey 2002) while IRD5, key component of IMD pathway, is the only protein from the IMD pathway shown to be SUMOylated (Fukuyama et al. 2013). Our lab observed an increase in global SUMOylation in response to an immune challenge. To unravel these changes in SUMOylation status in response to immune challenge, we performed SUMO-specific proteome analysis of S2 cells from *Drosophila*. Through this analysis, we identified ~900 proteins that show enhanced SUMOylation in response to infection. Among these proteins, some are already known to be involved in immune response, some are putatively identified to be influencing immune response dynamics, and some generally show enhanced SUMOylation in response to stress stimuli (Handu et al. 2015). Including our list, there are only two *Drosophila* SUMO proteomes (Handu et al. 2015; Nie et al. 2009). Like mentioned earlier, mammalian SUMO proteomes also identify the precise site of SUMOylation due to presence of short SUMO tag left behind post trypsin digestion. In *Drosophila*, however, the SUMO tag left on the target protein post trypsin digestion is longer. This makes it technically challenging to identify the target protein and the site of SUMOylation using Mass spectrometry. Hence, the site of SUMOylation needs to be identified using site directed mutagenesis approach.

Some researchers have used this site directed mutagenesis approach and studied SUMOylation in *Drosophila* by focusing on a single protein target. Although there are number of studies identifying the SUMOylation substrate and which confer biological function to SUMOylation, there are merely fifteen proteins for which site of SUMOylation and function are validated. These are listed in the table below.

Table 2-1: List of proteins which are already shown to be SUMOylated in *Drosophila*. The function of SUMO modification are also described in the reference mentioned.

Protein	Site of SUMOylation	Effect	Reference
Bicoid	K308	Inhibition of activity	*(Liu and Ma 2012)*
Medea	K113, K159, K222	Restriction of signaling range of Dpp in embryo	*(Miles et al. 2008)*
STAT92E	K187	Increase in transcription activity	*(Grönholm et al. 2010)*
p53	K26, K302	SUMOylation important for activity	*(Mauri et al. 2008)*
SU(VAR)3-7	K839	required for heterochromatic function	*(Reo, Seum, and Spierer 2010)*
Sal and Salr	Sal: 517-933 fragment Salr: 803-1126 fragment	Sub-nuclear localization and stability	*(Sánchez et al. 2010)*
soxNeuro	K439	represses transcriptional activity	*(Savare, Bonneaud, and Girard 2005)*
USP	K20 and 5 others	maintains USP stability - imp for 20E activity	*(Wang, Wang, and Li 2014)*
RpL22e	1to175	localisation to nucleoplasm in meotic spermatocytes	*(Kearse et al. 2013)*
dorsal	K382	Regulation of activity	*(Bhaskar et al., 2002)*
IRD5	K152	Expression of attacinA	*(Fukuyama et al. 2013)*
EcRB1	K871	Isoform-specific activity	***(Justyna 2013)***
EcR A	K842	"	"
Ecr B2	K662	"	"

This lack of comprehensive data on fly SUMOylation makes it challenging to identify target protein with high confidence and then to identify the site of SUMOylation. Keeping this mind, the goal of this Chapter is to predict potentially SUMOylated species in the fly using homology with

confident sets of SUMOylated proteins from Mammals. The homology-based list is then combined with experimentally determined SUMOylated species in *Drosophila* to generate a current database of SUMOylated proteins in the fly, christened FlySUMObase. This database is then analyzed to identify patterns in global SUMOylation as well as to predict SUMO targets for experimental validation. I have generated such a database and analyzed the same to predict systemic roles for SUMO in the cellular processes. Based on my analysis, I also predict possible SUMOylated proteins in the animal – and these predicted proteins such as Pont, Nph2, Iswi, as also members of the Mutli-aminoacyltRNA Synthetase (MARS) Complex become potential targets for experimental studies in our laboratory.

2.4 RESULTS

2.4.1 Making list of potential SUMO targets.

This database, christened FlySUMObase was created by merging different fly and human SUMO proteome datasets as described below.

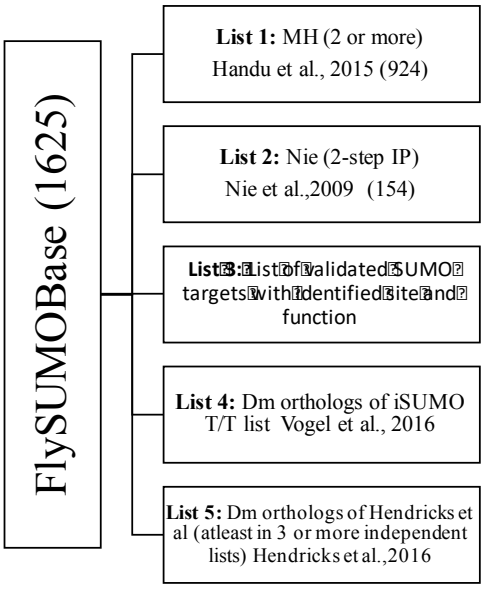

Figure 2-2: FlySUMObase, A confident dataset of proteins predicted to be SUMOylated in *Drosophila*. Schematics enlisting all the proteomes used to make the combined FlySUMOBase. List 1 and list 2 are experimental datasets obtained from *Drosophila* tissues. List 3 comprises of all the *Drosophila* proteins for whom, target site and biological significance of SUMOylation is known. List 4 includes *Drosophila* homologs of mammalian proteins which predicted to be SUMOylated with high significance. List 5 include *Drosophila* homologs of mammalian proteins which are shown to SUMOylated by at least 3 independent SUMO proteomes.

The details for generation of each list are described in the *Methodology* section.

2.4.2 Pont, NHP2 and Tsu emerge as high confidence SUMOylation targets.

All the lists used in FlySUMOBase have a different source. Despite this diversity, if a protein is part of multiple lists, the chances of it being SUMOylated are high. For this, it was necessary to analyze the overlap between the 5 lists used for generation of FLySUMOBase. The overlap analysis was done by generating Venn diagram using BioinforX software.

A

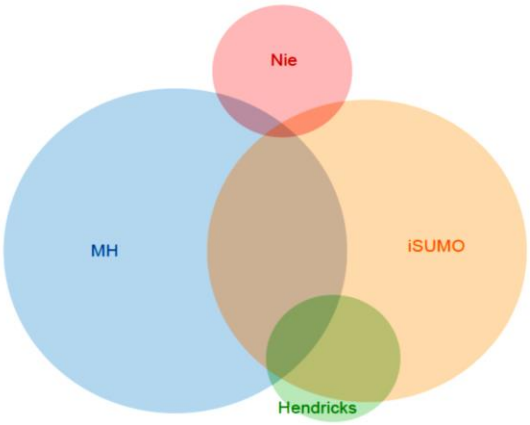

B

Set Name	Count No.
MH & iSUMO	264
MH & Hendricks	37
MH & Nie	14
iSUMO & Hendricks	118
iSUMO & Nie	12
Hendricks & Nie	3
MH, iSUMO & Hendricks	34
MH, iSUMO & Nie	7
MH, Hendricks & Nie	2
iSUMO, Hendricks & Nie	3
MH & iSUMO & Hendricks & Nie	2
Total	1612

Figure 2-3: Overlap analysis for datasets used in FlySUMOBase: (A) Scaled Venn diagram depicting the overlap between MH (Handu et al, part of 2 or more biological replicates), Nie (Nie et al list after 2-step IP), Hendricks (fly orthologs of proteins present in atleast 3 datasets) and iSUMO (fly orthologs of proteins from iSUMO prediction list). The maximum overlap is seen between MH and iSUMO. Only 2 or 3 proeins are common in 3 or more sets and most likely to be SUMOylated. **(B)** Table showing no. of genes common between different datasets.

This analysis showed very little overlap between datasets barring the exception of MH and iSUMO **(Figure 2.3)**. Only 2 proteins were identified by all the four datasets suggesting that the probability of these being SUMOylated is very high. These are NHP2 and Tsu. NHP2 functions in rRNA processing while Tsu (tsunagi) is part of the SPLICEOSOME COMPLEX C and important for many signaling pathways and thus fly development (Mohr, Dilan and Boswell, 2001). Interestingly, none of these proteins have been worked on as SUMOylation targets in *Drosophila*. On the other hand, out of the well-studied SUMOylated proteins in *Drosophila*, only two are present in this FLySUMOBase. These are Stat92E and Su(var)3-7. Thus, this list identifies many novel SUMOylation targets. One interesting example of this is Pont. This protein is identified to

be SUMOylated in all 7 mammalian SUMO proteomes (Hendriks and Vertegaal 2016) as well as our *Drosophila* immune SUMO proteome (Handu et al. 2015). The mammalian list identify K2 as the target site. This lysine is conserved in *Drosophila* and predicted by JASSA prediction tool as high confidence SUMOylation site.

2.4.3 Diverse biological processes enriched in FlySUMOBase.

Once the FlySUMObase was generated, I used the list for a systematic analysis of SUMOylated proteins in biological processes in *Drosophila*. I used blast2go® software (Götz et al. 2008) for enrichment analysis of biological processes in FLySUMOBase. This analysis, like many other SUMO proteomes, indicates that SUMOylated proteins are part of many different biological processes. Cell differentiation processes, biosynthesis and cellular transport processes are significantly enriched in FlySUMOBase along with others like the stress response and cellular component assembly **(Figure 2.4)**.

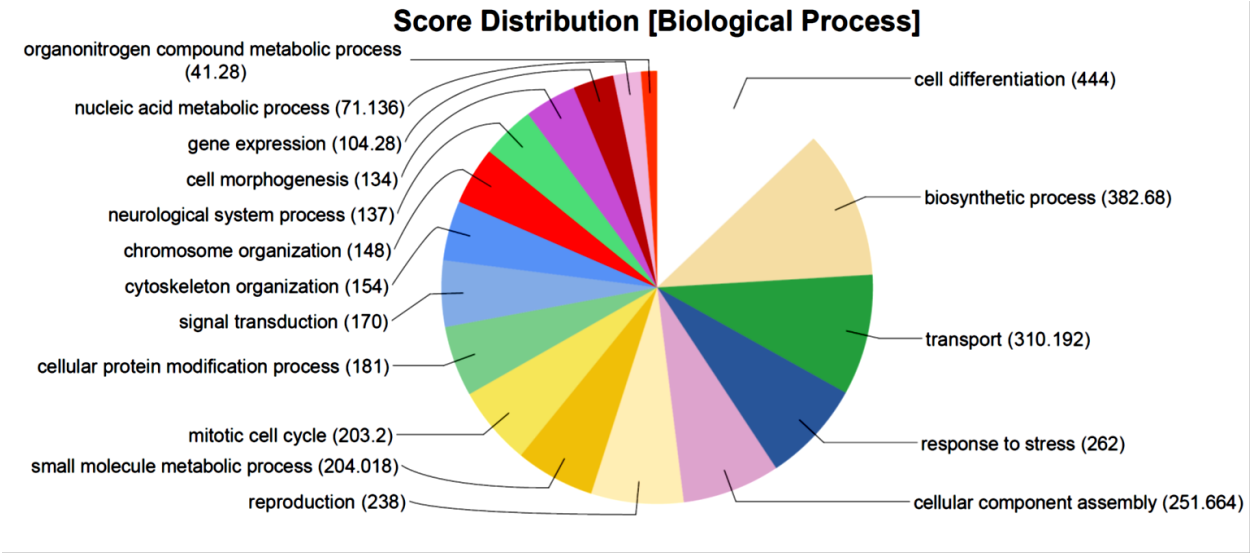

Figure 2-4: Analysis of 1625 proteins using GO ontology by blast2go®.(n=1625). Many processes are represented here with maximum targets functioning in cell differentiation, biosynthesis, stress response and transport. The protein modification components are also enriched as probable SUMOylation targets.

2.4.4 Proteins part of complexes are most likely to be SUMOylated.

It is a general notion, based on SUMO staining pattern, that most SUMOylated proteins are nuclear and very little SUMOylation is seen in cytoplasm. In light of this, the analysis done for these 1625 proteins for enrichment of cellular components, came as a surprise. This analysis, along with nuclear/chromosomal proteins, showed enrichment for proteins residing in the cytosol and the

mitochondria. This suggests that even if many nuclear proteins are SUMOylated, proteins present in other cellular compartments could also be SUMOylated.

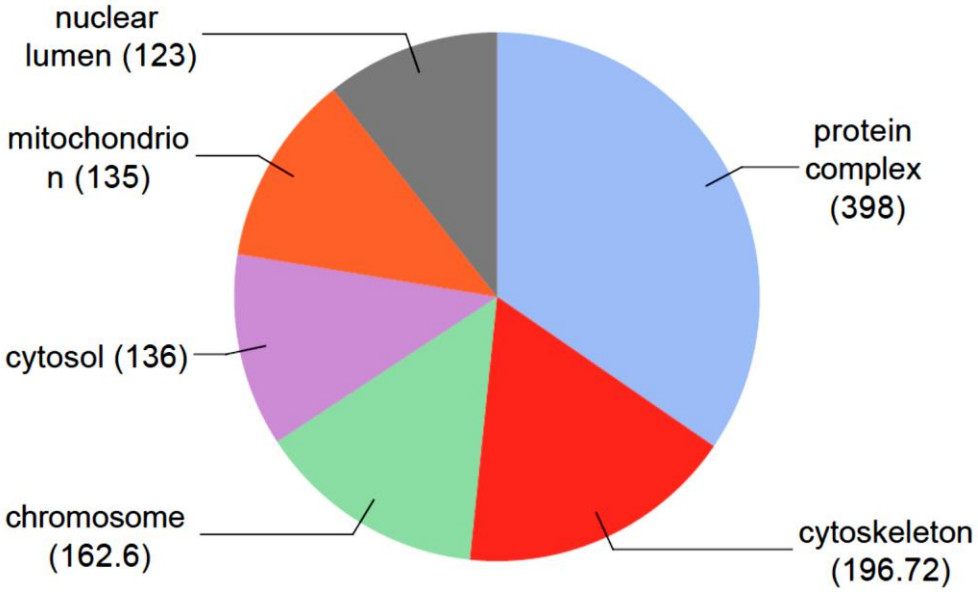

Figure 2-5: Analysis of FlySUMOBase using GO by blast2go to identify cellular components representing these targets (n=1625). Interestingly, the most enriched class was of protein complexes. Surprisingly, proteins from cytosol and mitochondria are also enriched as SUMOylation targets.

Another interesting feature of this analysis is the maximum enrichment seen in protein complex class **(Figure 2.5)**. As suggested by Handu et al., many protein complexes are likely regulated by dynamic SUMOylation (Handu et al. 2015). This could be due to SUMO-SIM interactions between different proteins of a given complex or through steric hindrance due to covalent modification by SUMO.

2.4.5. SUMOylation may regulate stability of certain protein classes.

Further analysis using PANTHER showed very significant enrichment of many protein classes. It also showed the down regulation of certain specific protein classes **(Figure 2.6).**

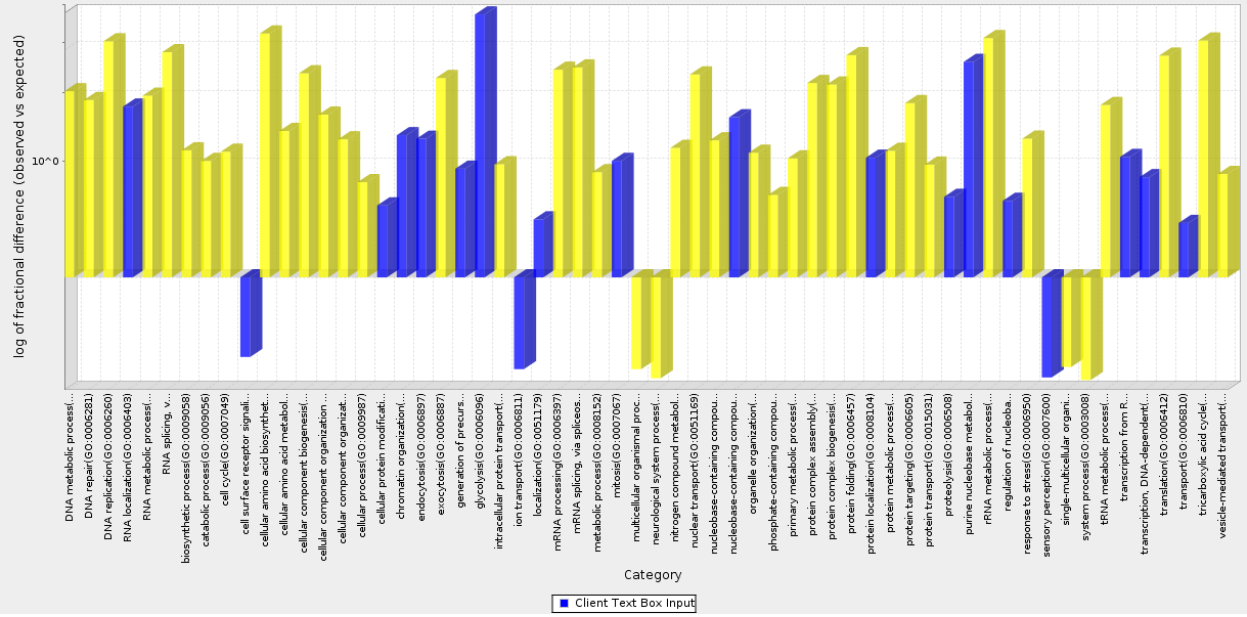

Figure 2-6: Enrichment analysis of FlySUMOBase for protein classes. Fold enrichment of proteins represented per biological process in FLySUMOBase as compared to reference database using PANTHER. Yellow bars represent process with significance $p<0.01$. Most processes show enrichment while some categories show fewer genes than expected.

This significant decrease in enrichment could suggest degradation of proteins in this class in response to SUMOylation or transcriptional regulation of these genes through SUMOylation. Neurological system processes class showed significant reduction suggesting some significant and unusual role for SUMOylation in neuronal regulation.

2.4.6. MARS complex dynamics is likely to be regulated by SUMO modification. FlySUMOBase was further analyzed using KEGG Pathway analysis to look for pathways that are regulated by SUMOylation. Proteins involved in RNA transport and carbon metabolism showed enrichment in KEGG pathway analysis. Proteins part of Spiceosome complex and Aminoacyl-tRNA biosynthesis are also enriched **(Figure2.7).** Many of the Aminoacyl-tRNA biosynthesis enzymes are part of complex called Multi-aminoacyl-tRNA synthetase complex (MARS). MARS complex includes 9 tRNA synthetases and 3 non-synthetase components. Many of the components of the MARS complex have been identified in our immune SUMO proteome and also comes up in the list of most likely SUMOylated proteins predicted by iSUMO.

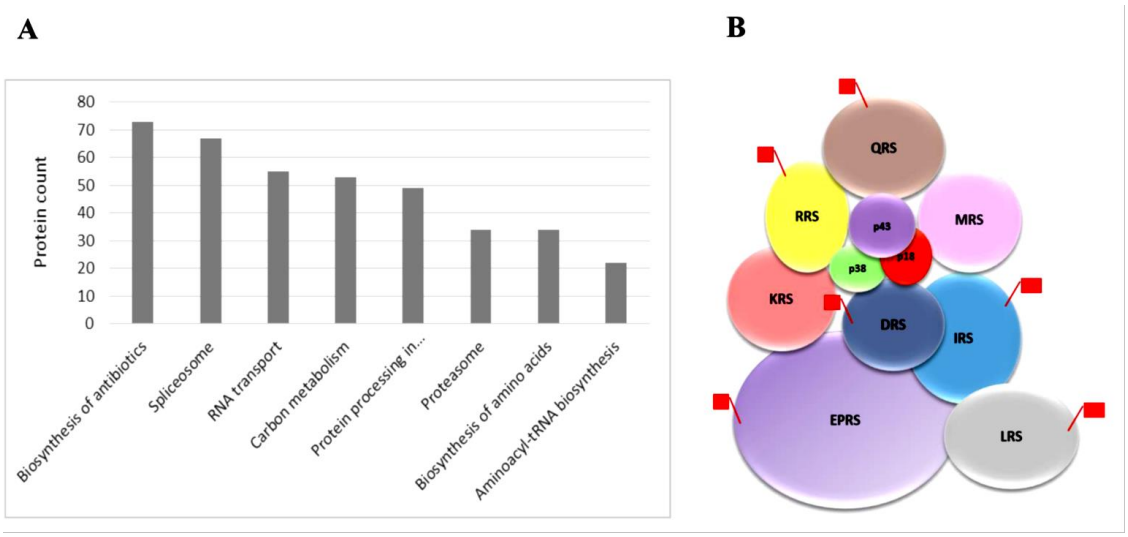

Figure 2-7: KEGG enrichment analysis of FlySUMOBase. KEGG module of DAVID identified number of proteins that show significant enrichment after normalizing to reference *Drosophila* dataset. The program calculates p-values and the proceses are arranged based on increasing p-value from felt to right. (n=1625). FlySUMOBase shows enrichment of protein complexes like SPLICEOSOME and MARS complex.

A couple of Aminoacyl-tRNA synthetases have also been identified by the 2-step pull-down done by Nie and her colleagues (Nie et al., 2009). Interestingly, the mammalian comprehensive list of SUMOylated proteins analyzed by Hendriks and his group picks up only one Aminoacyl- tRNA synthetase. This suggests that either the mammalian homologs are SUMOylated only under very specific conditions in vivo and could not be identified in cell culture studies done till date or are uniquely SUMOylated in the fly.

2.5 DISCUSSION

In theory, SUMOylated proteins can be identified by using Mass Spectrometry to identify any peptide fragment attached to the C-terminal tail of SUMO. This technique is used to identify SUMOylated proteins along with site of SUMOylation from the mammalian systems. In *Drosophila*, however, this is not feasible with current technology as the size of the SUMO+substrate fragments is too large to be measured accurately. Efforts have been made to decrease this fragment size by mutating the SUMO protein, but with little success as the mutations dramatically reduced the conjugation ability of SUMO (Minghua Nie, Unpublished). Thus, till technological changes make this problem go away, we have to identify SUMOylated targets using cruder techniques that involve biochemical purification of SUMOylated proteins and manual

identification of target site using site-directed mutagenesis of predicted lysines. Biochemical purification is usually done under denaturing conditions using 6XHis or biotin tags that allow researchers to separate SUMO-interacting proteins from SUMO-conjugated proteins. Even after using this methodology, target lists have problems of false positives and false negatives.

In this chapter I have used four current databases and generated a collated *Drosophila*-specific SUMO database. This database provides a consolidated list of proteins in *Drosophila* that may be SUMOylated. The database is arranged based on confidence score (CS) given to the predicted target. Prediction score is based on the number and identity of the lists the target belongs to. For instance, targets which are experimentally verified is a perfect 10, while proteins which are predicted by all 4 lists is assigned a CS 7. The targets where mammalian homolog is identified as confirmed SUMOylation target gets a higher CS as compared to others. Proteins which are present in Hendricks –fly orthologs (HN), Nie et al (Nie) and iSUMO-fly orthologs (S) have a higher CS while proteins which are part of MH and iSUMO have lower CS.

Table 2-2: List of top 20 proteins predicted by my analysis as high-probability targets in *Drosophila*. The list is arranged with descending order of confidence score (CS). Cs is given based on number of lists the protein is present in and which lists identify it as SUMOylation target. If the protein is present in all 4 lists that comprise FlySUMOBase, it get a higher CS as compared to protein present in only 2 lists. The table also consists of SUMOylation sites as predicted by Jassa for a given target. If the SUMOylation site for mammalian homolog of predicted target is identified, it is also enlisted in this table. The complete list is attached as Appendix.

Protein	# of Databases	CS[1]	PSS[2]	Sm[3]
NHP2	All 4 lists	7	K5,25,33,150	K5
tsu	All 4 lists	7	K159	K27
Top1	HN, N , S	6	K212,269,301,368,373,385,616,668	K153,117,148,164,336
RnrS	MH, N, S	5	K289,369	
Gdh	MH, N, S	5	NO site	
Tpp II	MH, N, S	5	K105,917,1207	
Moe	MH, N, S	5	K134	
RpS10b	MH, N, S	5	NO site	
pont	MH, HN, S	4	K2 (low PS)	K2
Mcm3	MH, HN, S	4	NO site	K450.462
Gnf1	MH, HN, S	4	K146,183,320,327,395	K568,498
Sym	MH, HN, S	4	K97,627,1122	K361, 483
Nup358	MH, HN, S	4	K889,1086,1745,2380,2582,2640	K1414,2571,2531, 2592, 1605, 2181, 2594,

Hop	MH, HN, S	4	K839	K123, 210,
Spt5	MH, HN, S	4	K452,612,1034	K143, 453
Uba2	MH, HN, S	4	K570	K236
CG2807	MH, HN, S	4	K302,532,843	K413, 400
lwr	MH, HN, S	4	NO site	K49
Rrp6	MH, HN, S	4	K711,743,769	K583
Iswi	MH, HN, S	4	K262,355,359,564,689,865	K944

When FlySUMOBase was analyzed with a focus of immunity, components of core immune signaling pathways along with other proteins having confirmed roles in immunity were identified. These are summarized in the table below:

Table 2-3: Predicted immune specific SUMO targets: Analysis of FlySUMOBase with special focus on immunity identified around 40 proteins with confirmed roles in immunity as potential targets for SUMOylation. The ones which are already validated are marked in bold.

Protein Class	Proteins	Average Confidence score
Toll pathway	**Dorsal**	10
JAK/STAT	**STAT92E**,	10
tRNA synthetases	**EPRS**, RRS, KRS, QRS, IRS, DRS, LRS, NRS, GRS, TRS, WRS, VRS, YRS	5
IMD pathway	IMD, **IRD5**, Caspar	5
JNK pathway	RI, Basket, **Jra, Kayak**, Rac1, Cpa, Cdc42, Ebi	5
Pvr/Ras/MAPK pathway	Pvr, Pvf2, Rolled, p38b	5
Phagocytosis	Colt, Psidin, TRAM, Hrs, deltaCOP. EcR, Flr, Mtr	5

2.6 CONCLUSION

In *Drosophila*, there are merely fifteen instances where a target protein along with the site of SUMOylation is identified and its functional relevance is known. Efforts to identify SUMOylation targets in *Drosophila* were done in our lab using S2 cells (Handu et al. 2015) and using developing embryo (Nie et al. 2009)**.** These two large scale proteomes, done with very different tissue types, are not enough to identify SUMOylation targets with high reliability in *Drosophila*. Hence, I have made efforts to analyse known mammalian SUMO proteomes wih respect to *Drosophila* by using fly orthologs of highly predictable SUMO targets from these published proteomes. This analysis

also identifies approximately 250 proteins as potential SUMOylation targets. This analysis identifies cell differentiation, cell division, stress response as probable biological process to hunt for a target and its role of SUMOylation. Also individual proteins such as Pont, Iswi, Nhp2 are identified as potential targets for SUMOylation in *Drosophila*. This list also findsSpliceosome and MARS complex as likely candidates to be regulated by SUMO modification. SUMOylation of the MARS complex will be further discussed in the next chapter.

2.7 METHODOLOGY

Generation of lists for FlySUMOBase: For understanding biological significance of SUMOylation, it is essential to identify the target protein along with the precise site of SUMOylation. In *Drosophila*, there is very limited understanding of SUMOylation based on two SUMO-specific proteomes and handful of individual targets. To help identify proteins that are potential SUMOylation targets in *Drosophila*, FlySUMOBase is needed. Following are the lists that I have used in creation of this database.

List 1 (MH (2 or more)): In order to understand role of SUMO modification in response to infection in *Drosophila*, we did pull-down of SUMOylated proteins post infection in *Drosophila* S2 cells. Proteins identified from this assay were further analyzed using LC/MS-MS. This was done in three biological replicates. I have chosen proteins which were present in at least two of the three replicates. This list consists of 924 unique proteins (Handu et al. 2015).

List 2 (Nie (2-step IP)): Minghua Nie et al have investigated proteins that are SUMOylated in early embryonic development stages of *Drosophila* using dual-tagged SUMO (smt3). They have performed a pull-down assay of SUMOylated proteins using stepwise affinity purification. In the first step, proteins were separated using a denaturing Ni-NTA column pulling down his-tagged protein. This was followed by purification using anti-FLAG IP. These two-step-purified proteins were identified by LC/MS-MS. These proteins include 154 unique proteins (Nie et al. 2009).

List 3: As mentioned earlier, in *Drosophila*, only for 15 proteins, the site of SUMOylation and associated function is identified. List 3 comprises of these 15 proteins. (Table2.1)

List 4 (iSUMO – fly orthologs): Vogel and her colleagues have extensively analyzed available human and yeast SUMO-specific proteomes. They have shown that most large scale SUMO-specific proteomes contain very few proteins that overlap with lists of bioinformatically predicted

SUMO targets. This suggests that most bioinformatically predicted proteins are not direct SUMO targets (false positives) or are SUMOyalted in context different from the tested scenarios. Further, by sequence-based prediction alone, the chance of identifying correct SUMO targets is only ~50% (Yao et al. 2017). Therefore, Vogel and colleagues have integrated other important parameters, such as protein–protein interaction, protein–nucleic acid interaction, and protein function. This has allowed them to predict 5-times more SUMO target proteins than existing tools could predict, while maintaining the false positive rate at 5%. From this list of most probable SUMO targets, I have selected those with an iSUMO score of ≥0.188. I further identified *Drosophila* orthologs of these proteins using DIOPT, a web-based tool. I shortlisted proteins with DIOPT score of ≥10 to ensure that they were true orthologs with high sequence similarity. This list, henceforth referred to as iSUMO-fly orthologs, was used for further analysis.

Flow Chart 1: Drosophila orthologs of most likely SUMOylated proteins predicted using iSUMO

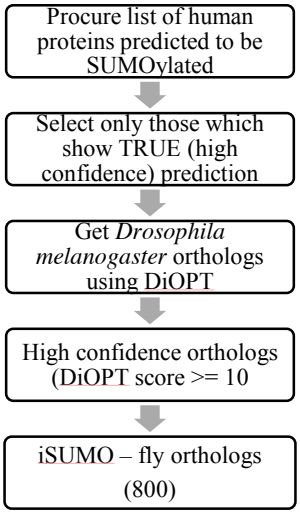

List 5 (Hendricks et al – fly orthologs): There are approximately 10 large-scale mammalian SUMO-specific proteome studies available to date, which have analyzed SUMO-specific proteomes in different stress conditions. These studies identify not only the proteins SUMOylated under specific conditions but also the sites at which they are SUMOylated. Unfortunately, these studies were performed at different times and with different analysis methods. Thus, they fail to provide a comprehensive overview of commonly SUMOlyated proteins and their most probable SUMOlyation sites. Hendricks et al have attempted to address this issue by procuring raw data from these studies and analyzing those entirely using advanced analysis tools. Through this

analysis, they have enlisted proteins that appear as SUMO targets in most studies (Hendriks and Vertegaal 2016). I have chosen a subset of proteins from the list made by Hendricks et al by keeping the following criterion in mind: each protein must be present in at least three independent lists post reanalysis. I have further identified *Drosophila* orthologs of these target proteins using DIOPT. I have used a cut-off DIOPT score of 10 to ensure that the identified ortholog is as true as possible. Finally, I have shortlisted 144 proteins from *Drosophila* whose mammalian orthologs are very likely to be SUMOylated. This list is attached in Appendix.

Flow Chart 2: Drosophila orthologs of SUMOylated proteins from Hendricks et al analysis.

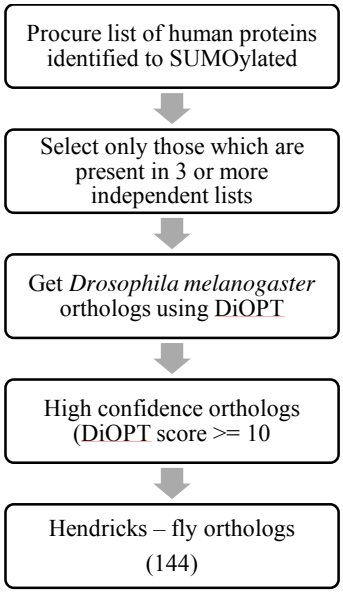

Identifying Drosophila homologs: The list of SUMOylated proteins from mammals was converted to UNIPROT IDs. These were used as input list in DIOPT (DRSC Integrative Ortholog Prediction Tool) *(Hu et al. 2011)*. The orhologs are given DIOPT score based on the sequence alignment analysis. I chose the ortholog which had the highest DIOPT score for a given protein. I did not consider the proteins whose orthologs had DIOPT score of 9 0r less.

Analysis of Database: FlySUMOBase gives a list of 1625 proteins that are potential targets for SUMOylation. Detailed analysis of this database is necessary to identify cellular components, biological process that are most enriched in FlySUMOBase. Here are various bioinformatical tools I have used for the enrichment analysis.

GO Ontology: FlySUMOBase were subjected to GO ontology using *Drosophila melanogaster* database as the reference list (Huang da, Sherman, and Lempicki 2009a, 2009b) and blast2go®

software. *p*-value was generated by Fisher Exact test along with robust False Discovery Rate (FDR) correction for multiple testing (Götz et al. 2008).

PANTHER analysis: PANTHER classification system 12.0 was used to compare FlySUMOBase with the reference *Drosophila* database. The Statistical enrichment test used for calculation of p-value for each enrichment category uses binomial test with Bonferroni correction (Mi et al. 2017). http://pantherdb.org/webservices/go/overrep.jsp

VENN diagram analysis: I used List1, 2, 4 and 5 for generating the VENN diagram using BioinfoX free online tool for data analysis. This tool generates a scaled VENN diagram based on the different number of proteins in each list. http://apps.bioinforx.com/bxaf7c/app/venn/app_overlap.php

2.8 CONTRIBUTIONS

In collaboration with MS Madhusudhan, we plan to carry out a systematic prediction of SUMOylated proteins in the fly. The data and analysis in the chapter has been done independently by myself and a similar but more thorough prediction and analysis, using three dimensional structural data is ongoing with Dr. Madhusudhan's lab.

2.9 SUPPLEMENTARY TABLES

These tables are placed in the appendix of the thesis as described below. Soft copies of the XLS files are available at the Ratnaparkhi Lab Web-Page (http://www.iiserpune.ac.in/~girish).

BIBLIOGRAPHY

Augustine, Robert C., Samuel L. York, Thérèse C. Rytz, and Richard D. Vierstra. 2016. 'Defining the SUMO System in Maize: SUMOylation Is Up-Regulated during Endosperm Development and Rapidly Induced by Stress', *Plant Physiology*, 171: 2191-210.

Bhaskar, Vinay, Matthew Smith, and Albert J Courey. 2002. 'Conjugation of Smt3 to Dorsal May Potentiate the *Drosophila* Immune Response', *Mol.and Cellular biology*, 22: 492-504.

Bruderer, Roland, Michael H. Tatham, Anna Plechanovova, Ivan Matic, Amit K. Garg, and Ronald T. Hay. 2011. 'Purification and identification of endogenous polySUMO conjugates', *EMBO Rep*, 12: 142-48.

Dantuma, N. P., and H. van Attikum. 2016. 'Spatiotemporal regulation of posttranslational modifications in the DNA damage response', *Embo j*, 35: 6-23.

Fukuyama, Hidehiro, Yann Verdier, Yongsheng Guan, Chieko Makino-Okamura, Victoria Shilova, Xi Liu, Elie Maksoud, Jun Matsubayashi, Iman Haddad, Kerstin Spirohn, Kenichiro Ono, Charles Hetru, Jean Rossier, Trey Ideker, Michael Boutros, Joëlle Vinh, and Jules A Hoffmann. 2013. 'Landscape of protein–protein interactions in *Drosophila* immune deficiency signaling during bacterial challenge', *Proceedings of the National Academy of Sciences* 110 10717-22.

Golebiowski, Filip, Ivan Matic, Michael H. Tatham, Christian Cole, Yili Yin, Akihiro Nakamura, Jürgen Cox, Geoffrey J. Barton, Matthias Mann, and Ronald T. Hay. 2009. 'System-Wide Changes to SUMO Modifications in Response to Heat Shock', *Science Signaling*, 2: ra24-ra24.

Götz, Stefan, Juan Miguel García-Gómez, Javier Terol, Tim D. Williams, Shivashankar H. Nagaraj, María José Nueda, Montserrat Robles, Manuel Talón, Joaquín Dopazo, and Ana Conesa. 2008. 'High-throughput functional annotation and data mining with the Blast2GO suite', *Nucleic Acids Research*, 36: 3420-35.

Grönholm, Juha, Daniela Ungureanu, Sari Vanhatupa, and Mika Rämet. 2010. 'Sumoylation of *Drosophila* Transcription Factor STAT92E', *J. of innate immunity*, 2: 618-24.

Handu, Mithila, Bhagyashree Kaduskar, Ramya Ravindranathan, Amarendranath Soory, Ritika Giri, Vijay Barathi Elango, Harsha Gowda, and Girish S Ratnaparkhi. 2015. 'SUMO Enriched Proteome for *Drosophila* Innate Immune Response.', *G3 (Bethesda, Md.)*, 91.

Hendriks, Ivo A, and Alfred C O Vertegaal. 2016. 'A comprehensive compilation of SUMO proteomics', *Nature Publishing Group*.

Hu, Yanhui, Ian Flockhart, Arunachalam Vinayagam, Clemens Bergwitz, Bonnie Berger, Norbert Perrimon, and Stephanie E Mohr. 2011. 'An integrative approach to ortholog prediction for disease-focused and other functional studies'.

Huang da, W., B. T. Sherman, and R. A. Lempicki. 2009a. 'Bioinformatics enrichment tools: paths toward the comprehensive functional analysis of large gene lists', *Nucleic Acids Res*, 37: 1-13.

———. 2009b. 'Systematic and integrative analysis of large gene lists using DAVID bioinformatics resources', *Nat Protoc*, 4: 44-57.

Jox, Theresa, Melanie K Buxa, Dorte Bohla, Ikram Ullah, Igor Mačinković, and Alexander Brehm. 2017. '*Drosophila* CP190 - and dCTCF - mediated enhancer blocking is augmented by SUMOylation', *Epigenetics & Chromatin*: 1-14.

Justyna, Seliga, Katarzyna, Bielska, El ˙zbieta Wieczorek, Marek, Orłowski, Rainer, Niedenthal, Andrzej O˙, Zyhar. 2013. 'Multidomain sumoylation of the ecdysone receptor (EcR) from *Drosophila* melanogaster', *Journal of Steroid Biochemistry and Molecular Biology*: 1-12.

Kearse, Michael G, Jill A Ireland, Smrithi M Prem, Alex S Chen, and Vassie C Ware. 2013. 'RpL22e , but not RpL22e-like-PA , is SUMOylated and localizes to the nucleoplasm of *Drosophila* meiotic spermatocytes © 2013 Landes Bioscience . Do not distribute © 2013 Landes Bioscience . Do not distribute': 241-58.

Kerscher, O. 2007. 'SUMO junction-what's your function? New insights through SUMO-interacting motifs', *EMBO Rep*, 8: 550-5.

Liu, Junbo, and Jun Ma. 2012. '*Drosophila* Bicoid is a substrate of sumoylation and its activator function is subject to inhibition by this post-translational modification', *FEBS Letters*, 586: 1719-23.

Matic, I., J. Schimmel, I. A. Hendriks, M. A. van Santen, F. van de Rijke, H. van Dam, F. Gnad, M. Mann, and A. C. Vertegaal. 2010. 'Site-specific identification of SUMO-2 targets in cells reveals an inverted SUMOylation motif and a hydrophobic cluster SUMOylation motif', *Mol Cell*, 39: 641-52.

Mauri, Federico, Laura M. McNamee, Andrea Lunardi, Fulvio Chiacchiera, Giannino Del Sal, Michael H. Brodsky, and Licio Collavin. 2008. 'Modification of *Drosophila* p53 by SUMO modulates its transactivation and pro-apoptotic functions', *Journal of Biological Chemistry*, 283: 20848-56.

Mi, Huaiyu, Xiaosong Huang, Anushya Muruganujan, Haiming Tang, Caitlin Mills, Diane Kang, and Paul D. Thomas. 2017. 'PANTHER version 11: expanded annotation data from Gene Ontology and Reactome pathways, and data analysis tool enhancements', *Nucleic Acids Research*, 45: D183-D89.

Miles, Wayne O, Ellis Jaffray, Susan G Campbell, Shugaku Takeda, Laura J Bayston, Sanjay P Basu, Mingfa Li, Laurel A Raftery, Mark P Ashe, Ronald T Hay, and Hilary L Ashe. 2008. 'Medea SUMOylation restricts the signaling range of the Dpp morphogen in the *Drosophila* embryo': 2578-90.

Miura, Kenji, Jing Bo Jin, and Paul M. Hasegawa. 2007. 'Sumoylation, a post-translational regulatory process in plants', *Current Opinion in Plant Biology*, 10: 495-502.

Nie, Minghua, Yongming Xie, Joseph a Loo, and Albert J Courey. 2009. 'Genetic and proteomic evidence for roles of *Drosophila* SUMO in cell cycle control, Ras signaling, and early pattern formation.', *PloS one*, 4: e5905.

Paddibhatla, Indira, Mark J. Lee, Marta E. Kalamarz, Roberto Ferrarese, and Shubha Govind. 2010. 'Role for Sumoylation in Systemic Inflammation and Immune Homeostasis in *Drosophila* Larvae', *PLoS Pathogens*, 6: e1001234.

Reo, Emanuela, Carole Seum, and Pierre Spierer. 2010. 'Sumoylation of *Drosophila* SU (VAR) 3-7 is required for its heterochromatic function', 38: 3-7.

Rodriguez, M. S., C. Dargemont, and R. T. Hay. 2001. 'SUMO-1 conjugation in vivo requires both a consensus modification motif and nuclear targeting', *J Biol Chem*, 276: 12654-9.

Sampson, D. A., M. Wang, and M. J. Matunis. 2001. 'The small ubiquitin-like modifier-1 (SUMO-1) consensus sequence mediates Ubc9 binding and is essential for SUMO-1 modification', *J Biol Chem*, 276: 21664-9.

Sánchez, Jonatan, Ana Talamillo, Fernando Lopitz-Otsoa, Coralia Pérez, Roland Hjerpe, James D Sutherland, Leire Herboso, Manuel S Rodríguez, and Rosa Barrio. 2010. 'Sumoylation modulates the activity of Spalt-like proteins during wing development in *Drosophila*.', *The Journal of biological chemistry*, 285: 25841-9.

Savare, Jean, Nathalie Bonneaud, and Franck Girard. 2005. 'SUMO Represses Transcriptional Activity of the *Drosophila* SoxNeuro and Human Sox3 Central Nervous System – specific Transcription Factors □', 16: 2660-69.

Wang, Jiawan, Sheng Wang, and Sheng Li. 2014. 'Sumoylation modulates 20-hydroxyecdysone signaling by maintaining USP protein levels in *Drosophila*', *Insect Biochemistry and Molecular Biology*, 54: 80-88.

Yao, Xiaotong, Shuvadeep Maity, Shashank Gandhi, Marcin Imielenski, and Christine Vogel. 2017. 'iSUMO - integrative prediction of functionally relevant SUMOylation events', *bioRxiv*.

Zhang, Jie, Yajuan Liu, Kai Jiang, and Jianhang Jia. 2017. 'SUMO regulates the activity of Smoothened and Costal-2 in *Drosophila* Hedgehog signaling', *Nature Publishing Group*, 7: 1-14.

Zhu, Jianmei, Shanshan Zhu, Catherine M. Guzzo, Nathan A. Ellis, Ki Sa Sung, Cheol Yong Choi, and Michael J. Matunis. 2008. 'Small Ubiquitin-related Modifier (SUMO) Binding Determines Substrate Recognition and Paralog-selective SUMO Modification', *Journal of Biological Chemistry*, 283: 29405-15.

Chapter 3

The Multiaminoactyl tRNA Synthetase (MARS) complex as a target for SUMO modification

3.1 SUMMARY

In Chapter 2, I have identified tRNA synthetases as confident targets for SUMO modification. In this chapter, I have cloned and expressed a number of tRNA Synthetases in order to validate their SUMOylation status using *in-vitro* SUMOylation. My findings confirm that members of the MARS Complex are SUMOylated and they present attractive targets for elucidating biological function of SUMO modification. EPRS and RRS are chosen as useful substrates to confirm SUMOylation in flies. With this goal in mind, transgenic animals expressing tagged versions of EPRS and RRS have been generated and are being tested for *in-vivo* SUMO modification.

3.2. ABBREVIATIONS

AATS: aminoacyl tRNA synthetase ; GAIT: γ-activated inhibition of translation; AIMP: aminoacyl tRNA synthetase- interacting multifunctional protein; MARS: multi-aminoacyl tRNA synthetase; IPTG: isopropyl β-D-1-thiogalactopyranoside; GST: glutathione – S-transferase

3.3 INTRODUCTION

Amino-acyl tRNA synthetases (AATS) are a conserved set of enzymes that charge a specific amino acid with its cognate tRNA, a role vital for correct translation of the genetic code. AATS are therefore critical for the survival of cells and animals null for any one member do not survive. A cognate tRNA synthetase exists for each and every amino-acid **(Figure 3.1).** The tRNA synthetases recognize specific pattern of nucleotides on cognate tRNAs **(Figure 3.2)**. Such pattern of nucleotides is termed as 'second genetic code' as the pairing of cognate tRNA and its specific amino acid by the synthetase is essential for correct translation of the genetic code (Martinis et al. 1999; Lee et al. 2004a).

Even though all the tRNA synthetases use very similar substrates, they differ significantly in size and shape. A tRNA synthetase could be as small as 49KDa for DRS or as big as113KDa for IRS in *Drosophila*. They also have acquired many additional domains in the course of evolution. A comparison between prokaryotic and eukaryotic AATS indicates that these domains probably add to the functional repertoire of AATS as the core charging domains are retained.

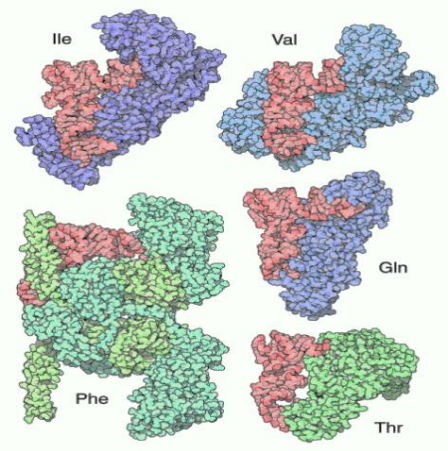

Figure 3-1: Structures depicting different ways in which Amino-acyl tRNA synthetases bind their cognate tRNA. Structures of amino acyl tRNA synthetases (green/blue) along with their cognate tRNA (pink). The shapes and sizes of individual AATs differ significantly, in spite of the common function of tRNA charging. The structures are downloaded from the RSCB protein data bank.

Over two decades ago, Pollard and group suggested existence of "non-canonical", i.e., more than just charging, function for tRNA synthetases. While working with temperature sensitive mutants of LeuRS, they saw rapid reduction in polypeptide chain initiation due to increased eIF2 phosphorylation. This phosphorylation of eIF-2 was readily rescued by LeuRS gain-of-function mutant but could not be rescued by charging the Leu-tRNA in vivo.

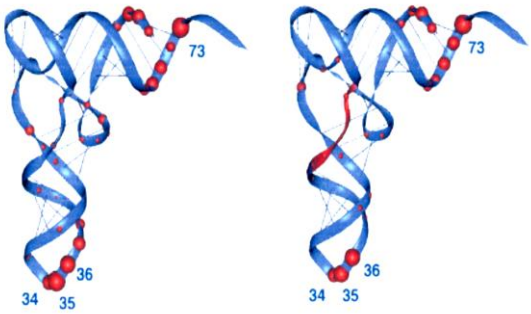

Figure 3-2: "Second genetic code". Specific residues on the tRNA help the specific AATS to recognize the correct pair of tRNA and amino acid. These nucleotides consist of the anticodon loop but also involves other regions of specific tRNAs. Regions of two different tRNAs recognised by different Amino-acyl tRNA synthetases are highlighted in red. Reproduced from (Martinis et al. 1999; Lee et al. 2004a)

This demonstrated that the charging activity by itself is not involved (Clemens et al. 1987; Pollard, Galpine, and Clemens 1989). This gave a new dimension to tRNA synthetase research, leading to mounting evidence regarding moonlighting effects by many other tRNA synthetases as summarized in the table below:

Table 3-1: AATs and their associated Moonlighting functions. Different tRNA synthetases are involved in variety of signalling pathways affecting immune response, angiogenesis and cell survival.

AATs	Function	*References*
TyrRS	Cleaved products post apoptosis act as cytokines, regulates angiogenesis, Mitochondrial splicing and neuronal degeneration.	*(Nangle et al. 2007; Kim, You, and Hwang 2011; Dyck and Lambert 1968)*
AsnRS	FGF2 induced survival in osteoblasts.	*(Park et al. 2009)*
TrpRS	Truncated amino-terminal acts as cytokine, suppresses angiogenesis. Elevated levels in salivary glands during development and immune stress	*(Kim, You, and Hwang 2011)*
GlycylRS	Mutants directly related to Charcot-Marie-tooth (CMT), a heritable peripheral neuronal disease	*(Antonellis et al. 2003; Seburn et al. 2006; Dyck and Lambert 1968; Nangle et al. 2007)*
SerRS (Zebrafish)	Angiogenesis	*(Fukui, Hanaoka, and Kawahara 2009; Herzog et al. 2009)*
MRS, YRS, LRS, IRS,	Nascent tRNA proofreading in nucleus followed by cytoplasmic export	*(Lund and Dahlberg 1998)*
EPRS	Translational suppression on INF-γ signalling in humans	*(Jia, Arif, Ray, and Fox 2008; Mukhopadhyay et al. 2009; Arif et al. 2010)*
MRS	rRNA synthetase tumor suppression and translational regulation	*(Ko et al. 2000; Kwon et al. 2011)*

It is interesting to note that 9 of the 19 tRNA synthetases, namely RRS, MRS, LRS, IRS, DRS, QRS, EPRS, KRS, form a Multi Amino-acyl tRNA synthetase (MARS) complex. This complex also consists of 3 non-tRNA synthetase proteins, p43 (AIMP I), p38 (AIMP II) and p18 (AIMP III). The composition of MARS is conserved through *Drosophila* to mammals, the only deviation being the complex seen in *C. elegans*.**(Figure 3.3)** (Kerjan, Cerini, and Mirande 1994).

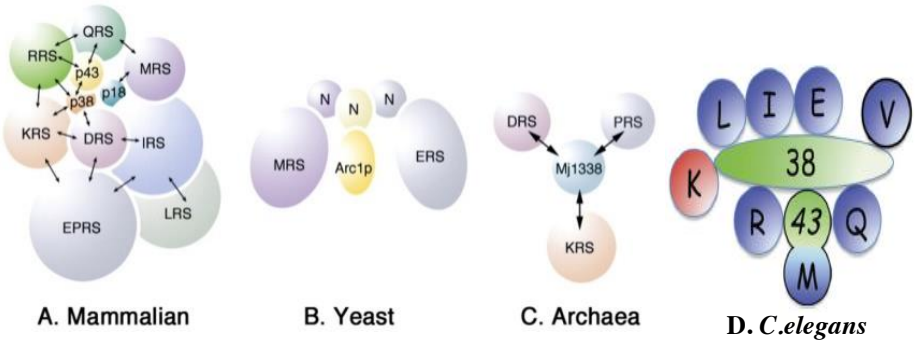

Figure 3-3: The comparative composition of MARS complex with its AIMP (Aminoacyl tRNA synthetase- interacting multifunctional protein) components. The complex in A is conserved from *Drosophila* to mammals with a known exception in *C.elegans*. *C.elegans* do not contain a fused EPRS or the auxiliary protein p18 but still has the other components of the MARS complex conserved. Figure modified from (Lee et al. 2004b; Havrylenko et al. 2011)

In flies and mammals, the Glutamyl-Prolyl tRNA synthetase (EPRS) is a bifunctional enzyme with N-terminal Glutamyl synthetase domain, C-terminal Prolyl tRNA synthetase domain brought together with connecting WHEP repeats. As an exception, *C. elegans* have two independent Glutamyl and Prolyl tRNA synthetases although a modified MARS complex exists in *C. elegans*. Regulation of the complex dynamics and availability of individual components for specific function had been puzzle untill post-translation modofication by phosophorylation for some of the components was identified. For example, Phosphorylation of Glutamyl-Prolyl tRNA synthetase (EPRS) on INF-γ signalling leads formation of GAIT (γ activated inhibition of translation) complex by release of EPRS from the MARS complex and interaction with NSAP1. The GAIT complex contains EPRS, ribosomal protein L13, NSAP1 and GAPDH. This complex then binds to different mRNAs involved in Interferon response through phosphorylated EPRS WHEP domain and inhibit translation **(Figure 3.4)** (Jia, Arif, Ray, Fox, et al. 2008; Mukhopadhyay et al. 2009; Arif et al. 2011)

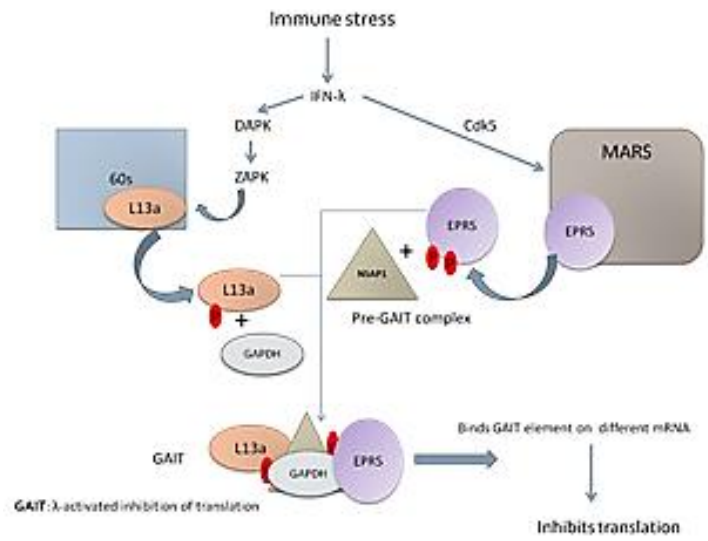

Figure 3-4: Regulation of GAIT complex formation. Phosphorylation of WHEP domain on INF λ signalling leads formation of GAIT (λ activated inhibition of translation) complex containing EPRS, ribosomal protein L13, NSAP1 and GAPDH. This complex then binds to different mRNAs containing GAIT element. (Jia, Arif, Ray, Fox, et al. 2008; Arif et al. 2009; Arif et al. 2011) Adapted from (Gebauer, Preiss, and Hentze 2012).

In addition to EPRS, other tRNA synthetases and auxillary components of MARS complex are also regulated by post-translational modification.For example, Mitogen-activated protein kinase causes phosphorylation of Lys tRNA synthetase (KRS) in stimulated mast cells. This phosphorylation leads to its translocation from MARS complex into the nucleus. In the nucleus, KRS causes immune regulatory genes expression by interacting with a transcription factor called microphthalmia associated transcription factor (mITF). Release of KRS from MARS complex also activates TNF production from macrophages. Detection of auto-antibodies against most tRNA synthetases in almost 30% autoimmunity cases suggests that the enzymes are secreted under specific pathological and/or physiological conditions (Levine, Rosen, and Casciola-Rosen 2003).

The auxillary componets of the MARS complex have multiple effects in critical regulatory processes. MARS complex is hypothesized to sequester these components and release them only under specific signals. For instance, AIMP1, when released, activates caspase 3 via phosphorylation of c-Jun kinase, thus stimulating apoptosis. AIMP2 and AIMP3 also contribute to regulation of cell death. On genotoxic damage, AIMP2/p38 and AIMP3/p18 are released form MARS complex and translocated to the nucleus where AIMP2 activates p53 directly and AIMP3 activates p53 through the activation of the kinases ataxia telangiectasia mutated (ATM) and ATM- and Rad3-related (ATR) (Quevillon et al. 1997; Park, Ewalt, and Kim 2005; Park and Kim 2006).

AIMP2,also regulates apoptosis by down-regulating TNF receptor associated factor 2 (TRAF2) and fuse-binding protein (FBP).

Various studies have shown AaRS and AIMPs to be implicated in tissue specific cancers. For instance, CRS is expressed as a fusion protein with anaplastic lymphoma kinase (Cools et al. 2002). Mitochondrial IleRS expression was altered in hereditary nonpolyposis colorectal cancer (HNPCC) and Turcot syndrome cancer by promoter mutations (Miyaki et al. 2001). A preferential expression of PheRS was observed in acute phase chronic myeloid leukemia and solid tumors (Rodova, Ankilova, and Safro 1999). KRS over-expression was also observed in breast cancer (Park, Ewalt, and Kim 2005). As stated earlier; the AIMPs are involved in regulated angiogenesis. Thus, the synthetases along with the AIMPs might have implications in cancer progression.

In all, the AIMPs perform tumor suppression function as individual proteins while helping complex formation and stability, as components of MARS. Also, the non-canonical activity of most of these components is regulated by modification of these proteins in response to specific signals. In the light of this, the fact that we identified many of the MARS complex components in our SUMO proteome and also in my extensive analysis of published SUMO proteomes, suggests a key role for SUMOylation of these proteins.

3.4 RESULTS.

3.4.1 Knockdown of tRNA synthetases causes lethality in flies.

As tRNA syntheatses play a critical role in protein translation, knockdown of these would have deleterious effects. In order to confirm this, I knocked down few of these tRNA synthetases using ubiquitous and tissue specific Gal4 lines. The UAS-RNAi lines for knockdown were obtained from NIG, Japan. Knockdown of many of the synthetases showed larval or pupal lethality. The absence of embryonic lethality indicate maternal deposition of these tRNA sythetases. It is interesting to note that, knockdown of Prolyl synthetase alone, CG12186, has no effect on fly development. This might be due to presence of full length EPRS in the background. Alternately, this may indicate that the line is not functional.

Table 3-2: Effect of tRNA synthetases knockdown using different Gal4 drivers. Driver used included ubiquitous Actin Gal4, wing-specific Gal4 driver MS1096and eye specific driver (Eyeless). With most combinations, larval or pupal lethality was observed.

Aats RNAi	**Gal4**		
Gene	**Actin**	**MS1096**	**Eyeless**
CG12186	No visible phenotype	No visible phenotype	No visible phenotype
IleRS	X	No wings	X
LeuRS	X	Larval lethal	X
AlaRS	X	Pupal lethal	X
AspRS	1st instar larval lethal	Pupal lethal	Larval lethal
AsnRS	No visible phenotype	Pupal lethal	X
TyrRS	Pupal lethal	Very few flies eclosed. No wings	X
ThrRS	No visible phenotype	X	14% emerged. Smaller eye or complete loss of eye.
TrpRS	No visible phenotype	Pupal lethal	Pupal lethal
PheRS	1st instar larval lethal	X	Pupal lethal

Note: X indicates no cross set for that combination.

3.4.2. Sub-cloning and expression of MARS complex components in *E. coli.*

All the components of MARS complex were subcloned in pGEX4T1 with N-terminal GST tag using homologous recombination. The detailed cloning strategy is described in Methodolgy section. The clones were screened by colony PCR and confirmed to be correct and in-frame with GST using sequencing. The confirmed clones were transformed in BL21 DE3 *E.coli* strain and used for expression. Primary culture from these positive clones was grown overnight at 37 ºC and used for secondary culture. Secondary culture was grown at 37 ºC till O.D 0.6-0.8 was achieved and induced with varying IPTG concentrations from 0.5mM to 2.5mM and expression was tried at a range of temperatures from 18 to 37 ºC. Best expression was achieved at 1mM IPTG concentration and 25 ºC.

Table 3-3: Summary of all MARS complex components expressed using pGEX4T1. All the clones were confirmed by sequencing. Protein expression conditions for all components was standardized successfully.

Components	pGEX cloned	Expressing correctly
EPRS-WHEP	✓	✓
EPRS-Glu	✓	✓
EPRS-Pro	✓	✓
RRS	✓	✓
IRS	✓	✓
LRS	✓	✓
KRS	✓	✓
DRS	✓	✓
MRS	✓	✓
QRS	✓	✓
CG12304	✓	✓
CG30185	✓	✓
CG8235	✓	✓

3.4.3. *In bacto* SUMOylation

Once expression for all components was standardized, all components were expressed using *in bacto* SUMOylation assay as explained in *Methodology* section **(Figure3.9)**. In brief, each clone was individually co-transformed with Q_{SUMO} or $Q_{SUMO-\Delta GG}$ in BL21 DE3 cells and expressed using 1mM IPTG and 25 ºC. The protein was immunoprecitated using Anti-GST Glutathione beads and SUMOylation was checked using SUMO-specific Anti-6X-His Western. I discovered RRS to be SUMOylated **(Figure3.5),** while many other components were not SUMOylated, under *in bacto* conditions.

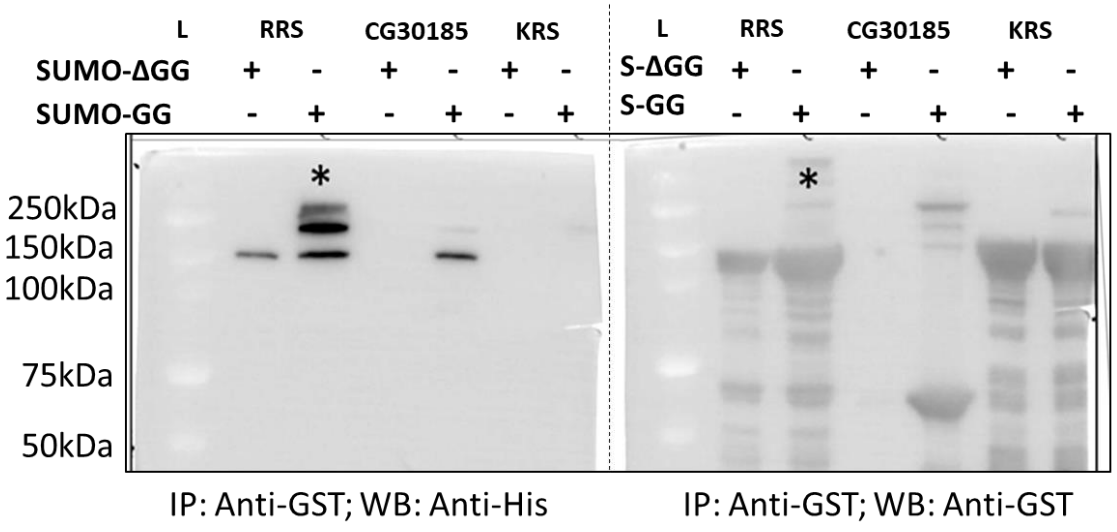

Figure 3-5: Western blot showing multiple SUMOylations for Arginyl tRNA synthetase (RRS). Δ indicates inactive SUMO-ΔGG (S- ΔGG) while Q indicate active SUMO-GG (S-GG). * indicate bands specific to SUMOylation. Additional bands with higher molecular weight (15kDa extra) are observed in SUMO-GG lane for Arginyl tRNA synthetase which are not seen in SUMO- ΔGG. These bands also cross-react with Anti-His Western confirming SUMOylation. Absence of any band in Anti-His blot for Lysyl tRNA synthetase indicates no SUMOylation.

EPRS is SUMOylated at multiple sites and all the sites fall within the WHEP domain (Smith et al. 2004) . Full length SUMO-deficient EPRS ($EPRS^{FL\text{-}5M}$) was cloned in pGEX using overlapping PCR. *EPRS cds* was divided into three fragments: Glutamyl synthetase domain sequence (Glu Fragment), Prolyl synthetase domain sequence (Pro Fragment) and SUMO-deficient WHEP (5M-WHEP). At first, 5M-WHEP and Pro Fragment were combined using overlapping PCR to form 5M-WHEP-Pro fragment. This was then fused to Glu-Fragment to form $EPRS^{FL\text{-}5M}$ **(Figure3.6A).** This was then cloned into pGEX4T1 and confirmed by colony PCR **(Figure3.6B)** and sequencing.

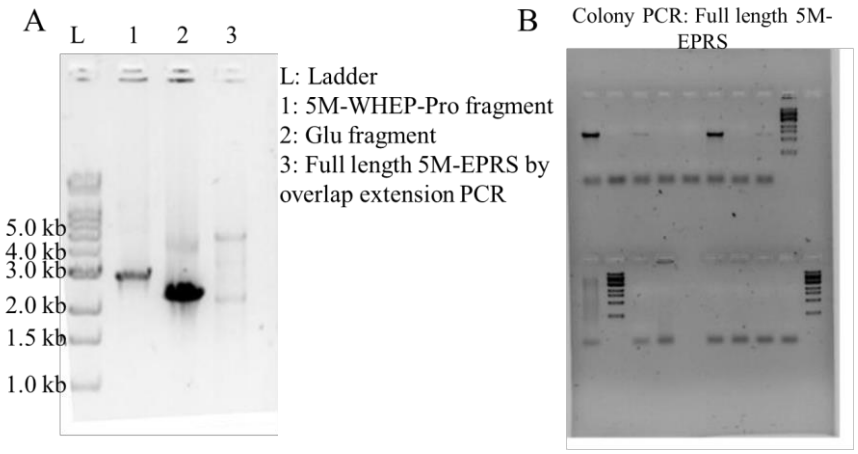

Figure 3-6: Cloning of $EPRS^{FL\text{-}5M}$ in pUASp, fly expression vector. **A)** Overlap PCR using Glutamyl, WHEP and Prolyl segments of EPRS to obtain a FL 5.1kb amplicon. This was then cloned into pGEX for bacterial expression, pRM-HA for S2 cells and pUASp for maternal and zygotic expression in flies. **B)** Confirmation of pGEX-$EPRS^{FL\text{-}5M}$ by colony PCR. These colonies were confirmed by sequencing.

I have cloned all the MARS complex components in pRM-Ha3 and pIEX6 using homologous recombination. All the clones were confirmed by sequencing. Cloning in pIEX6 was done to express the components in large scale in SF9 insect cells to try and assemble the complex with SUMOylated and deSUMOylated form. Cloning of these components in pRM-HA3 with N-terminal myc-tagged was used to test SUMOylation of these components using *Drosophila* macrophage-like S2 cell line.

3.4.4. Cloning into transposon based vectors and Generation of transgenic animals.

I sub-cloned wild-type EPRS, SUMO-deficient EPRS (EPRS^{5M-FL}) and wild type RRS with N-terminal myc-tag in pUASp P-element vector **(Figure3.9)** between two P-element ends using restriction digestion and ligation cloning. Details are mentioned in *Materials and Methods*. The clones were confirmed by sequencing. The plasmids were purified and sent for injections. Transgenics were identified by presence of red eye selection marker present in pUASp. These lines were then balanced using chromosome specific balancer. One example of genetics of balancing, if the insertion is on 2nd chromosome, is described in **Figure 3.7.**

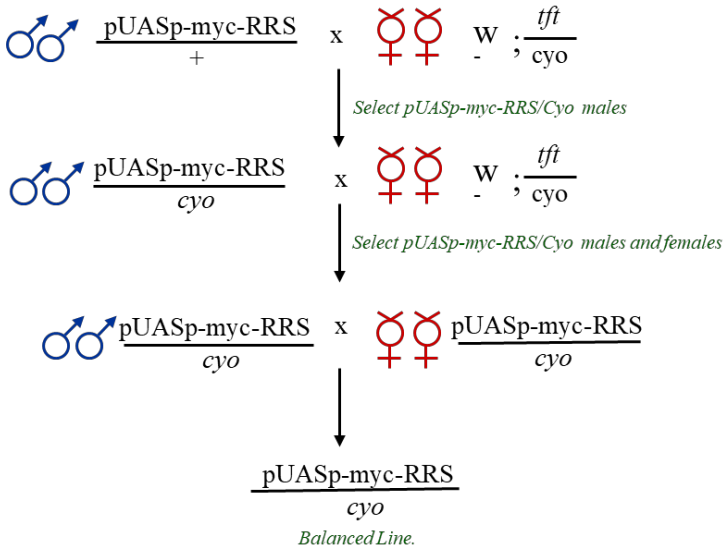

Figure 3-7: Schematic representation of balancing the transgenic line: An example of balancing insertion on the second chromosome. Single transgenic male is crossed to 2nd chromosome double balancer line. In the next generation, Red-eyed *cyo* males are crossed again to 2nd chromosome double balancer line. If the insertion is on 2nd chromosome as in this example, in the next generation, all red eyed flies would have curled wings (cyo). The red eyes male and female flies are then crossed for maintaining of the transgene.

I have generated transgenic lines for different constructs of EPRS and RRS. The list is summarized in table below.

Table 3-4: Table summarizing all the transgenics generated for EPRS and RRS. Multiple transgenic lines with insertions on either 2nd or 3rd chromosome were obtained. These were balanced accordingly using chromosome specific balancer lines.

LINE	VEctor	Transgenic Scored?	Inserts on multiple Chromosomes?
RRS (myc tagged)	pUASp	Yes	yes (multiple lines on II or III chromosome)
EPRS-WHEP(myc tagged)	pUASp	Yes	yes (multiple lines on II or III chromosome)
EPRS-WHEP 5M (myc tagged)	pUASp	Yes	yes (multiple lines on II or III chromosome)
EPRS-FL 5M (myc tagged)	pUASp	Yes	yes (multiple lines on II or III chromosome)
EPRS(untagged)	pUASp	Yes	yes (multiple lines on II or III chromosome)
EPRS-WHEP (untagged)	pUASp	Yes	yes (multiple lines on II or III chromosome)
EPRS-WHEP5M (untagged)	pUASp	Yes	yes (multiple lines on II or III chromosome)

Prajna Nayak, a graduate student in the laboratory has confirmed their expression using Anti-myc immunohistochemistry and she is using these transgenic lines for further investigation.

3.5. CONCLUSIONS

I have identified RRS as a novel SUMOylation target, demonstrated SUMOylation using *in bacto* conditions. I have cloned and made multiple transgenic lines for EPRS and RRS which are being used to understand if SUMOylation of RRS and EPRS have functional significance in flies, in their canonical or non-canonical function or in maintaining MARS complex stability.

3.6. MATERIALS AND METHODS

Fly stocks: Knockdown line for tRNa synthetases were obtained from NIG, Japan. EPRS and RRS variant transgenic lines were generated in NCBS fly facility and balanced in house. All fly stocks were maintained on standard media at 25 °C.

Subcloning. *Source of cDNA*. Genes were cloned into pGEX-4T1 bacterial expression vector (Promega). The cloning was done using homologous recombination. GOI amplification primers were designed to have 20bp homology with vector and 20bp with gene of interest (GOI). Forward primer had vector homology with C-terminal GST sequence and insert homology with first 20bp of N-terminal of GOI coding sequence. Reverse primer had last 20bp of C-terminal of GOI coding sequence and 20bp of the vector The amplified GOI is transformed along with linearized vector into Recombinase expressing *E.coli strain*. The colonies are screened by colony PCR and confirmed by sequencing.

In bacto SUMOylation assay system: We use Quadruplet construct (QSUMO vector, a generous gift from Minghua Nie, Al Courey's Lab), containing His-SUMO (active GG-form or inactive (ΔGG-form), streptavidine-Ubc9 and SUMO activation enzymes Sae1/Sae2. This vector expressed along with GST-tagged substrate can be tested for SUMOylation.

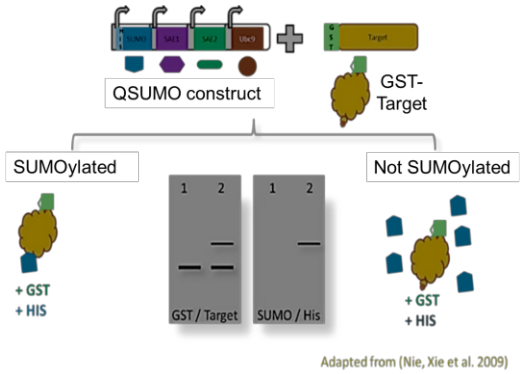

Figure 3-8: *In bacto* system: The SUMOylation machinery components, His-tagged SUMO-GG, Sae1/Sae2, Ubc9 are cloned into quadrant vector with separate T7 promoter for each component. Similarly, an inactive His-tagged SUMO-ΔGG is also expressed as negative control. AGST tagged substrate protein expressed along with his-tagged SUMO can be tested for SUMOylation (Nie et al. 2009).

Test protein expression was induced using 0.5mM to 2mM isopropyl β-D-1-thiogalactopyranoside (IPTG) concentrations at 25-37 °C. For most MARS components, 1mM IPTG at 25 °C for 3hrs was used. If the test protein is target for SUMOylation, it would show up only in active SUMO-

GG lanes on both anti-GST Western (Rb Anti-GST 1:5000) as well as anti-His Western (Mouse Anti-His 1:3000) blots.

Cloning in pUASp: Genes were subcloned in pUASp **(Figure3.9)** using restriction digestion and ligation cloning. EPRS was cloned between Not1 and Xba1 sites, downstream of UAS. pUASp was linearized using Not1 and Xba1 double digestion at 37 ºC for 6hrs followed by 1h of phosphatase treatment at 37 ºC. Linearized vector was purified using Gel Extraction kit. Insert was PCR amplified using Not1 at 5' end and Xba1 site at 3' end followed by double digestion with Not1 and Xba1 and purification. Vector and insert were mixed in 1:3 ratio and ligated using Takara Ligation Mighty Mix. The ligated product was transformed in *E.coli* DH5α cells. Colonies were screened using colony PCR and confirmed by sequencing.

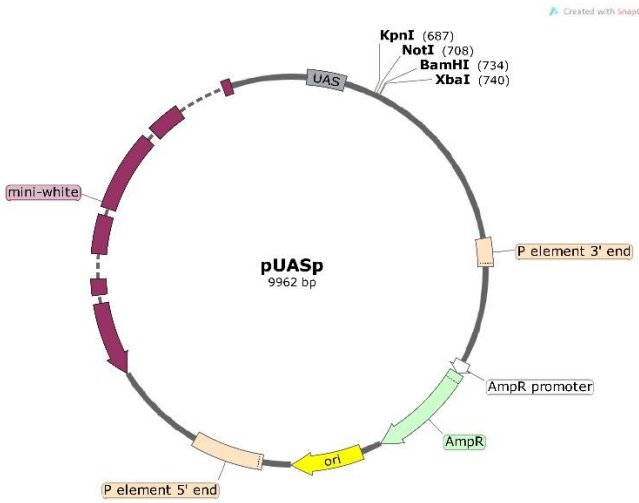

Figure 3-9: pUASp vector map. pUASp vector is used for expression of transgenes in maternal as well as embryonic tissues. The gene of interest is cloned within the MCS, downstream of UAS. The vector gets integrated in *Drosophila* genome using P-element based insertion. The transgenic flies are identified by red eyes, due to mini-white gene present in the vector.

3.7. CONTRIBUTIONS.

The tRNA synthetases were my first choice for elucidation function in response to SUMO modification. However, the absence of null regents and the difficulties associated with working with proteins with critical amino-acid charging functions led me to switch targets in the fourth year of my Ph.D. At that point in time, I chose Caspar, a negative regulator of IMD signaling, with a null allele available to start null/rescue experiments as my primary validation target. The EPRS/RRS work will be continued by Pranja Nayak, a graduate student who joined the laboratory in 2014.

BIBLIOGRAPHY

Antonellis, Anthony, Rachel E Ellsworth, Nyamkhishig Sambuughin, Imke Puls, Annette Abel, Shih-Queen Lee-Lin, Albena Jordanova, Ivo Kremensky, Kyproula Christodoulou, Lefkos T Middleton, Kumaraswamy Sivakumar, Victor Ionasescu, Benoit Funalot, Jeffery M Vance, Lev G Goldfarb, Kenneth H Fischbeck, and Eric D Green. 2003. 'Glycyl tRNA synthetase mutations in Charcot-Marie-Tooth disease type 2D and distal spinal muscular atrophy type V.', *American journal of human genetics*, 72: 1293-9.

Arif, A., J. Jia, R. A. Moodt, P. E. DiCorleto, and P. L. Fox. 2011. 'Phosphorylation of glutamyl-prolyl tRNA synthetase by cyclin-dependent kinase 5 dictates transcript-selective translational control', *Proceedings of the National Academy of Sciences*, 108: 1415-20.

Arif, A., J. Jia, R. Mukhopadhyay, B. Willard, M. Kinter, and P. L. Fox. 2009. 'Two-site phosphorylation of EPRS coordinates multimodal regulation of noncanonical translational control activity', *Mol Cell*, 35: 164-80.

Arif, Abul, Jie Jia, Robyn A Moodt, Paul E Dicorleto, and Paul L Fox. 2010. 'Phosphorylation of glutamyl-prolyl tRNA synthetase by cyclin-dependent kinase 5 dictates transcript- selective translational control', *PNAS*, Early edit: 1-6.

Clemens, M J, a Galpine, S a Austin, R Panniers, E C Henshaw, R Duncan, J W Hershey, and J W Pollard. 1987. 'Regulation of polypeptide chain initiation in Chinese hamster ovary cells with a temperature-sensitive leucyl-tRNA synthetase. Changes in phosphorylation of initiation factor eIF-2 and in the activity of the guanine nucleotide exchange factor GEF.', *The Journal of biological chemistry*, 262: 767-71.

Cools, Jan, Iwona Wlodarska, Riet Somers, Nicole Mentens, Florence Pedeutour, Brigitte Maes, Christiane De Wolf-Peeters, Patrick Pauwels, Anne Hagemeijer, and Peter Marynen. 2002. 'Identification of novel fusion partners of ALK, the anaplastic lymphoma kinase, in anaplastic large-cell lymphoma and inflammatory myofibroblastic tumor.', *Genes, chromosomes & cancer*, 34: 354-62.

Dyck, P J, and E H Lambert. 1968. 'Lower motor and primary sensory neuron diseases with peroneal muscular atrophy. I. Neurologic, genetic, and electrophysiologic findings in hereditary polyneuropathies.', *Archives of neurology*, 18: 603-18.

Fukui, H., R. Hanaoka, and a. Kawahara. 2009. 'Noncanonical Activity of Seryl-tRNA Synthetase Is Involved in Vascular Development', *Circulation Research*, 104: 1253-59.

Gebauer, Fátima, Thomas Preiss, and Matthias W Hentze. 2012. 'From cis-regulatory elements to complex RNPs and back.', *Cold Spring Harbor perspectives in biology*, 4: a012245.

Havrylenko, Svitlana, Renaud Legouis, Boris Negrutskii, and Marc Mirande. 2011. 'Caenorhabditis elegans evolves a new architecture for the multi-aminoacyl-tRNA synthetase complex.', *The Journal of biological chemistry*, 286: 28476-87.

Herzog, W., K. Muller, J. Huisken, and D. Y.R. Stainier. 2009. 'Genetic Evidence for a Noncanonical Function of Seryl-tRNA Synthetase in Vascular Development', *Circulation Research*, 104: 1260-66.

Jia, J., A. Arif, P. S. Ray, and P. L. Fox. 2008. 'WHEP domains direct noncanonical function of glutamyl-Prolyl tRNA synthetase in translational control of gene expression', *Mol Cell*, 29: 679-90.

Jia, Jie, Abul Arif, Partho S Ray, Paul L Fox, Jie Jia, Abul Arif, Partho S Ray, and Paul L Fox. 2008. 'WHEP Domains Direct Noncanonical Function of Glutamyl-Prolyl tRNA Synthetase in Translational Control of Gene Expression', *Molecular Cell*, 29: 679-90.

Kerjan, Pierre, Claire Cerini, and Marc Mirande. 1994. 'The multienzyme complex containing nine aminoacyl-tRNA synthetases is ubiquitous from *Drosophila* to mammals', *Biochimica et Biophysica Acta*, 1199: 293-97.

Kim, Sunghoon, Sungyong You, and Daehee Hwang. 2011. 'Aminoacyl-tRNA synthetases and tumorigenesis: more than housekeeping.', *Nature Reviews*, 11: 708-19.

Ko, Young-gyu, Young-sun Kang, Eun-kyoung Kim, Sang Gyu Park, and Sunghoon Kim. 2000. 'Nucleolar Localization of Human Methionyl – tRNA Synthetase and Its Role in Ribosomal RNA Synthesis', 149: 567-74.

Kwon, Nam Hoon, Taehee Kang, Jin Young Lee, Hyo Hyun Kim, Hye Rim Kim, Jeena Hong, Young Sun Oh, Jung Min Han, Min Jeong Ku, Sang Yeol Lee, and Sunghoon Kim. 2011. 'Dual role of methionyl-tRNA synthetase in the regulation of translation and tumor suppressor activity of aminoacyl-tRNA synthetase-interacting multifunctional protein-3.', *Proceedings of the National Academy of Sciences of the United States of America*, 108: 19635-40.

Lee, Sang Won, Byeong Hoon Cho, Sang Gyu Park, and Sunghoon Kim. 2004a. 'Aminoacyl-tRNA synthetase complexes: beyond translation', *Journal of Cell Science*, 117: 3725-34.

———. 2004b. 'Aminoacyl-tRNA synthetase complexes: beyond translation.', *Journal of cell science*, 117: 3725-34.

Levine, Stuart M, Antony Rosen, and Livia A Casciola-Rosen. 2003. 'Anti-aminoacyl tRNA synthetase immune responses: insights into the pathogenesis of the idiopathic inflammatory myopathies.', *Current opinion in rheumatology*, 15: 708-13.

Lund, E., and James Dahlberg. 1998. 'Proofreading and Aminoacylation of tRNAs Before Export from the Nucleus', *Science*, 282: 2082-85.

Martinis, Susan A., Pierre Plateau, Jean Cavarelli, and Catherine Florentz. 1999. 'Aminoacyl-tRNA synthetases: A new image for a classical family', *Biochimie*, 81: 683-700.

Miyaki, M, T Iijima, K Shiba, T Aki, Y Kita, M Yasuno, T Mori, T Kuroki, and T Iwama. 2001. 'Alterations of repeated sequences in 5' upstream and coding regions in colorectal tumors from patients with hereditary nonpolyposis colorectal cancer and Turcot syndrome.', *Oncogene*, 20: 5215-18.

Mukhopadhyay, Rupak, Jie Jia, Abul Arif, Partho Sarothi Ray, and Paul L Fox. 2009. 'The GAIT system : a gatekeeper of inflammatory gene expression', *Trends in biochemical sciences*: 324-31.

Nangle, Leslie A, Wei Zhang, Wei Xie, Xiang-lei Yang, and Paul Schimmel. 2007. 'Charcot – Marie – Tooth disease-associated mutant tRNA synthetases linked to altered dimer interface and neurite distribution defect', 104.

Nie, Minghua, Yongming Xie, Joseph a Loo, and Albert J Courey. 2009. 'Genetic and proteomic evidence for roles of *Drosophila* SUMO in cell cycle control, Ras signaling, and early pattern formation.', *PloS one*, 4: e5905.

Park, Sang Gyu, Karla L Ewalt, and Sunghoon Kim. 2005. 'Functional expansion of aminoacyl-tRNA synthetases and their interacting factors: new perspectives on housekeepers.', *Trends in biochemical sciences*, 30: 569-74.

Park, Sang Gyu, and Sunghoon Kim. 2006. 'Do aminoacyl-tRNA synthetases have biological functions other than in protein biosynthesis?', *IUBMB life*, 58: 556-8.

Park, Su Jin, Seong Hwan Kim, Han Seok Choi, Yumie Rhee, and Sung-Kil Lim. 2009. 'Fibroblast growth factor 2-induced cytoplasmic asparaginyl-tRNA synthetase promotes survival of osteoblasts by regulating anti-apoptotic PI3K/Akt signaling', *Bone*, 45: 994-1003.

Pollard, Jeffrey W, Angela R Galpine, and Michael J Clemens. 1989. 'A novel role for aminoacyl-tRNA synthetases in the regulation of polypeptide chain initiation', 9: 1-9.

Quevillon, S, F Agou, J C Robinson, and M Mirande. 1997. 'The p43 component of the mammalian multi-synthetase complex is likely to be the precursor of the endothelial monocyte-activating polypeptide II cytokine.', *The Journal of biological chemistry*, 272: 32573-9.

Rodova, M, V Ankilova, and M G Safro. 1999. 'Human phenylalanyl-tRNA synthetase: cloning, characterization of the deduced amino acid sequences in terms of the structural domains and coordinately regulated expression of the alpha and beta subunits in chronic myeloid leukemia cells.', *Biochemical and biophysical research communications*, 255: 765-73.

Seburn, Kevin L, Leslie a Nangle, Gregory a Cox, Paul Schimmel, and Robert W Burgess. 2006. 'An active dominant mutation of glycyl-tRNA synthetase causes neuropathy in a Charcot-Marie-Tooth 2D mouse model.', *Neuron*, 51: 715-26.

Smith, Matthew, Vinay Bhaskar, Joseph Fernandez, and Albert J Courey. 2004. '*Drosophila* Ulp1, a nuclear pore-associated SUMO protease, prevents accumulation of cytoplasmic SUMO conjugates.', *The Journal of biological chemistry*, 279: 43805-14.

Chapter 4

SUMOylation of Caspar regulates the *Drosophila* innate immune response

4.1 SUMMARY

In *Drosophila*, Caspar is a protein involved in the immune deficiency (IMD) pathway. The IMD pathway, with its component the NFκB effector Relish, is one of the three central immune pathways regulating host defense in *Drosophila*, the other being the Toll/ NFκB pathway. Caspar is a negative regulator of IMD/NFκB signaling. Earlier, we had shown that Caspar is a target of SUMO modification. In this Chapter, I demonstrate that SUMOylation of Caspar at K551 is important for robust host defense and that the absence of SUMOylation leads to immune response weakening. To investigate Caspar SUMOylation, I have generated two basic tools: a Caspar^{K551R}fly line wherein Caspar is resistant to SUMOlyation generated using Crisper/Cas9-based genome editing and an anti-Caspar antibody to visualize Caspar expression as well as to discover Caspar-interacting proteins.

4.2 ABBREVIATIONS

IMD: immune deficiency pathway; DREDD: Death related ced-3/Nedd2-like caspase; FAF1: Fas-associated factor1; CRISPR- Clustered Regularly Interspaced Short Palindromic Repeats

4.3 INTRODUCTION

In *Drosophila*, the immune deficiency (IMD) pathway is activated in response to infection by gram negative bacteria, when DAP-type peptidoglycan from the bacterial cell wall binds to the cell surface receptor PGPRP-LC. This triggers a cascade of signaling, which involves DREDD-dependent cleavage and nuclear translocation of Relish, a fly NF-kB (Leulier et. al. 2003). Relish then activates transcription of several antimicrobial peptides such as *attacinD (attd), drosocin (dro)* and *dipterecin (dipt)*, some of which are potent antagonists of gram negative bacteria. While

Akirin is a single known positive regulator of the IMD/ NF-kB pathway (Bonnay et. al. 2014), many players are involved in its negative regulation (**Figure4.1**). The basal negative regulators ensure inactivation of the pathway in the absence of infection to avoid inflammation. In the absence of infection, the IMD/ NF-kB pathway is suppressed at several levels. For example, in the absence of infection, PGPRP-LF (peptidoglycan (PGN)-recognition protein LF) forms inactive heterodimers with PGPRP-LC, which forms active PGPRP-LC homodimers in the presence of infection; this dimerization indicates the pathway suppression at the level of bacterial recognition (Mellroth et. al. 2005). Similarly, within the cytoplasm, proteins like Posh, CYDL, and dUSP36 regulate expression levels of IMD pathway components by Ub-mediated proteosomal degradation, indicating pathway suppression at another level (Meinander et. al. 2012). Other proteins like DNR and Caspar regulate DREDD activity and retain Relish into the cytoplasm. Caudal, on the other hand, inhibits Relish activity in the nucleus; this affects AMP production without affecting other pathway components (Clayton et. al. 2013). Apart from these constitutive negative regulators, PIRK and ROS regulate the IMD pathway via feedback inhibition (Lee and Ferrandon 2011)..

Many of the key players in the IMD pathway were identified during genetic screens. Caspar, for example, when over-expressed, suppress IMD mutant phenotype (Kim, Lee et al. 2006). Caspar deficient flies showed untimely activation of Relish and production of AMPs without infection. Supporting the above observation, overexpression of Caspar led to inhibition of Relish translocation and consequent inhibition of the immune response. Although no direct physical contact between Caspar, Relish, and DREDD has been demonstrated, it is generally believed that Caspar perturbation affects DREDD-dependent cleavage of Relish, blocking its nuclear translocation (Kim *et al*., 2006).

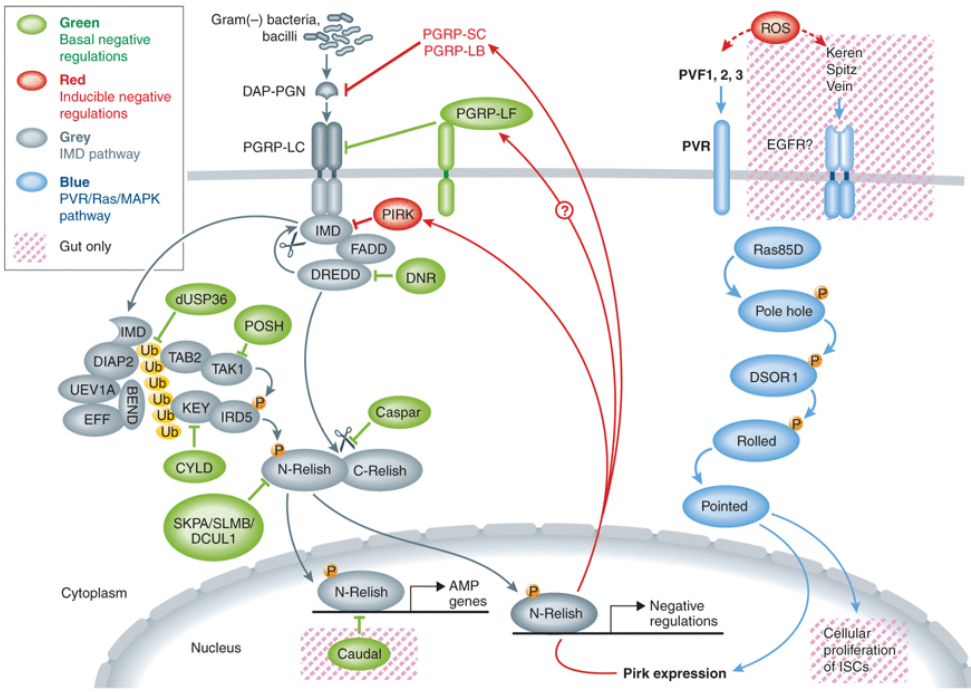

Figure 4-1: Regulation of the IMD pathway. In response to infection by gram-negative bacteria, PGPRP-LC is activated, which in turn activates the IMD pathway and DREDD. IMD, through a series of interactions, activates IDR5, which consequently phosphorylates Relish. Activated DREDD, in turn, cleaves Relish. The cleaved N-terminal fragment of Relish translocates to the nucleus and activated the transcription of AMP genes, resulting in the production of AMPs in the hemolymph at approximately 1mM concentration. Alternatively, PIRK regulates the IMD pathway via feedback inhibition. In the absence of infection, proteins like DNR, CYD, dUSP36, POSH, and Caspar inhibit this cascade and prevent inflammation. The IMD pathway is also regulated through the gut via Pvr/Pvf-dependent Ras/MAPK pathway. Image reproduced from (Lee and Ferrandon 2011)

Caspar was identified as a *Drosophila* homolog of human FAF1, Fas-associated factor1 (**Figure4.2**). FAF1, like Caspar, contains Ubiquitin association domain (UAS), Ubiquitin-like regulatory domain (Ubx), Fas-associating region, and a DED-interaction region. These different domains allow FAF1 to interact with multiple proteins. For example, FAF1 interacts with VCP through UBX domain and regulates ER-associated degradation (ERAD) pathway (Lee, Park et al. 2013). FAF1, through its UAS domain, interacts with K48-linked Ub polymers, which are then recruited for ERAD-mediated degradation (Song et. al. 2005). On the contrary, phosphorylation of FAF1 leads to Ub-independent, proteasome-dependent degradation of Aurora-A. Like Caspar in *Drosophila*, FAF1 acts as a negative regulator of TNFα-induced activation of NF-kB pathway. FAF1 inhibits IKK activation by physically binding to IKKβ (Park, Moon et al. 2007). Recent studies have contradictory findings regarding the role of FAF1 in viral immunity (Kim JH et. al. 2017). FAF1 acts as a negative regulator of viral immunity by inhibiting translocation of Interferon

regulatory factor3 (IRF3) into the nucleus in response to dsDNA infection in HeLa cells (Song, Lee et al. 2016). Alternatively, FAF1 positively regulates immune response against RNA viruses in mice by binding to NLRX1 and activating MAVS-RIG-1 antiviral signaling (Kim, Park et al. 2017).

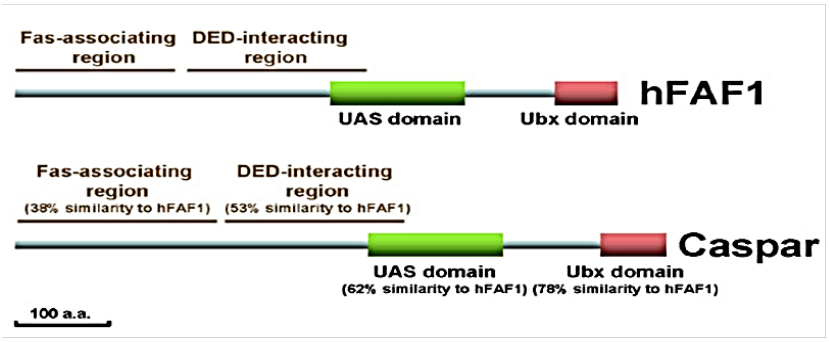

Figure 4-2: Domain structure of human FAF1 and *Drosophila* Caspar. Both proteins contain Ub-association domain (UAS), Ub-like regulatory domain (Ubx), Fas-association region and DED-interacting region. These domains possess varied functions in mammals. (Image reproduced from Kim et al., PNAS, 2006)

FAF1 is better characterized in mammalian systems than its *Drosophila* ortholog and is associated with a variety of functions. Very few of these functions are equivalent to those performed by Caspar in *Drosophila*. Most are dependent on multiple protein–protein interactions. These interactions can be modulated by post-translational modifications such as phosphorylation, acetylation, and SUMOylation.

Previously, we have identified Caspar as a target of SUMO modification using quantitative proteomics. K551 is conserved in all model organisms and may be a potential site for SUMO modification in other species as well. We validated Caspar SUMOylation and identified the lysine residue, K551, as a site of SUMO modification. Another predicted SUMO modification site, K436, does not appear to be so (Handu, Kaduskar et al. 2015) (**Figure 4.3**).

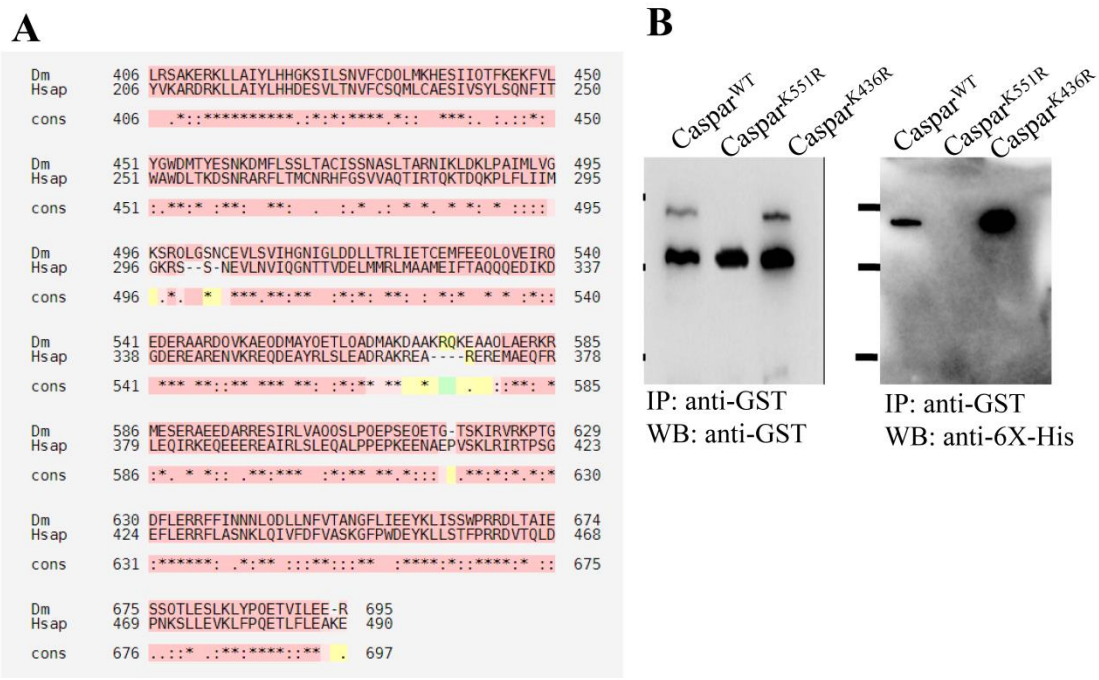

Figure 4-3: Caspar is SUMOylated at K551. (A) Protein sequence alignment of human FAF1 with *Drosophila* Caspar. The figure shows a section of the sequence alignment that contains the predicted SUMO acceptor site (VK^{551}AE) and that it is conserved in flies and humans. (B) Caspar is SUMOylated at K551 when tested using the in bacto SUMOylation assay. An additional band corresponding to SUMOylation is present in the Caspar (WT) and Caspar (K436R) lanes but not in the Caspar (K551R) lane. Image adapted from Handu et al., 2015.

4.4 RESULTS

4.4.1. Caspar is SUMOylated in adult flies.

Earlier, we have shown SUMOylation of Caspar using *in bacto* system (**Figure4.3**), a system developed by Nie et al.., and the S2 cell system (Handu *et al*.,2015). To study the biological significance of SUMOylation in infection and immunity in adult flies, it was important to demonstrate that Caspar is SUMOylated in adult flies. A transgenic fly line expressing Caspar:HA:FLAG (DPiM, See Methods) was crossed with a transgenic line expressing 6XHis:SUMO. In the F1 generation, adult flies overexpressed both Caspar and SUMO. Next, lysates of these flies were made in denaturing conditions (8M Urea). SUMOyalted proteins were purified in denaturing conditions by Ni-NTA affinity chromatography. Anti-Casp antibody staining was used to show that Caspar was one of the SUMOylated proteins in the cell (**Figure4.4**).

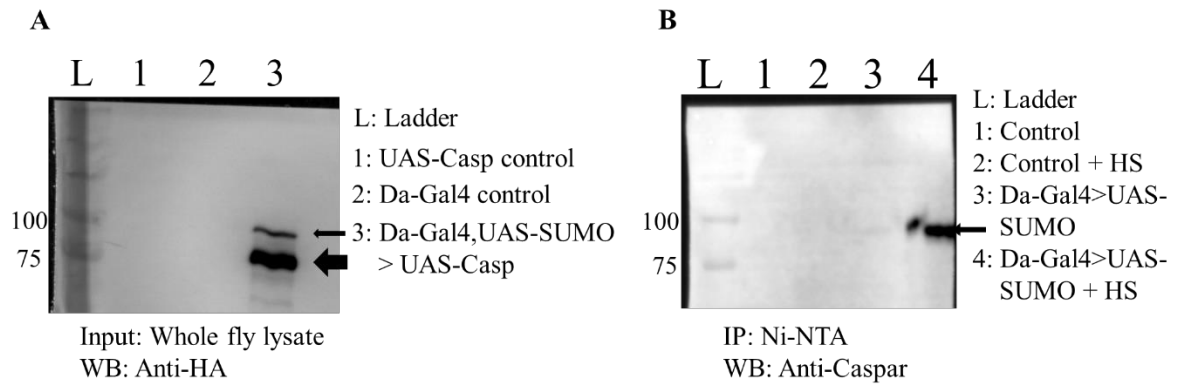

Figure 4-4: Caspar is SUMOylated in flies. To confirm Caspar SUMOlyation in adult flies, I performed Western blot analysis using Caspar overexpression and heat shock strategy**.** In heat shock strategy, flies of genotypes mentioned in the figure were incubated at 37 °C for 1h. The flies of mentioned genotypes were lysed in RIPA and processed with Laemmli dye. The proteins in the lysate were separated using SDS-PAGE and probed using indicated antibodies. **(A)** HA-FLAG-tagged Caspar was expressed ubiquitously along with 6X-His-tagged SUMO. Whole fly lysates for each genotype were probed with Anti-HA antibody to visualize overexpressed Caspar. Upon electrophoretic separation, a band corresponding to the molecular weight of Caspar was observed along with an additional higher molecular weight band (15kDa) in Lane 3 (indicated by arrows). **(B)** Flies overexpressing 6x-His-tagged SUMO were subjected to heat shock (HS). His-tagged proteins were separated from the lysates of HS as well as control files under denaturing conditions using the pull down technique. Further, the proteins were probed with Caspar-specific antibody. A single prominent band corresponding to the molecular weight of SUMOylated Caspar was observed in SUMO overexpressing HS flies (Lane 4); such a band was absent in control or control with HS (Lanes 1 and 2). In summary, these Western blot analyses confirm Caspar SUMOylation.

Caspar-null flies are embryonic lethal, indicating the crucial role of Caspar in early development of *Drosophila*. I wanted to investigate if SUMOylation of Caspar is essential for its function in development. For this investigation, I decided to replace wild-type Caspar with SUMO-deficient Caspar ($Caspar^{K551R}$). As one of the strategies to achieve this, I used a classical genetics approach and expressed $Caspar^{K551R}$ in a $Caspar^{null}$ background ubiquitously using UAS-Gal4 system (**Figures 4.5 and 4.7**).

I sub-cloned $Caspar^{WT}$ and $Caspar^{K551R}$ in pUASp-attB, a fly expression vector. Details of cloning are mentioned in the *Material and Methods* section. The accuracy of cloning was confirmed using sequencing and consequently, transgenic flies were obtained. These flies were used for further experiments.

4.4.2. Expression of wild-type Caspar using *Daughterless-Gal4* rescues lethality.

At first, I checked if the embryonic lethal phenotype of Caspar-null can be rescued by over-expressing wild type Caspar. I performed a series of genetic crosses as shown in **Figure 4.5**. The

desired genotype of *Caspar-null/Caspar-null; Daughterless-Gal4/UAS-Caspar-HA-FLAG* was obtained in F2 generation, confirming that embryonic lethality of Caspar-null was rescued. In this fly, the endogenous *caspar* is deleted and Caspar expression is driven by Daughterless-Gal4 (Da-Gal4). The expression of wild-type Caspar using Da-Gal4 is confirmed using Western blot (**Figure 4.6**). This expression is sufficient to rescue lethality seen in Caspar-null flies.

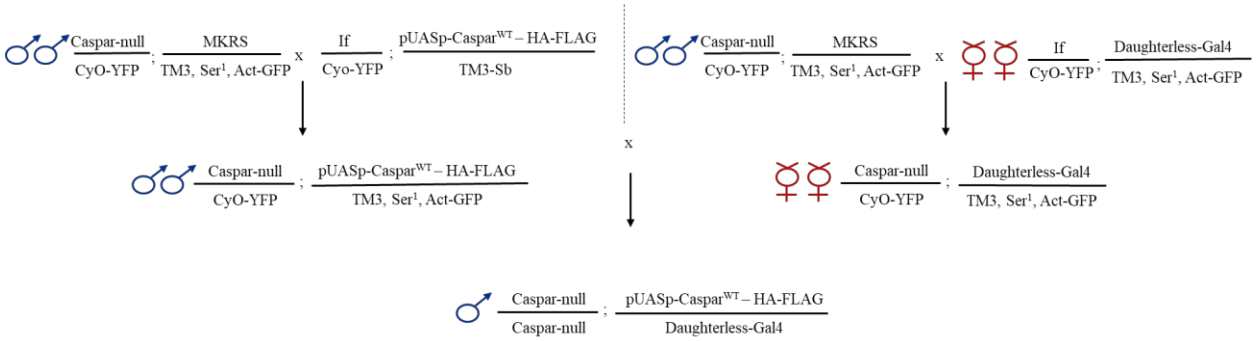

Figure 4-5: The series of genetic crosses performed to generate rescued Caspar-null with overexpression of wild-type Caspar. In the first set of crosses, Caspar-null chromosome was brought together with either UAS-Caspar or Daughterless-Gal4. This was done by using If/Cyo; MKRS/serrate, 2nd, 3rd chromosome double balancer. In the second step, Caspar-null/Cyo; UAS-Caspar/Serrate flies were crossed to Caspar-null/CyO; Daughterless-Gal4/Serrate. As *CyO* and TM3-*serrate* are balancers, homozygous flies for either of the genotypes do not survive. Caspar-null/Caspar-null flies are lethal. If over-expression of Caspar using Daughterless-Gal4 is sufficient to compensate for Caspar function during early development, flies of Caspar-null/Caspar-null; UAS-Caspar/Daughterless-Gal4 are obtained.

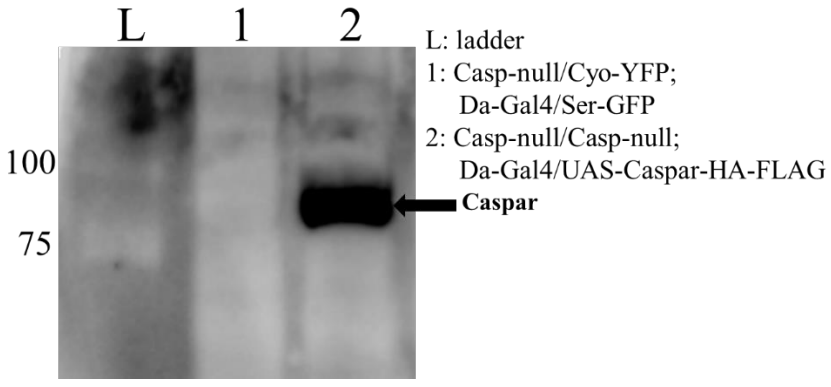

Figure 4-6: Expression of wild-type Caspar in the rescue line. Western blot analysis was performed to confirm the expression of Caspar in the rescue line. UAS-Caspar-HA-FLAG was expressed using Da-Gal4 in the rescue line (Lane 2), but not in the control flies. The flies of the indicated genotypes were lysed in

RIPA and processed with Laemmli dye. The lysate proteins were separated using SDS-PAGE and probed with Anti-HA antibody. A band corresponding to the molecular weight of Caspar was observed in the rescue line (Lane 2) as indicated by arrow but not in control line (Lane 1).

4.4.3. SUMO-deficient Caspar (Caspar^{K551R}) expression can also rescue Caspar-null lethality.

Expression of wild-type Caspar using Daughterless-Gal4 was sufficient to rescue lethality caused by the deletion of endogenous *caspar*. Moreover, Caspar^{K551R} also completely rescued Caspar-null lethality. I confirmed the expression of myc-tagged Caspar^{K551R} with the help of genomic PCR (**Figure 4.8A**) and quantitative real-time PCR (Figure **4.8B and C**) using *myc*-specific primers. The flies that expressed only Caspar^{K551R} and no endogenous Caspar did not show any visibly distinct phenotype. This confirmed that Caspar^{K551R} substitutes for the functions of Caspar in *Drosophila* development and that Caspar SUMOylation does not play a significant role in early developmemt. When *caspar* transcript levels were compared among control flies, flies rescued with wild-type Caspar, and those rescued with Caspar^{K551R}, they were variable (**Figure 4.8C**).

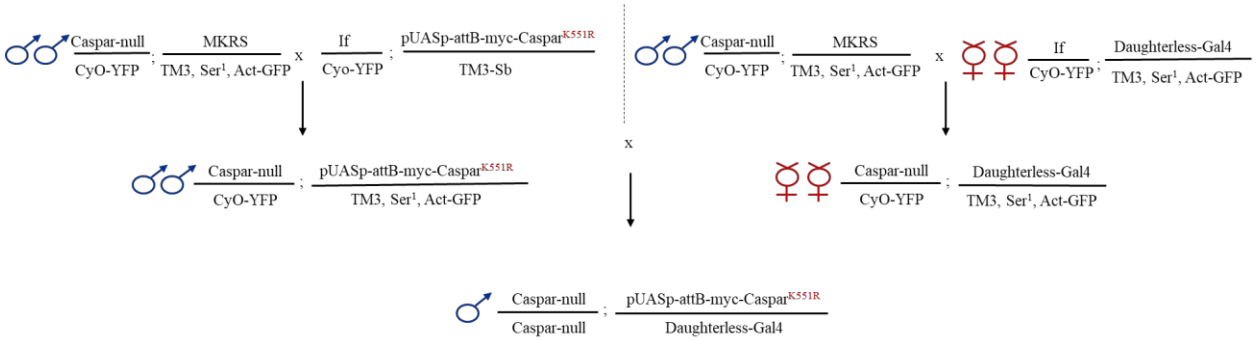

Figure 4-7: The series of genetic crosses performed to generate rescued Caspar-null by overexpressing SUMO-deficient Caspar (Caspar^{K551R}).

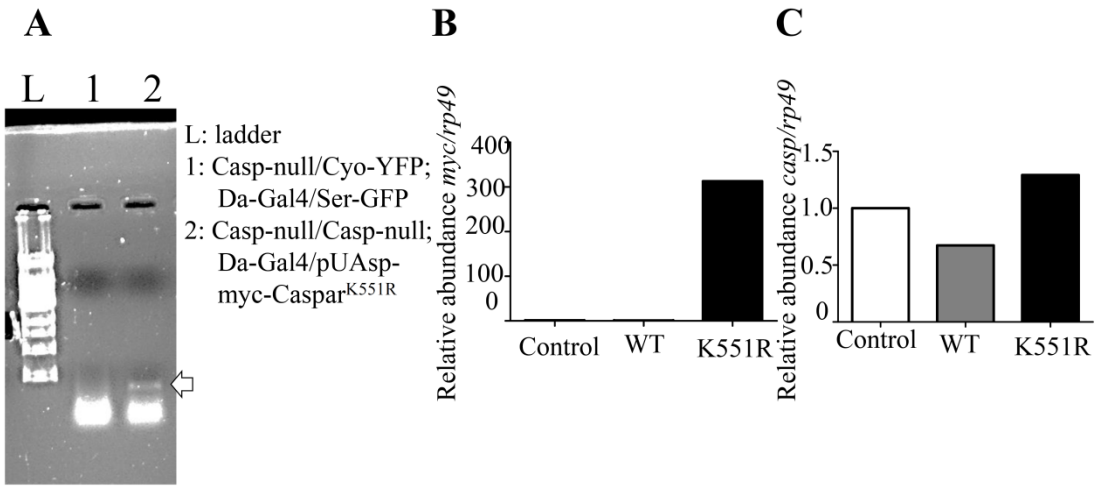

Figure 4-8: Expression of Caspar^{K551R} in the rescued Caspar-null line. The expression of *myc*- tagged Caspar^{K551R} in the rescue line *Casp-null/Casp-null; Da-Gal4/UAS-myc-Casp^{K551R}* (K551R) is confirmed using genomic PCR and quantitative real time PCR. (A) Genomic PCR: Genomic DNA was isolated from the rescue line and amplified using a *myc*-specific forward primer and a caspar-specific reverse primer. The amplification was observed only in the SUMO -resistent rescue line (K551R) and not in the Control (CS) or rescue with wild-type Caspar (WT); (B) Quantitative RT-PCR: Total RNA was isolated from K551R and control adult flies, and cDNA was synthesized. The expression of myc-tagged Caspar K551R was confirmed by qRT-PCR using *myc*-specific primers. The histogram shows relative abundance of CasparK551R in comparison with *rp49;* (C) *caspar* specific quantitative RT-PCR: Expression of Caspar^{K551R} (*Casp-null/Casp-null; Da-Gal4/UAS-myc-Casp^{K551R}*) and Wild-type Caspar (*Casp-null/Casp-null; Da-Gal4/UAS-Casp-HA-FLAG)* was quantified using quantitative RT-PCR. Compared to the expression in control flies, expression in wild-type Caspar lines was lower, whereas that in Caspar^{K551R} lines was higher. The fold change in expression was normalized to *rp49* expression levels and the histogram was plotted using GraphPad 5.0

Expressing various proteins using UAS-Gal4 system is insufficient to understand endogenous expression patterns as well as to compare total protein levels between wild-type and mutant variants.

4.4.4. Caspar-specific antibody was generated and validated.

Purification of Caspar for antibody production. To generate Anti-Caspar antibody, purifying Caspar was essential. To achieve this, full length Caspar was sub-cloned with N-terminal 6X-His tag in pET45b vector. Accuracy of cloning was confirmed by sequencing. Details of cloning are described in *Materials and Methods*. 6X-His-tagged Caspar was expressed in BL21DE3 cells using 1mM IPTG induction at 25 °C. The cell lysate was run over Ni-NTA beads and the bound protein of interest was eluted using increasing concentrations of Imidazole (50mM–150mM).

Eluate obtained with each Imidazole concentration was analyzed on SDS-PAGE to check the quantity and quality of the purified protein (**Figure 4.9A**). The 150mM eluate showed fewer undesired proteins as compared to elutions at 50mM and 100mM. However, the amount of Caspar is also least in 150mM eluate. On the other hand, maximum amount of protein was observed in the eluate obtained with 50mM Imidazole. For antibody production, purified protein is required in large quantities. To achieve higher quantities of the purified protein, the 50mM and 100mM eluates were subjected to size exclusion chromatography using fast protein liquid chromatography (FPLC). Multiple fractions from each eluate were collected. One percent of each fraction was analyzed on SDS-PAGE (**Figure 4.9B, C and D**). The fractions B6 and B7 from the 50mM eluate showed maximum protein quantity (Figure10). Protein from these fractions was quantitated using a protein estimation kit and the findings were recorded. These fractions were lyophilized, and in total, approximately 3 mg protein was sent for antibody production.

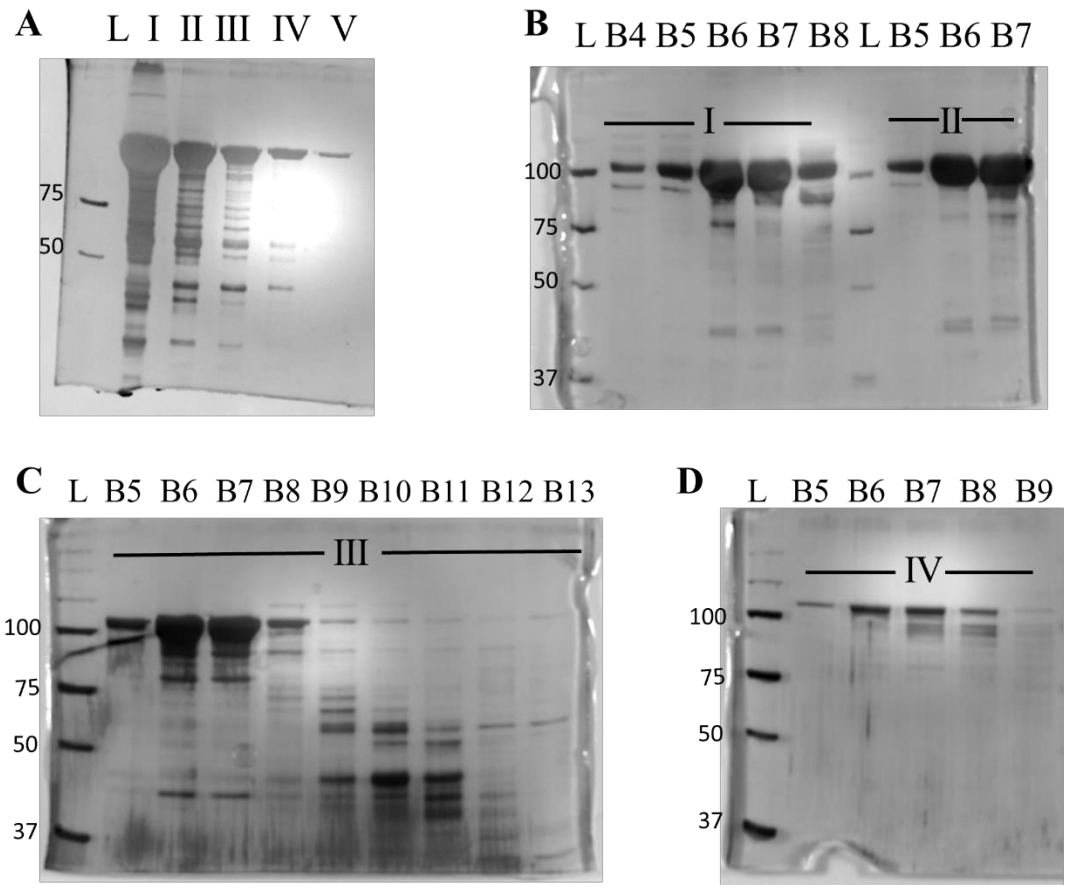

Figure 4-9: Protein purification using Ni-NTA and FPLC. Caspar was expressed in *Escherichia coli* BL21 DE3 cells with 1mM IPTG at 25 °C. Bacteria were lysed in 10mM Imidazole and the lysate was run over Ni-NTA beads. The bound protein was eluted using 50–150mM Imidazole. (A) One percent of eluate

obtained with each concenration of Imidazole was analyzed by SDS-PAGE. The gels were stained with Commassie R250 for protein visualization. Purified protein was observed in the 150mM eluate, but its amount was low (Lanes IV and V). Maximun amount of protein was observed in the 50mM eluate (Lanes I and II). All eluates were were subjected to FPLC-based protein seperation. Different fractions were collected between 50ml to 80ml elution. The fractions expected to contain Caspar were analyzedby SDS-PAGE followed by staining with Commassie-R250 for protein visualization (Panels B, C, and D; Lanes B4 to B13) . (B) Fractions collected from the 50mM eluate as input (Lane groups I and II) show highest amount of Caspar (Lanes B6 and B7). A similar trend was observed in fractions collected from the 100mM eluate (C) and the 150mM eluate (D).

In size exclusion-based FPLC, proteins are separated on the basis of their size, i.e., larger molecules exit the column earlier than smaller molecules. When the 50mM eluate was subjected to FPLC, Caspar exited the column at around 60 ml; the elution volume corresponds to 150 kDa proteins. This 150 kDa peak observed in the elution profile indicates that Caspar exists in dimeric form *in bacto*. (**Figure 4.10**). I confirmed that SUMOylation has no effect on dimerization when SUMO and Caspar are co-expressed *in bacto*..

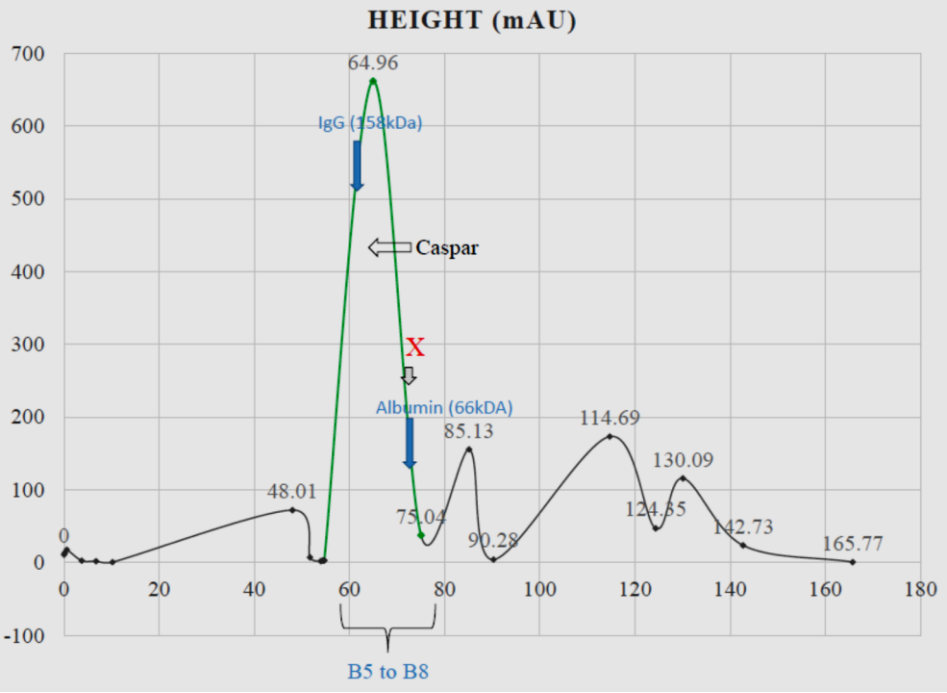

Figure 4-10: Elution profile size exclusion-based FPLC purification of the 50mM eluate. Column properties: matrix, Sephadex G-200; dimensions, 30 cm × 10mM; eluent, TBS; flow rate, 1 ml/min. The 50mM eluate was subjected to size exclusion-based FPLC. Each peak in the elution profile represents a protein present in the eluate. The highlighted peak corresponds to 150 kDa when compared to retention time of IgG. Fractions B5–B8 collected from FPLC confirm the presence of Caspar in the highlighted peak. Based on the retention time of Albumin (human) with molecular weight of 66kDa, Caspar (75 kDa) is predicted to elute at around 80 min (indicated by X). Caspar, alternatively, has a retention time of 64.96 min, closer to that of IgG (158 kDa), indicating that Caspar exists as a dimer in bacterial cells.

The purified Caspar was injected in rabbits in boosters as described in the table below. Different bleeds were tested for specific antibody production. Antibody specificity was checked by Bioklone using Indirect ELISA (**Figure 4.11A**). Further, the obtained antibody was tested at various dilutions ranging from 1:500 to 1:20,000 using Western blot analysis. Control and Caspar-null adult fly lysates were used to test the antibody. A band corresponding to the molecular weight of Caspar (75kDa) was observed in the control lysate but not in the Caspar-null lysate (**Figure 4.11B**). This confirmed the specificity of the generated antibody. The best working conditions for the Western blot were 1:20,000 dilution in 5% milk, and incubation at 4 °C overnight.

Table 4-1: Description of generation of Caspar antibody.

Booster No.	Date of Immunization	Bleed No.
-	-	Pre-immune bleed
Primary Immunization	27.01.2017	-
First Booster	17.02.2017	-
		Test bleed
Second Booster	10.03.2017	
		First bleed
Third Booster	31.03.2017	
		Second bleed
Fourth booster	21.04.2017	
		Third Bleed

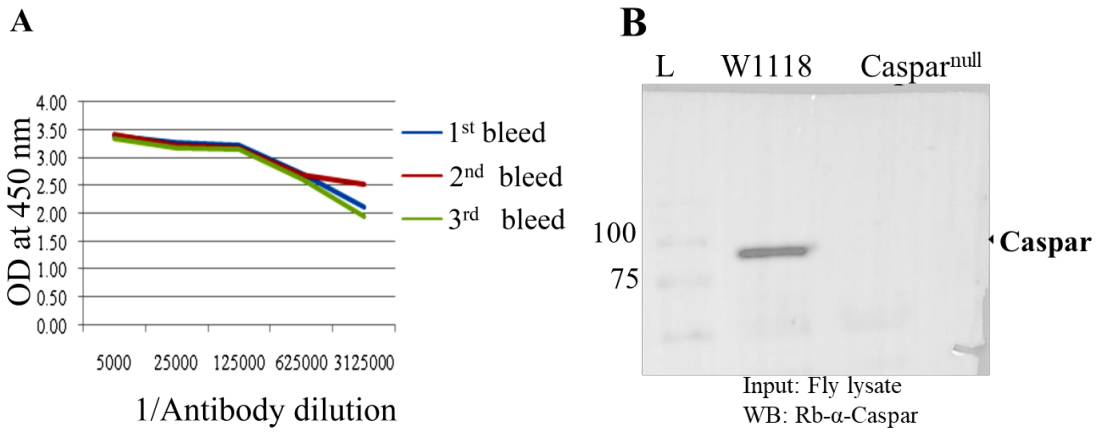

Figure 4-11: Validation of generated Rb-Anti-Caspar antibody. (A) Indirect ELISA. All the bleeds collected during antibody production were tested against purified Caspar in indirect ELISA. All the bleeds showed binding with the purified Caspar. Image Courtsey: Bioklone (B) Western Blot analysis. Caspar antibody was tested on Control and Caspar-null fly lysates. Conditions used were: 1:20,000 dilution in 5% milk, overnight at 4 °C. Band specific to Caspar is observed in control lysate but is not present in the Casp-null fly lysate, confirming specificity of the antibody.

The antibody was also validated by knockdown and over-expression of Caspar in wing disc using *Apterous*-Gal4. Neel, a 3rd year BS/MS student from lab standardized conditions in which the antibody works in IHC. The conditions that best worked for IHC: 1:500 dilution, 1XRoche blocking reagent, overnight at 4 °C. Over-expression of Ha-tagged Caspar showed co-localization of Caspar antibody staining with HA-staining as compared to control. On the other hand, when Caspar was knocked down, the staining with Anti-Caspar antibody also diminished, confirming specificity of the antibody in IHC (**Figure 4.12B**).

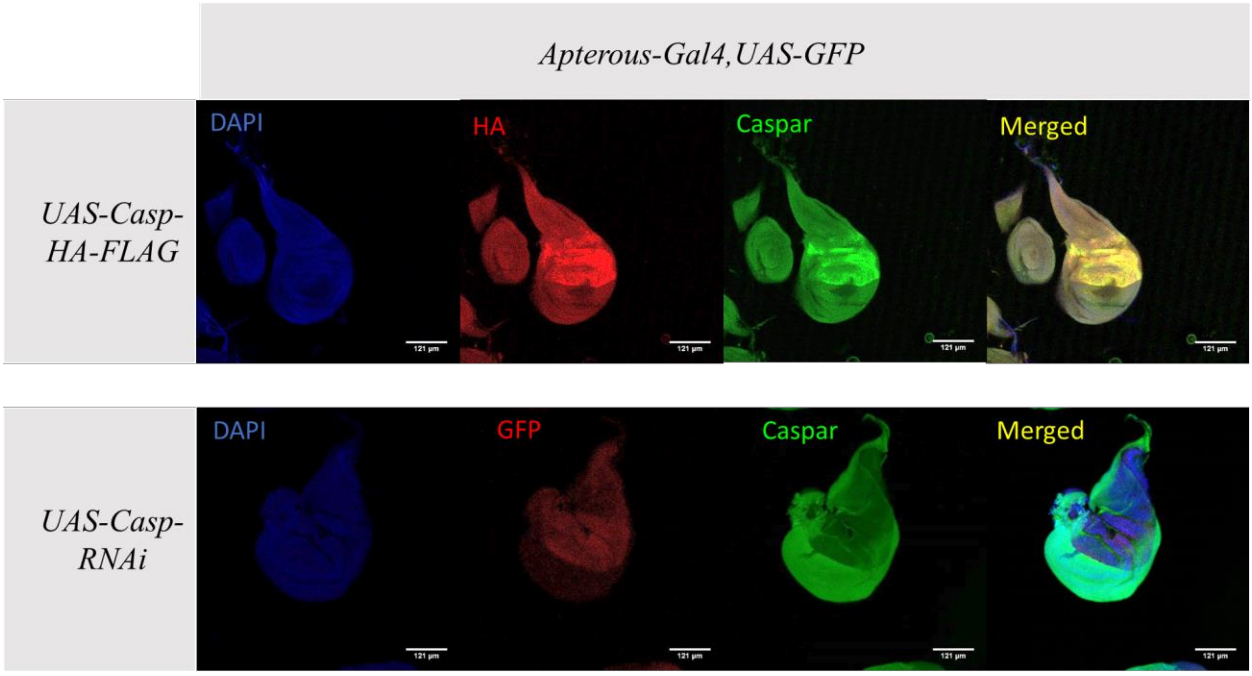

Figure 4-12: Confirming specificity of antibody using IHC. Caspar was over-expressed (UAS-Caspar-HA-FLAG), upper panel or knockdown (UAS-Caspar-RNAi), lower panel, using Apterous-Gal4. Apterous expresses only in cells of dorsal compartment of wing. This allows over-expression of Caspar only in the dorsal compartment as confirmed by HA-staining (B). Caspar antibody also shown enhanced staining in the same compartment (C), (D). Knockdown of Caspar using Apterous-Gal4, UAS-GFP shows diminished staining with Caspar antibody (G) in the compartment expression GFP (F), (H). Both over-expression and knockdown of Caspar, thus, help confirm specificity of the in-house generated antibody. Data Courtesy: Neel Wagh

Experiments to understand more about tissue-specific expression and sub-cellular localization of endogenous Caspar using the generated antibody are on-going.

4.4.5. Generation of Caspar^{K551R} using CRISPR-Cas9 based mutagenesis.

For understanding biological effects of SUMOylation of a given protein, it is necessary that the expression pattern is the same as the endogenous protein and the levels of wild-type and mutant protein are comparable. This removes any artefacts due to difference in levels or expression patterns. . Post-translational modifications can modulate subtle changes which can be missed in over-expression systems. The application of CRISPR-Cas9 mediated site-directed mutagenesis at the genomic locus allows to retain the natural expression patterns and regulation. This led me do use CRISPR-Cas9 technology to generate SUMO-deficient variant of Caspar (Caspar^{K551R}).

Generation and screening of Caspar$^{K551R.}$ There are three components to CRISPR-Cas9 based mutagenesis: Cas9 to generate a DNA double strand break, gRNA to guide Cas9 to target site, and ssODN as template for homologous recombination based repair. To generate Caspar^{K551R}, gRNA was designed very close to the site of desired mutation, facilitating DNA break near the mutation site. The replacement single stranded DNA (ssODN) template carrying K551R mutation and a newly introduced BssHII restriction enzyme target sequence at the mutation site is provided along with Cas9 and gRNA. This allows DNA break repair by homologous recombination using the provided template, thus, generating K551R mutation in Caspar. Details of design, gRNA cloning in pBFv.U6 and generation of transgenic lines is attached in Appendix III. The transgenic flies expressing gRNA is crossed to flies expressing Cas9 and embryos expressing Cas9 and gRNA are collected. In these embryos, ssODN, single stranded DNA template containing K551R and novel restriction site included in at site of mutation was injected. The flies that emerged from these embryos were used for screening of K551R mutation.

A

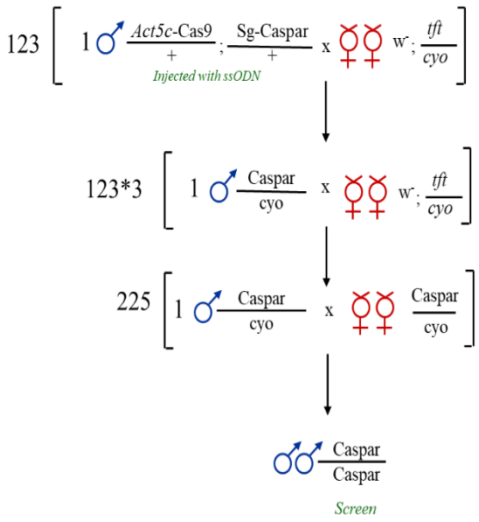

B

	Event	What's happening	Numbers	PCR Screen
1	Cross	Sg2-Caspar X Actin5c-Cas9		
2	Embryo collection	Inject with Caspar^{K551R} HR ssODN	320 embryo injected and distributed in 4 vials	
3	Hatched flies from the vials: Collect males; Ignore females	Cross to the balancer	120* (1 male X w-;*tft/cyo*) ***120 Primary lines***	120 males used for PCR and BssII digestion. **No Hits**
4	Use 120 Primary lines	3 lines per primary line is generated	120*3*(1 male X w-;*tft/cyo*)	
5	103*3**(1 male X w-;*tft/cyo*) *Balanced lines*	17 sterile males	**309 Secondary lines** (labelled as A/B/C per primary line)	225 mlaesused for PCR and BssII digestion.
6	PCR and RE screen for all Secondary balanced lines	**positive lines identified**	**2**	Yes
7	Confirmation of desired mutation	PCR and sequence the genomic locus for muation	2	**Confirmed mutants**

Figure 4-13: Schematic of genetics for screening and balancing of Caspar^{K551R} flies. (A) Genetics of balancing Caspar^{K551R} flies. 123 injected individual males were crossed with white eyed 2nd chromosome balancer line. From F1 generation, 3 males from each male progeny were separately balanced using white eyed 2nd chromosome balancer (123*3). Single homozygous balanced fly from each cross (225) were used for mutation screening. **(B) Summary of the generation and screening of Caspar^{K551R} flies.** Table describing step-wise generation of the caspar^{K551R} using CRISPR-Cas9 methodology and screened by PCR and restriction digestion.

Strategy for screening Caspar^{K551R} mutants included genomic PCR followed by restriction digestion of the PCR product with unique enzyme BssHII, included at the site of mutation generating two DNA fragments of 300bp and 250bp. I tried screening the injected males from the first step but did not find any mutants. This is because restriction digestion requires the presence of target sequence on both the DNS strands. If the mutation is present only on one chromosome in the injected male, a mixed PCR product of wild-type and mutant sequence will be obtained. This PCR product would have a small population mutant product , but the digestion would be too faint to detect. For this, I decided to make pure lines from each injected male. Genomic DNA isolated from these males was used as template for PCR and screened by digestion with BssHII. I identified 2 mutants from a screen of 225 flies (**Figure 4.14**).

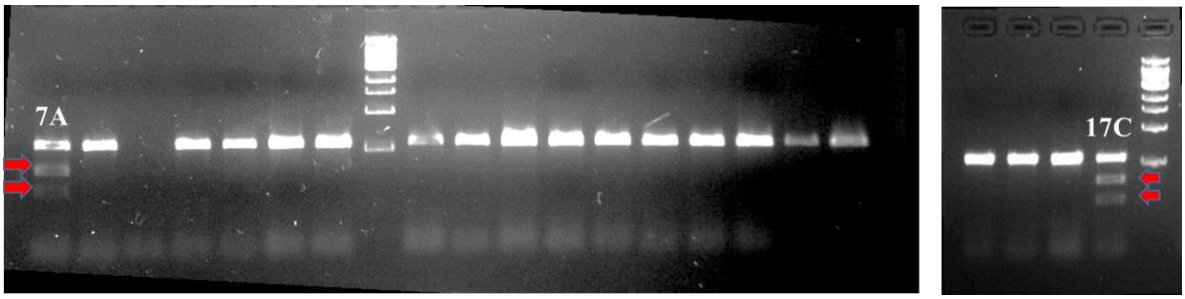

Figure 4-14: Screening of flies for Caspar^{K551R} mutation. Genomic DNA from 225 balanced homozygous males was isolated and used as template for PCR using *caspar*-specific primers generating product of 550bp. The PCR product was then digested with BssHII. PCR products from two of the 225 screened lines showed digestion with BssHII and bands at 250bp and 300bp were obtained. This indicated mutation at desired location. The K551R mutation in these PCR products were further confirmed by sequencing.

Caspar expression was confirmed from the two identified mutants using quantitative RT-PCR (**Figure 4.15B**) and Western using in-house generated antibody (**Figure 4.15A**). Both the mutant lines showed near equal Caspar expression. The Western blots also confirmed expression of full-length Caspar. SUMOylation in some cases is known to affect stability of proteins. In case of Caspar, however, the sumo-deficient variant did not show stability issues in normal conditions. It would be interesting to check stability of mutant Caspar in stress conditions. These Caspar^{K551R} mutants will be used for further experiments.

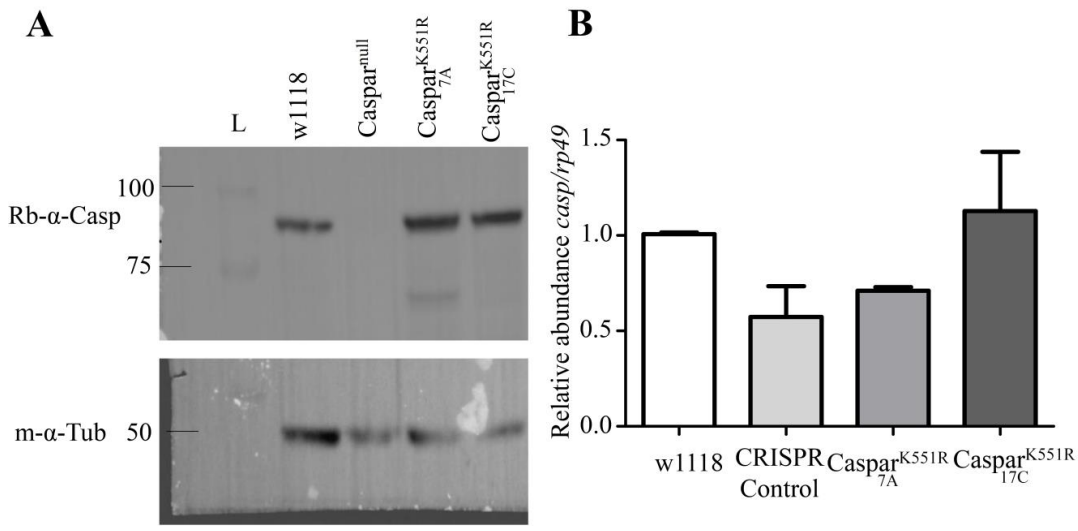

Figure 4-15: CRISPR-Cas9 generated CasparK551R flies show comparable levels of Caspar. (A) Western blot analysis confirming expression of Caspar. Lysates from wild-type, Caspar-null and Caspar^{K551R} mutants, labelled (7A and 17C) were processed, run on SDS-PAGE gel and probed with anti-Caspar antibody. Band corresponding to Caspar were observed in all lysates except Caspar-null. Both the mutants showed expression of full-length Caspar at levels comparable to wild-type (WT). (B) Quantitative RT-PCR showed *caspar* expression almost equal to wild type. A control line from the CRISPR-Cas9 experiment which did not have the mutation, was also used. The fold expression was normalized to *rp49*. Graph was plotted using GraphPad 5.0 and analyzed using 1-Way ANOVA and no significant difference was seen.

4.4.6. Biological significance of SUMOylation of Caspar.

4.4.6.1 *Caspar^{K551R} mutant flies shows reduced life-span post infection*. Earlier report indicated that over-expression of Caspar reduced life-span of flies post infection (Kim et al., 2006). For SUMO-deficient mutants flies, I started by checking the effect of infection on life-span in these mutants. A set of 100 wildtype and Caspar^{K551R} flies were pricked with culture of *E.coli* grown overnight and another set was used as unpricked control. The flies were reared at 25 °C and transferred every 2 days to fresh food vial. The SUMO-deficient flies showed shortened life-span (Median survival = 30 days) when infected as compared to control infected flies (Median survival = 44 days). The uninfected mutants also show increased lethality rate (Median survival = 34 days) as compared to uninfected control flies (Median survival = 46 days) (Figure16A).

(**Figure 4.16A**).

4.4.6.2 *Caspar^{K551R} mutant flies show defective antimicrobial peptide synthesis*.

Caspar is a negative regulator of the IMD pathway. It blocks relish cleavage and inhibits synthesis of *attacins and dipterecin*. In order to understand if the shortened life-span post infection in these mutants is indeed a result of hampered immune response, I checked synthesis of *dipterecin* using quantitative RT-PCR. 1-3 day old control and mutant flies were pricked with overnight grown *E. coli* culture. After 6h of infection, RNA from infected and uninfected flies was isolated using Trizol®, cDNA was synthesized and used for qRT-PCR. The infected SUMO-deficient mutant flies show significant reduction in *dipterecin* synthesis compared to the infected control flies (Figure13B). In absence of infection as well, the basal levels of *dipterecin* were reduced in these mutants.

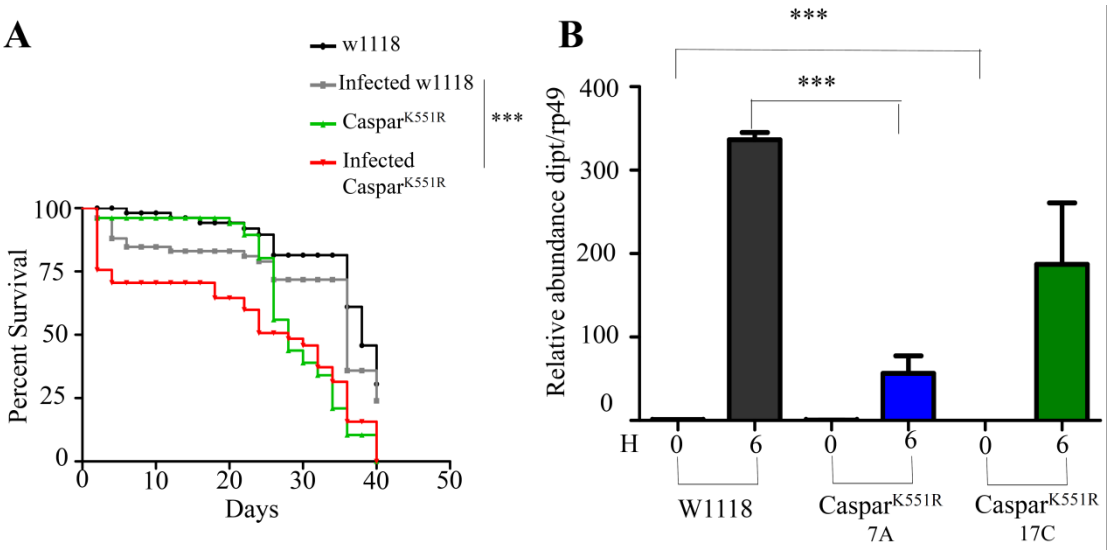

Figure 4-16: Caspar^{K551R} are more susceptible to gram-negative infection. (A) Caspar^{K551R} show reduced life-span post infection. 100 flies from each genotype were used. The 'infected' set for each genotype was pricked with overnight grown culture of *E. coli*. Flies were maintained at 25 °C and fresh food was provided every alternate days. Lethality as monitored every 2nd day. Caspar^{K551R} flies had reduced life-span as compared to control flies. The graph was plotted using GraphPad 5.0 and analyzed by Long-Rank test for trend. **(B) Caspar^{K551R} show significant decrease antimicrobial peptide production.** Total RNA was isolated from 5 control and infected wild-type and mutant flies and cDNA was synthesis. Antimicrobial peptide response for these flies was checked using qRT-PCR. The mutants showed significant reduction in *dipterecin* transcripts as compared to control. The experiment was done in biological triplicate. Graph was plotted using GraphPad 5.0 and analyzed by 1-Way ANOVA.

4.4.6.3 *Caspar^{K551R} / Caspar-null flies show enhanced bacterial clearance defects*.

Homozygous Caspar^{K551R} flies show altered immune response. In order to confirm that these phenotypes are specific to the mutation in Caspar, Caspar^{K551R}/Caspar-null flies were tested for

immunity defects. At first, expression of Caspar in these flies was checked using Western blot and qRT-PCR. As expected, Caspar^{K551R}/Caspar-null flies showed lowered levels of Caspar than wild-type and Caspar^{K551R}/Caspar^{K551R} flies (**Figure 4.17A, B**). These flies also showed immune defects as seen by reduced ability to clear bacterial load (**Figure 4.18A, B**).

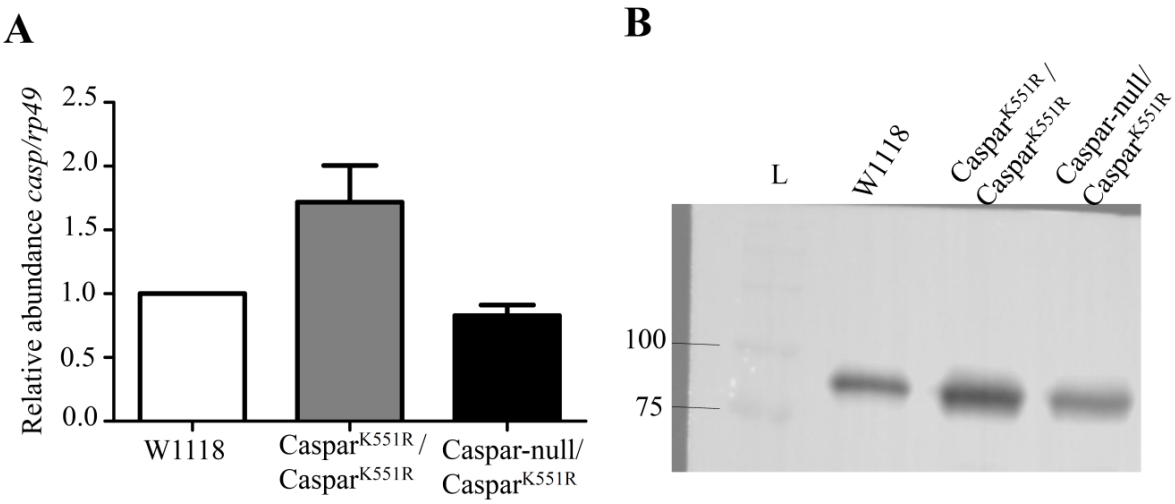

Figure 4-17: Caspar expression in different Caspar^{K551R} allelic combinations.(A) Quantitative RT-PCR for *caspar*. 5 flies from each genotype were used for qRT-PCR. Total RNA was isolated and cDNA was synthesized**.** *caspar* expression was quantitated and normalized to *rp49*. The experiment was done in biological triplicate with 5 flies per replicate. Graph was plotted using GraphPad 5.0 and analysis was done with 1-Way ANOVA. No significant difference was observed between w1118 and Caspar^{K551R}**. (B) Western blot confirming Caspar expression.** Protein was isolated from 5 flies per genotype, processed with Laemmli buffer and proteins were separated using SDS-PAGE. Western blot analysis was done using Rb-α-Caspar antibody.

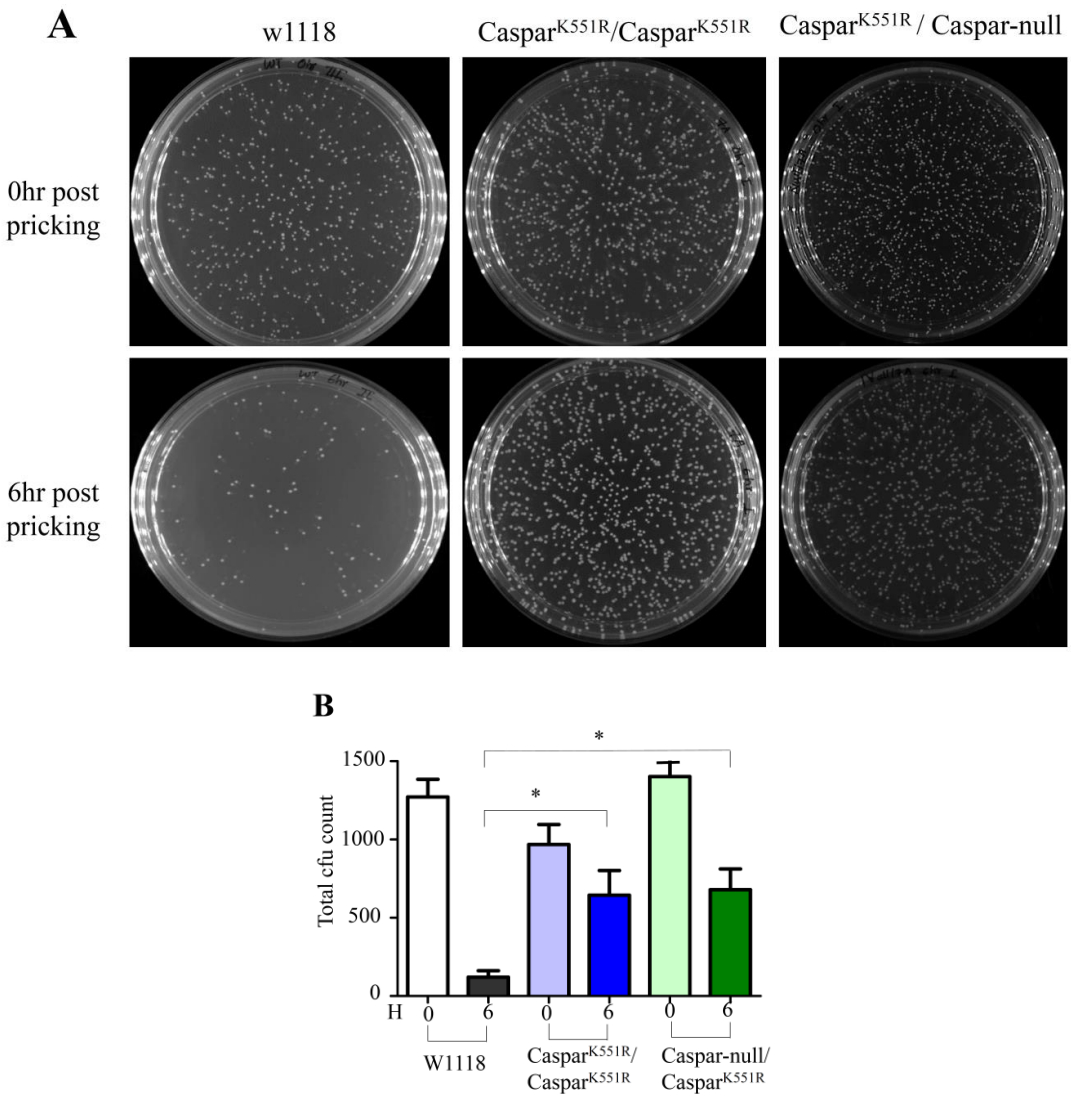

Figure 4-18: Caspar^{K551R} decreases bacterial clearance ability of *Drosophila*. (A) Representative images of bacterial clearance assay. Control and SUMO-deficient Caspar mutant flies were infected with overnight grown ampicillin resistant *E. coli* culture. One set of flies were surface sterilized immediately after pricking, crushed in 100ul LB and plated on LA plated with ampicillin. The bacterial colonies were counted post 24h incubation at 37 °C. This was the 0hr (initial load) reading. The initial load in all genotypes was comparable. The other set of flies were surface sterilized 6h post pricking, processed similar to 0h and total colony count was taken. (B) Quantitation of bacterial clearance assay. The plates were imaged and the images were processed using ImageJ particle analysis tool. The experiment was done in biological triplicate with 4 flies per replicate per genotype. Graph plotted using GraphPad 5.0 and analyzed by 1-Way ANOVA.

4.4.6.4 *Caspar^{K551R} mutants have shortened life-span under stress conditions*.

While working with Caspar^{K551R}mutants, I observed that these mutants are not able to handle stress conditions like starvation and high temperature. To confirm my observation, I checked life-span of these mutants under stress conditions. Adult 1-2 day old 60 flies of control, homozygous Caspar^{K551R} and Caspar^{K551R}/Caspar-null were transferred to 29 °C and lethality was monitored every alternate day. I observed significant reduction in life-span for mutant flies as compared to control under high temperature stress. While the Control flies showed minimal lethality, homozygous Caspar^{K551R}/Caspar^{K551R} flies had median survival of 24 days while the Caspar^{K551R}/Caspar-null flies had median survival of only 8 days (**Figure 4.19A**). Life-span for Caspar^{K551R}/Caspar^{K551R} flies was also affected when flies were reared on sucrose-only media (**Figure 4.19B**). Control flies survived only for 14 day under these conditions. Even though the difference in median survival of control and mutant flies is one day, the mutant flies start dying as early as day 2 and lethality accelerates each day. This phenotype suggested defective storage of energy reservoirs. As described in the next chapter, lipids play critical roles in energy storage and homeostasis. Therefore, I decided to compare total cellular lipid content in Control, Caspar^{K551R}/Caspar^{K551R} and Caspar^{K551R}/Caspar-null flies. I isolated total lipids from 5 flies per genotype and ran these on silica TLC plate. The lipids were visualized using phosphomolibdic acid. I observed decrease in Monoalk(en)yl diacylglycerol (MeDAG) (**Figure 4.20A**). These ether lipids are synthesized by peroxisome specific alkyl-DHAP synthase, known as alkylglycerone-phosphate synthase (*agps)*, in flies, and stored in lipid droplets. MeDAG levels vary between different cell types and depend on lipid droplet – peroxisome interaction. Decrease in MeDAG levels is correlated with decrease in peroxisomes (Bartz, Li et al. 2007). Interestingly, reduced peroxisome numbers show impaired innate immune response and shortened life-span post infection (Di Cara, Sheshachalam et al. 2017). This could suggest a link between Caspar SUMOylation and peroxisomal regulation.

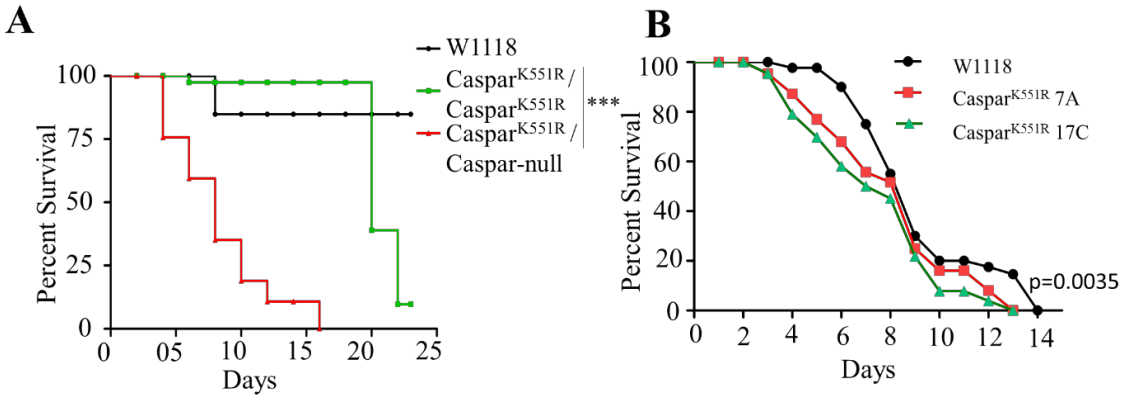

Figure 4-19: Caspar^{K551R} show reduced life-span under stress conditions. (A) Survival analysis of control, *Caspar^{K551R}/Caspar^{K551R} and Caspar^{K551R}/Caspar^{-null}* flies at 29 °C shows dramatic reduction in SUMO-deficient Caspar flies as compared to control. Mean survival for *Caspar^{K551R}/Caspar^{K551R}* was 24 days while for *Caspar^{K551R}/Caspar^{-null}* was just 8 days. 60 flies per genotype were used for the analysis and plotted using GraphPad 5.0. Significance was calculated using Log-Rank test for trend. p<0.0001 **(B)** Survival of Control and *Caspar^{K551R}/Caspar^{K551R}* flies in sucrose only media was measured with 160 flies per genotype. Although both control and mutant flies died within 15 days, the mutants die faster in early days of the assay ("Gehan-Breslow-Wilcoxon Test" p = 0.0008).

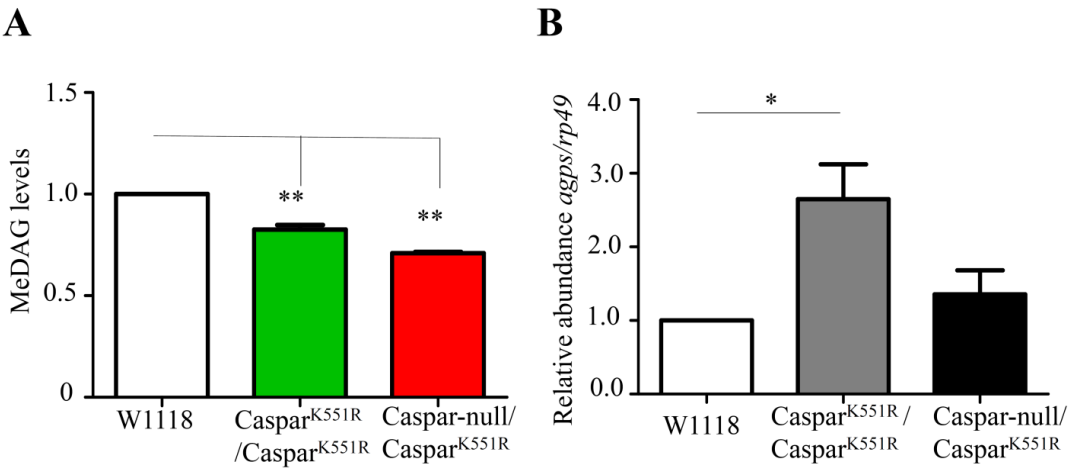

Figure 4-20: Caspar^{K551R} have reduced levels of MeDAG. (A) Quantitation of MeDAG from TLC. Total cellular lipids were isolated from 5 flies per genotype per replicate. The isolated lipids were run on silica TLC plate and visualized using phosphomolibdic acid. The lipids were quantitated using ImageJ and plotted using GraphPad 5.0. The data was analyzed by 1-Way ANOVA. ** = p < 0.05 **(B) qRT-PCR for *agps*.** Total RNA was isolated from 5 flies per genotype per replicate and cDNA was synthesized. The relative levels of *agps* were calculated by normalizing to r*p49*. Graph plotted using GraphPad 5.0. Data was analyzed by 1-Way ANOVA. * = p<0.05

4.5. DISCUSSION

NF-kB signaling is crucial for *Drosophila* development and immune function. The IMD/ NF-kB pathway is activated in response to infection by gram-negative bacteria. Tight regulation of immune pathways is important not only for robust immune response but also for normal development of the fly. Any perturbation in this regulation causes a plethora of developmental defects and/or lethality. Such regulation occurs at transcriptional as well as post-translational level.. In the case of the IMD pathway, SUMOylation of IRD5 regulates IMD pathway activation (Fukuyama, Verdier et al. 2013). Knockdown of SUMO causes dysregulation of innate immunity in flies Although various reports (Bhaskar, Valentine et al. 2000, Chiu, Ring et al. 2005, Fukuyama, Verdier et al. 2013), confirm the role of SUMOylation in the regulation of *Drosophila* immunity, only a couple of studies demonstrate target-specific role of SUMOylation in this regulation and its biological significance. Our group has earlier published a report on immune-specific SUMO proteome in which approximately 700 proteins which change their SUMOylation status in response to infection were identified. This list of proteins comprises direct SUMOylation targets and their interactors, including proteins that belong to the Toll and IMD pathways. We identified Caspar, a regulator of the IMD pathway activation, as a direct target of SUMOylation at K551. We have shown that stress modulates Caspar SUMOylation in S2 cells (Handu, Kaduskar et al. 2015). To understand the biological significance of Caspar SUMOylation, in the first step, I demonstrated that Caspar is indeed SUMOylated in adult flies. Caspar-null flies are homozygous lethal. This suggests the role of Caspar in *Drosophila* early development, independent from its role in immunity. I showed that SUMO-deficient Caspar can rescue lethality of Caspar-null flies using a classical genetics-based approach involving null-rescue experiments. This indicates that SUMOylation of Caspar may not have critical contribution to function of Caspar in early development. Recent technological advancements in genome editing using CRISPR-Cas9 have helped in understanding the role of post-translational modifications. This technique allows site-specific mutagenesis of the genome DNA. This ensures endogenous expression and regulation of the mutant protein. I utilized this technique to successfully generate genome-edited SUMO-deficient Caspar ($Caspar^{K551R}$) flies. The mutant was validated by a Caspar-specific antibody that we generated in our lab.

Caspar^{K551R} flies showed shortened life-span and lowered *dipterecin* production compared to control flies, indicating weak immune response against infections by gram-negative bacteria. Similar phenotypes are seen by over-expression of Caspar (Kim, Lee et al. 2006). This suggests that Caspar^{K551R} acts as potent form of Caspar, negatively regulating immune response even after infection. Caspar^{K551R}/Caspar-null flies show more severe immunity defects, confirming specificity of the phenotypes seen in Caspar^{K551R} /Caspar^{K551R} flies.

In addition to shortened life span and defects in antimicrobial peptide synthesis and bacterial clearance, Caspar^{K551R} /Caspar^{K551R} flies also showed reduced levels of MeDAGs. These lipids are synthesized by peroxisome-specific enzymes and stored in lipid droplets. Reduction in the levels of these lipids is associated with reduced peroxisome number or activity (Bartz, Li et al. 2007). According to a recent report, the activity of peroxisomes is associated with robust immune response through phagocytosis (Di Cara, Sheshachalam et al. 2017). Caspar^{K551R} /Caspar^{K551R} flies show dramatic reduction in phagocytosis, resulting in ineffective bacterial clearance. It will be interesting to investigate the status of peroxisomes in the SUMO-deficient Caspar flies.

Caspar has been recently identified as a genetic interactor of Iswi in cell cycle regulation by regulating apoptosis. FAF1, a mammalian homolog of Caspar, is already established as a key player in vertebrate cell division and apoptosis. Cell cycle regulation emerged as one of cellular processes regulated by SUMOylation in FlySUMOBas analysis. Although Caspar function in cell cycle regulation is not well characterized, it will be worth investigating the role of Caspar SUMOylation in the context of apoptosis and cell cycle regulation.

4.6. MATERIALS AND METHODS

Cloning in pUASp-attB and generation of transgenic lines: Caspar variants (wild-type, SUMO-deficient) were sub-cloned in pUASp-attB, with N-terminal HA-tag, using restriction digestion–ligation method.

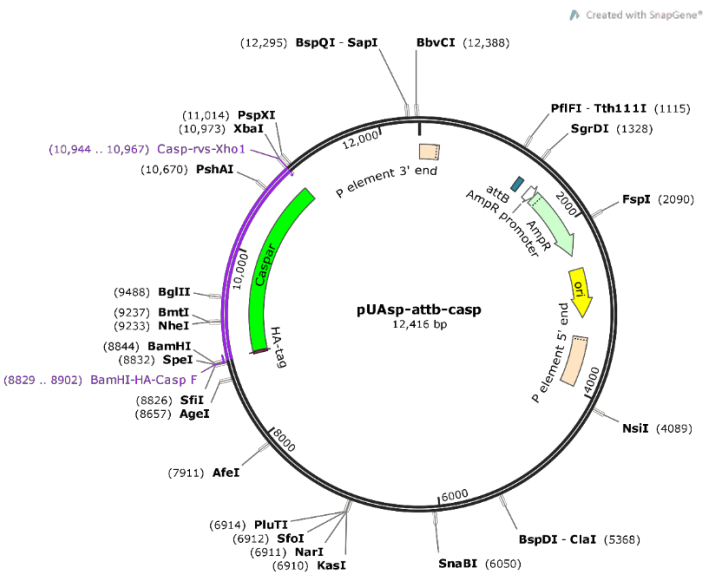

Figure 4-21: pUASp-attB-HA-Caspar vector map. N-terminal HA-tagged Caspar was cloned within the MCS between BamH1 and Xho1 restriction sites.

Cloning in pET45b vector for expression of 6X-His tagged Caspar: Caspar and Caspar^{K551R} were cloned in bacterial expression vector pET45b using restriction digestion cloning.

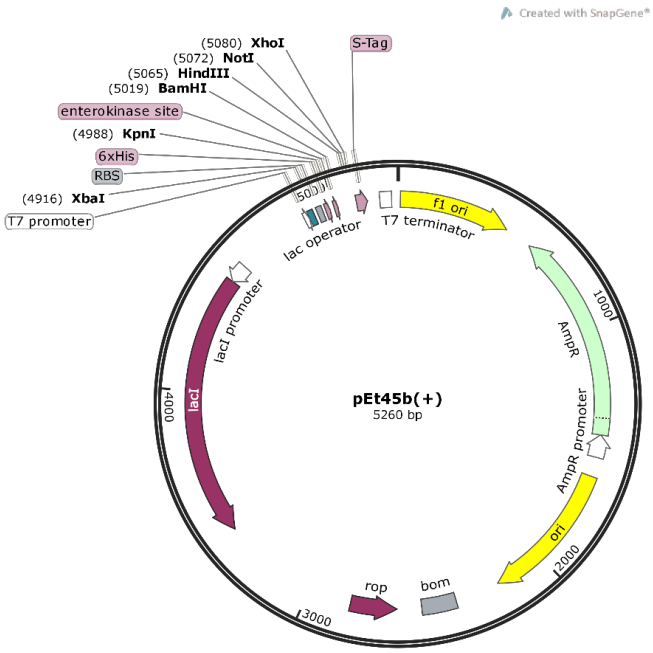

Figure 4-22: pEt45b Vector map.

Fly stocks: UAS-Caspar-HA-FLAG lines was obtained from NCBS-DPiM collection. Daughterless-Gal4 line was obtained from Bloomington stock center. All the transgenic lines were

injected at NCBS fly facility. All flies were maintained on normal media at 25 °C unless otherwise stated.

FPLC:

Western blot analysis: Five male flies were used to make whole body lysates using 100 µl 1X SDS-PAGE loading buffer as a lysing agent. The lysate was boiled at 95 °C for 10 min followed by centrifugation at 10000 g for 20 min. The processed proteins were used for Western blot analysis. Rb-anti- Caspar was used in 1:20,000 dilution in 5% Milk. Mouse-Anti-Tubulin (Sigma) antibody was used in1:20,000 dilution.

Survival Analysis. For survival assays, 1–3-day-old males from each genotype were maintained on standard medium at 25 °C or 29° C. For survival post infection, flies were pricked with 20 h-old culture of ampicillin-resistant *E*. *coli* (DH5α). Dead flies were removed every day and food vials were changed every alternate day. Surviving flies were scored till all the flies were dead, at both temperatures. Kaplan–Meier and Log Rank tests were performed using GraphPad Prism 5.0 to analyze the data. (Lemaitre, Bruno, et al, 1995, Lemaitre, Bruno, et al. 1996 Regan, Regan, J. C et al 2016).

Bacterial clearance assay. 1–3-day-old male flies from each genotype were pricked with *E*. *coli* and maintained at 25 °C for 6 h. Four live flies from each genotype were surface sterilized using 70% ethanol. Flies were air-dried and washed twice with autoclaved MQ under sterile conditions, crushed in 100 µl of LB and plated on ampicillin-containing agar plates. The number of bacterial colonies was counted using ImageJ particle analysis tool and it was plotted in the form of a histogram. Results were analyzed using One-way ANOVA.

Lipid extraction for thin layer chromatography (TLC): Lipid isolation was done using a modified Folch extraction protocol (Kamat, Camara et al. 2015). Briefly, five whole adult males were crushed in 1 ml DPBS in a glass vial, 1 ml methanol was added, and the mixture vortexed. Thereafter, 2 ml of chloroform was added to and the mixture was further vigorously vortexed. The sample was then centrifuged at 2800 g for 5 min to separate the aqueous and organic phases. The organic phase (bottom) containing lipids was collected in a clean glass vial. To selectively isolate phospholipids, the aqueous layer was acidified using 2.5% v/v formic acid, and re-extracted using 2 ml choloroform, and the two phases were separated by centrifugation at 2800 g for 5 min. The

two organic phases were pooled and dried using N_2 gas. The extracted lipids were subjected to TLC analysis. TLC was performed using mobile phase of Hexane:Ethylacetate:Acetic acid in 80:20:1 ratio. The plate was developed using 20% phosphomolybdic acid (PMA) in ethanol by heating at 95 °C for 1-2 min.

Quantitative real time PCR: Total RNA was extracted from all the samples 6 h post infection (Direct-zol™ RNA MiniPrep Cat. No. R2050). cDNA was then synthesized from 1 ug total RNA using High capacity cDNA synthesis kit (Cat No. 4368814). Quantitative PCR experiments were accomplished with a Realplex^2 and using SYBR Green (KAPA CatNo.# KK4601). Relative gene expression was calculated after normalization to the control RpL32/rp49 mRNA.

4.7. PERMISSIONS

Two images were reproduced from published sources. For both the images, publishing journal grants permission for non-commercial use of material published in their journals.

BIBLIOGRAPHY

Bartz, R., W. H. Li, B. Venables, J. K. Zehmer, M. R. Roth, R. Welti, R. G. Anderson, P. Liu and K. D. Chapman (2007). "Lipidomics reveals that adiposomes store ether lipids and mediate phospholipid traffic." J Lipid Res **48**(4): 837-847.

Bhaskar, V., S. A. Valentine and A. J. Courey (2000). "A functional interaction between dorsal and components of the Smt3 conjugation machinery." J Biol Chem **275**(6): 4033-4040.

Chiu, H., B. C. Ring, R. P. Sorrentino, M. Kalamarz, D. Garza and S. Govind (2005). "dUbc9 negatively regulates the Toll-NF-kappa B pathways in larval hematopoiesis and drosomycin activation in *Drosophila*." Dev Biol **288**(1): 60-72.

Di Cara, F., A. Sheshachalam, N. E. Braverman, R. A. Rachubinski and A. J. Simmonds (2017). "Peroxisome-Mediated Metabolism Is Required for Immune Response to Microbial Infection." Immunity **47**(1): 93-106 e107.

Fukuyama, H., Y. Verdier, Y. Guan, C. Makino-Okamura, V. Shilova, X. Liu, E. Maksoud, J. Matsubayashi, I. Haddad, K. Spirohn, K. Ono, C. Hetru, J. Rossier, T. Ideker, M. Boutros, J. Vinh and J. A. Hoffmann (2013). "Landscape of protein-protein interactions in *Drosophila* immune deficiency signaling during bacterial challenge." Proc Natl Acad Sci U S A **110**(26): 10717-10722.

Handu, M., B. Kaduskar, R. Ravindranathan, A. Soory, R. Giri, V. B. Elango, H. Gowda and G. S. Ratnaparkhi (2015). "SUMO-Enriched Proteome for *Drosophila* Innate Immune Response." G3 (Bethesda) **5**(10): 2137-2154.

Kamat, S. S., K. Camara, W. H. Parsons, D. H. Chen, M. M. Dix, T. D. Bird, A. R. Howell and B. F. Cravatt (2015). "Immunomodulatory lysophosphatidylserines are regulated by ABHD16A and ABHD12 interplay." Nat Chem Biol **11**(2): 164-171.

Kim, J. H., M. E. Park, C. Nikapitiya, T. H. Kim, M. B. Uddin, H. C. Lee, E. Kim, J. Y. Ma, J. U. Jung, C. J. Kim and J. S. Lee (2017). "FAS-associated factor-1 positively regulates type I interferon response to RNA virus infection by targeting NLRX1." PLoS Pathog **13**(5): e1006398.

Kim, M., J. H. Lee, S. Y. Lee, E. Kim and J. Chung (2006). "Caspar, a suppressor of antibacterial immunity in *Drosophila*." Proc Natl Acad Sci U S A **103**(44): 16358-16363.

Lee, J. J., J. K. Park, J. Jeong, H. Jeon, J. B. Yoon, E. E. Kim and K. J. Lee (2013). "Complex of Fas-associated factor 1 (FAF1) with valosin-containing protein (VCP)-Npl4-Ufd1 and polyubiquitinated proteins promotes endoplasmic reticulum-associated degradation (ERAD)." J Biol Chem **288**(10): 6998-7011.

Lee, K. Z. and D. Ferrandon (2011). "Negative regulation of immune responses on the fly." EMBO J **30**(6): 988-990.

Park, M. Y., J. H. Moon, K. S. Lee, H. I. Choi, J. Chung, H. J. Hong and E. Kim (2007). "FAF1 suppresses IkappaB kinase (IKK) activation by disrupting the IKK complex assembly." J Biol Chem **282**(38): 27572-27577.

Song, S., J. J. Lee, H. J. Kim, J. Y. Lee, J. Chang and K. J. Lee (2016). "Fas-Associated Factor 1 Negatively Regulates the Antiviral Immune Response by Inhibiting Translocation of Interferon Regulatory Factor 3 to the Nucleus." Mol Cell Biol **36**(7): 1136-1151.

Chapter 5

Age dependent regulation of the *Drosophila* innate immune response by regulation of Sphingolipid homeostasis

5.1. SUMMARY

Mt2 mutant flies have shortened lifespan and an altered immune response. Their ability to defend themselves from bacterial infections declines with age. On day 2, flies are mildly deficient in their ability to clear infection. By day 15 however, Mt2 mutant flies show an 80% reduction in the ability to fight with bacterial infections (Varada et al., 2017, Ph.D. Thesis) via both the cellular as well as humoral response. In Mt2 mutants, using quantitative lipidomics, I observed age-associated decrease in TAG content and accumulation of bioactive lipids S1P and ceramides in 15-day old flies. Mt2 mutant flies also show decreased Sply activity causing lipid homeostasis defects. The disturbance of lipid homeostasis correlates strongly with the decline in immune function, suggesting that Mt2 may function to regulate lipid homeostasis, which in turn is critical for a robust immune response in an ageing animal.

5.2. ABBREVIATIONS

Mt2: DNA methytransferase 2; LD: lipid droplets; TAG: triacylglycerides;
CE: cholesterol esters; DGAT: diacylglycerol acyltransferases;
ACAT: acyl-CoA:cholesterol acyltransferases; IP: inositol phosphate
S1P: spingosine-1-phosphate; C1P: ceramide-1-phosphate
PE: phosphoethanolamine; PIP2: phosphatidylinositol 4,5-bisphosphate
GPI: glycosylphosphatidylinositol; TLC: thin layer chromatography

5.3. INTRODUCTION

DnMt2 (called *Mt2* here forth), a DNA/RNA methyltransferase (MT). Vertebrates have multiple DNA MTs, classified as *DnMt1, Mt2, DnMt3a, DnMT3b*, based on their activity and structural features (Okano, Xie, and Li 1998). DnMt1 and DnMt3 are DNA MTs and play crucial roles in regulating epigenetic modifications and transferring these through replication. Mt2, however, is RNA MT, important for tRNA methylation and thus, stability of tRNAs in vertebrates (Tuorto et al. 2015). Deletion of Mt2 has no visible effect on mice under normal conditions. However, their ability to handle stress conditions is significantly hampered. These mutants also show defective differentiation in adipose tissue and Many of the Mt2 mutant defects in mice are seen in combination with mutations in Nsun2, another tRNA MT (Tuorto et al. 2012). This suggests that most of the defects are specific to altered tRNA methylation and Mt2 plays secondary role in tRNA methylation in mice. *Drosophila,* has only a single MT which shows maximum homology with vertebrate Mt2 (Tang et al. 2003). In *Drosophila*, Mt2 is characterized as a DNA-MT, where Mt2 null flies show altered DNA methylation pattern although no direct evidence of Mt2 methylating DNA is available. Recent research, however, suggests that Mt2 might function primarily as a RNA-MT (Goll et al. 2006; Schaefer et al. 2010), with methylation enhancing tRNA stability similar to observations made in mice (Tuorto et al. 2015). *Mt2* null flies ($Mt2^{-/-}$) do not show overt developmental abnormalities and lifespan is near normal under non-stressed conditions. Under stress (Schaefer et al. 2010; Thiagarajan, Dev, and Khosla 2011; Becker et al. 2012), $Mt2^{-/-}$ flies show a shorter lifespan (Lin et al. 2005). Flies grown in overcrowded conditions develop melanotic spots (Durdevic et al. 2013), suggesting disturbances in immune function. Infection studies also suggest that Mt2 plays an important role in acute immune response to *Drosophila* C virus (DCV) by binding to and possibly methylating viral RNA (Durdevic et al. 2013).

While investigating protein profile defects in Mt2 null flies, I observed lowered lipids in these Mt2 mutants. In this chapter, I have tried to investigate this observation in detail and its role in age dependent alteration in immune response seen in these Mt2 mutants.

Lipids are classically known as energy reserves and building blocks of cells. This notion had overshadowed any possibility that lipids can act not only as structural moieties but also be involved in signaling. As early as 1930, Watson and Mellanby showed that when mice were fed with high-

butter diet, they developed increased susceptibility to tar-induced skin tumors, linking dietary fat to tumorogenesis. (Watson and Mellaby 1930). The quest to investigate the role of lipids in tumor progression significantly contributed to unraveling roles of lipids in immunity.

In 1953, Hokin and Hokin demonstrated that incorporation of ^{32}P into the phospholipids was accompanied with increased secretion of amylase from pancreas. This suggested direct correlation between increased lipid phosphorylation and amylase secretion. This study also lead to the idea that lipids might be important in a signaling pathway that makes the pancreas secrete amylase in response to external stimuli of cholinergic drugs. (Hokin and Hokin 1953). Unfortunately, this study did not bring lipid biology in limelight. The importance of lipids in crucial cellular processes was realized when Khan et al showed that exogenous application of sphingosine, a lipid moiety, inhibits protein kinase C activity, and thereby affects function of platelets (Khan et al. 1991) This study was followed by multiple reports uncovering roles of lipids such as inositol phosphates and sphingosine and its modified forms in various cellular pathways. The last couple of decades have seen an increasing number of studies highlighting the importance of lipids in energy homeostasis and cellular signaling.

Lipids in metabolism: Lipid metabolic pathways are very well conserved from yeast to humans. Lipids are storehouses of energy synthesized mainly during high-fed conditions and metabolized for energy requirements during starvation through β-oxidation in mitochondria or peroxisomes. They are generally stored in the form of lipid droplets (LDs).

LDs are congregations of lipid esters and proteins involved in lipid metabolism encapsulated in a phospholipid monolayer. All cells contain LDs. For example, white adipocytes contain LDs that predominantly comprise triglyceraldehydes (TAGs). The enzymes involved in synthesis of TAGs and CEs, diacylglycerol acyltransferases (DGATs) and acyl-CoA:cholesterol acyltransferases (ACATs), respectively, are a part of the endoplasmic reticulum (ER) membrane. This implies that CEs are synthesized and stored within the ER membrane bilayer. The ER membrane accumulates the lipids to certain extent; however, beyond a certain limit, it pinches off from the ER to form LDs. Evidence for direct regulation of LDs through the ER comes from perturbations in membrane trafficking. Rab18 is an LD-associated Rab, which regulates LD size and volume depending on cellular metabolic state. Rab18 recruitment to LDs is dependent on the metabolic state of LDs and overexpressing Rab18 affects ER-LD dynamics. This suggests regulation of ER–LD interaction

through metabolism (Martin et al. 2005). In *Drosophila*, a link between LD metabolism and regulation comes from Fujimoto and Parton. They identified phosphotidylcholine availability as key factor in maintaining LD size to volume ratio (Fujimoto and Parton 2011). Another example for link between metabolism and LD size came from Peng Li's group, where they showed that mice having a mutation in *cedia*, a gene important for LD size regulation, are lean and show high energy consumption. These mice have low plasma levels of free fatty acids (FFA) and TAG. These mice are also resistant to obesity and diabetes induced by high-fat diet. Interestingly, Cedia localizes not only in LDs but also in the mitochondria, where it interacts with Ucp1 and regulates its activity, thus in turn regulating lipid metabolism, obesity, and diabetes (Zhou et al. 2003).

Lipids being storehouses of energy, it is not surprising that their storage and the metabolic state of the organism, its dietary intake, and growth signals such as insulin and TOR are directly linked.

Lipids and signaling: Besides being directly involved in regulating metabolism and energy supply, lipids are identified as active signaling molecules. Some have even been designated as secondary messengers along with cAMP. These signaling lipids are synthesized when required, have short life span, and act through G-protein coupled receptors. Among the signaling lipids, inositol phosphates and sphingolipids are the important ones.

Inositol phosphates: Inositol phosphates are the first lipids identified to have a direct role in signaling, as demonstrated by Hokin and Hokin. IPs are diverse compounds in which inositol ring is modified by phosphates at three or more sites. They are diffusible molecules formed mainly by phospholipase C (PLC) located in the plasma membrane. They are synthesized by the hydrolysis of lipids within the plasma membrane in response to external stimuli. They act through Ca^{2+} sensitive G-protein coupled receptors located on the ER and trigger the release of intracellular Ca^{2+}. Increased cytosolic Ca^{2+} levels in turn activate PLC. Activated PLC then phosphorylates multiple targets regulating various cellular processes (**Figure 5.1**).

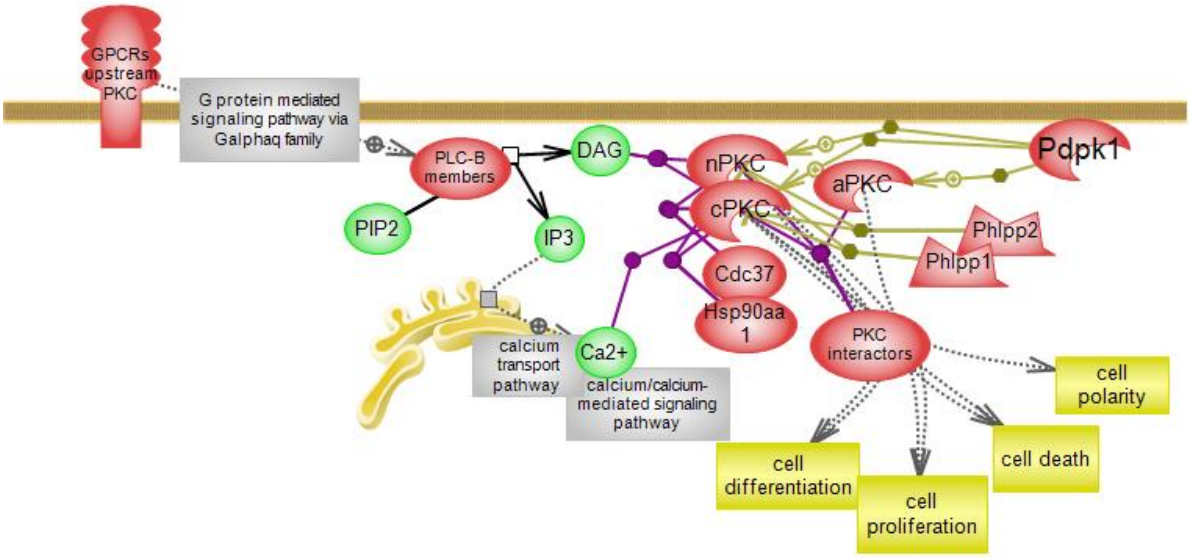

Figure 5-1: Mechanism of intracellular Ca2+ release mediated by IP3: Membrane PIP_2 is converted to IP_3 with the help of membrane-bound PLC. IP_3 then binds to IP_3-sensitive G-Protein coupled receptor located in the ER, which leads to opening of calcium channels. This causes intracellular Ca^{2+} release. The released Ca^{2+}, along with membrane-located DAGs, activates protein kinase C, which in turn phosphorylates downstream substrate proteins. Image reproduced from RGD database (Shimoyama et al. 2015).

Sphingolipids: Sphingolipids are a class of bioactive lipids with sphingosine backbone. They were first identified in 1870 in ethanolic fractions, and were named after the Greek mythological creature "Sphinx", as their functions were difficult to interpret at that point of time. Since then, sphingolipids are attributed to variety of functions.

Sphingosine-1-P (S1P) is synthesized by two isoenzymes Sphk1 and Sphk2. It binds to S1P receptors, a family of G-protein coupled receptors and initiates downstream signaling. S1P is present at very low levels within cells. This regulation is achieved by Sphk1/2 and S1P lyase along with a newly proposed phosphohydrolase.

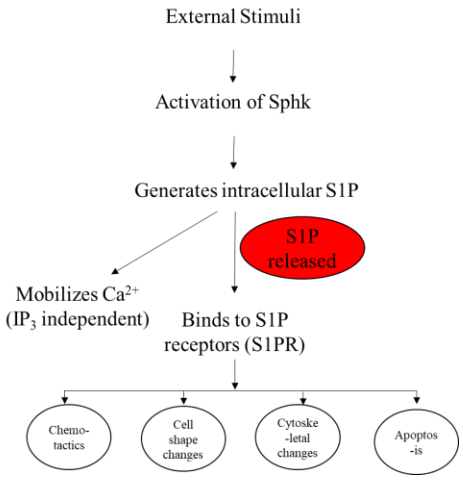

Figure 5-2: Schematics describing S1P signaling: External cues lead to release of S1P, which in turn causes intracellular Ca^{2+} release. Ca^{2+} activates Akt, which then phosphorylates many downstream substrates. S1P, as a ligand, also binds to S1P receptors on different cell surfaces and affects multiple cellular processes such as chemotaxis, survival, and cell shape determination in tissue-specific manner.

S1P regulates multiple cellular processes (**Figure5.2**). It regulates cell–cell and cell–matrix adhesion by regulating PTEN signaling and by disrupting adherent junctions important for the adhesions. It also regulates actin and myosin cytoskeleton remodeling through Rac and Rho GTPases. These processes are important for cell migration and thus, unsurprisingly, S1P is crucial in germ cell migration, immune cell migration, and cancer metastasis. Cell migration is an important process in heart development (Kupperman et al. 2000) and blood vessel formation (Vouret-Craviari et al. 2002); these are also regulated by S1P. S1P also acts in receptor-independent manner to regulate intracellular Ca^{2+}, a mechanism independent of IPs described earlier. S1P activates Ras and ERK signaling independent of S1P receptors. Extracellular addition of S1P is enough to inhibit outgrowths from AV canal cultures (Wendler and Rivkees 2006). It causes neurite retraction and cell rounding in PC12 cells (Van Brocklyn et al. 1999). Regulation of cell morphology is a direct result of regulation of ERM (ezrin-radixin-moesin) family of proteins by S1P and ceramides. While S1P activates ERM proteins by phosphorylation, ceramides lead to dephosphorylation and inactivation. ERM proteins modulate actin cytoskeleton and actin–membrane interaction, thus controlling cell morphology and cell division (Freymuth and Fitzsimons 2017; Adada et al. 2014).

S1P signaling leads to Akt phosphorylation, inhibits NFκ-B activation, and regulates male germ cell apoptosis (Suomalainen, Pentika¨inen, and Dunkel† 2005). In endothelial cells, S1P-induced Akt phosphorylation is essential for their chemotaxis (Lee et al. 2001). Depression patients show

elevated levels of S1P and ceramides. S1P acts through dopaminergic neurons by promoting mitochondrial function and regulating ROS levels (Sivasubramanian et al. 2015). In a different study, S1P inhibits HDACs in specific neurons, causing specific memory and fear extinction in mice (Hait et al. 2014). In *Drosophila*, *sply* mutants show increased cellular apoptosis in ovaries and testes, causing developmental defects (Phan et al. 2007).

These examples show tissue-specific functions of S1P. The levels of S1P are regulated in tissues by regulating S1P lyase expression. S1P lyase is regulated by GATA-like transcription factors. For example, in *Caenorhabiditis elegans,* S1P lyase expression occurs mostly in the gut (Mendel et al. 2003) and altering this expression leads to feeding problems, delayed growth, intestinal damage, and reproductive abnormalities (Mendel et al. 2003); these findings emphasize the role of S1P signaling in animal development.

Ceramides: Ceramides are the most toxic lipids that accumulate in obese individuals. Accumulation of ceramides causes inhibition of IP_3-induced Akt signaling. Inhibition of Akt signaling eventually leads to disruption of many cellular processes (Stratford et al. 2004). Ceramide synthesis manipulation is sufficient to reverse insulin resistance caused by glucocorticoids, inflammation, and high-fat diet. Ceramides also interact with mitochondria in inducing apoptosis by increasing permeability of the membranes. Moreover, inhibition of ceramide synthesis prevents destruction of β-cells in diabetes.

Ceramide synthesis occurs via ceramide synthases (CerS) along with S1P acylation and sphingomyelinases (SMases). CerS are distributed in various tissues in mammals and have tissue-specific functions, as summarized in Table 1.

Table 5-1: Tissue-specific expression of ceramide synthases (CerS) and phenotypes associated with tissue specific knockout of CerS in mice (Park and Park 2015). For example, in the brain, CerS2 knockdown causes demyelination of neurons, whereas in the liver, it leads to increased insulin resistance and fatty liver. On the contrary, CerS6 knockdown in the liver results in increased insulin sensitivity: an effect opposite to that of CerS2 knockdown. CerS3 and CerS4 knockout in skin-specific manner show independent defects.

Ceramide synthase	Tissue expressed	Effects of knockdown
CerS1	Brain	Cerebellar ataxia; Purkinje cell death
CerS2	Brain	Demyelination; Abnormal rhythmic EEG activity
CerS2	Liver	Fatty liver on HFD; insulin resistance, Hepatoadenoma

CerS2	Adrenal Gland	Pheochromocytoma
CerS2	Lung	Macrophage infiltration; susceptible to *Pseudomonas aeruginosa* infection
CerS3	Skin	Transepidermal water loss; vulnerable to *C. albicans* infection
CerS4	Skin	Alopecia; Reduced wax diesters in sebum
CerS5	Brain	Altered behavior
CerS6	Liver	Increased insulin sensitivity

Phosphorylated ceramides (C1P) also act as signaling molecules. Formation of C1P is regulated by ceramide kinases (CerK) and perturbation of CerK by RNAi or chemical inhibitors affects various cellular processes. C1P acts as a mitogen, triggering division of fibroblasts and macrophages. It also regulates apoptosis. C1P causes activation of arachidonic acid (AA) through phospholipase A2, leading to inflammatory response. C1P functions mostly within the cell by moving through the subcellular organelles; however, it also works as a secreted ligand. C1P is identified as a fusogenic agent and is hypothesized to function by altering membrane fluidity; this property facilitates phagosome formation and thus regulates phagocytosis (Hinkovska-Galcheva et al. 2005)

Drosophila Lipids

The first study on *Drosophila* lipids was performed in 1959, in which Wren and Mitchell isolated very complex lipids from 25 ethanolic fractions from flies (Wren and Mitchell 1959). Soon after, in 1967, Alec and colleagues showed that limiting glycerol from fly diet led to increase in hydrocarbons and decrease in glycerides (KEITH 1966); this was the first report to demonstrate diet-induced changes in lipid composition in flies. Butterworth, in 1969, isolated a lipid moiety found only in adult male flies. This lipid accumulated with age and was found only in ejaculatory bud of the male flies. Further, Brain Oliver and colleagues found that male flies have more saturated cholesterol esters while female flies mainly have polyunsaturated ones. These studies suggested sex-specific role for lipids in *Drosophila*.

LDs, as mentioned earlier, are storehouses of lipids and associated proteins. In flies, LDs are associated with histones. LDs are toxic to gram-positive and gram-negative bacteria, and this toxicity acts through the associated histone molecules (Anand et al. 2012; Welte 2015).

Like in mammals, lipid homeostasis is critical for fly development. It is mainly regulated via hormones and transcription factors expressed specifically in the gut. For example, Lemaitre and colleagues showed that a MAP kinase variant, p38c, is expressed specifically in the fly intestine, and it regulates lipid metabolism, oxidative stress, and in turn immune homeostasis along with Atf2. Flies with p38c deletion show lipid accumulation and increased antimicrobial peptide production. This phenotype is similar to obesity induced inflammation seen in humans (Chakrabarti, Poidevin, and Lemaitre 2014). Lipid homeostasis is also achieved by the interplay of multiple nutrient signals. For instance, insulin receptor (InR) interacts with PI3K and leads to Akt activation, which consequently increases glucose uptake and fatty acid and protein synthesis. Insulin also directly regulates fatty acid metabolism by repressing *pudgy*, a gene involved in fatty acid β-oxidation (Liu and Huang 2013). As shown in a study, IP_3R mutant flies tend to store excess fat and become unnaturally obese even on normal diet. This leads to altered fat storage and membrane lipid composition. Interestingly, this phenotype can be rescued by increasing insulin signaling, (Subramanian et al. 2013). The very first example identifying glycosphingolipid metabolism genes involved in critical developmental pathways was demonstrated by Goode and colleagues. They identified two genes, *egghead* and *brainiac*, showing embryonic developmental defects similar to Notch mutants along with some additional defects in polarity and adhesion of follicle cells in flies (Goode, Wright, and Mahowald 1992). These two genes were later shown to be involved in glycosphingolipid synthesis. Recently, genetic screen performed to investigate the genes important in intracellular trafficking of Notch identified lipid metabolism genes like *spt* and *acc*. Both the genes showed defective apoptosis and tissue overgrowth (Kraut 2011). Apart from the abovementioned examples, mutations in many other genes important in lipid metabolism show various defects in fly development. These are summarized in Table 5.2.

Table 5-2: Summary of genes involved in lipid metabolism and phenotypes associated with their mutations (Liu and Huang 2013; Kraut 2011). Mutations in genes involved in lipid metabolism have different phenotypes in different tissues. For example, mutation in DAG kinase improves motor activity in fly Huntington model but causes retinal degeneration in the eye. Many of these mutations mimic mammalian models of lipid-associated disorders, thus making flies ideal model organisms for studying mammalian metabolic disorders.

Gene	Decription	Phenotype
Tafazzin	Phospholipid/glycerol acyltransferase	reduced cariolipin decreased locomotory activity abnormal mitochondria
Giotto	Phosphatidylinositol transfer protein;	cytokinesis failure in mitotic neuroblasts cytokinesis failure in meotic spermatogenesis
Midway	Diacylglycerol O-acyltransferase 1	reduced neutral lipids in female germline; egg chamber degeneration
Fan	*MSP domain containing protein*	defective spermatogenesis
wun and wun2	phospholipid dephosphorylation	defects in germ cell migration abnormal upregulation of immune response
Bmm	lipid catabolic process	accumulation of TAGs; phenotypes similar to obese mice models , growth inhibition
DAGKε	diacylglycerol kinase activity	improves motor dysfunction in fly Huntington disease model; shows retinal degeration
apoD	Lipocalin/cytosolic fatty-acid binding domain	age associated lipid peroxides accumulation; regulated by JNK signaling; protection from Aβ-42 in cytotoxicity in Alzimer's fly model
Lace	Helps serine C-palmitoyltransferase activity	Imaginal disk apoptosis; Rescues photoreceptor degeneration in PLC mutants

Schlank	sphingosine N-acyltransferase activity	Failure of fat storage
Des-1	sphingolipid delta-4 desaturase activity	Failure of spindle assembly and cytokinesis during spermatocyte meiosis
dCerk	ceramide kinase activity	Phototransduction defect; Fail to localize PLC-β; Effect on PIP2 distribution in photoreceptor membrane
nCDase	Hydrolyzes the sphingolipid ceramide into sphingosine and free fatty acid at neutral pH	Failure of synaptic vesicle fusion and synaptic transmission; Overexpression rescues retinal degeneration in arrestin and PLC mutants; Down-regulated upon sugar feeding
alkCDase	Hydrolyzes the sphingolipid ceramide into sphingosine and free fatty acid at alkaline pH	Increase in ceramide levels; Increased resistance to oxidative stress; Increased lifespan; Defective mushroom and ellipsoid body.
SphK1/2	D-erythro-sphingosine kinase activity	Flight impairment; Reduced fecundity
Sply	sphinganine-1-phosphate aldolase activity	Increased sphingosine, S1P levels; Increased Δ4,6-sphingadienes; Flight muscle degeneration; Apoptotic ovaries and testes
GlcT-1	glucosylceramide biosynthetic process	Apoptosis in embryo; overexpression suppresses apoptosis induced by reaper and grim
Egghead/	beta-1,4-mannosyltransferase activity	Notch-like neuronal hypertrophy;
brainiac		Defective EGF-R signaling in oocyte (ventralized follicle cells)

β4GalNacTA/B		Defective neuromuscular junction innervation and coordination; Similar to egghead/brainiac defective oocyte
α4GT1/2		Overexpression suppresses Mindbomb Notch-like phenotype and inhibits apoptosis in eye disk

Lipids as post translational modifiers: Approximately 1000 unique proteins are identified as targets of lipid modification. Every lipid modification confers unique properties to the target protein such as ability to interact with other proteins or stability (Baumann and Menon 2002). Additionally, lipid modifications enable target proteins to localize in different organelle membrans or plasma membrane lipid rafts. Although some lipid modifications such as palmitoylation or addition of GPI anchors are reversible, some modifications such as myristylation are irreverisble. Some proteins are modified by more than one lipid moeities to regulate stability and signaling. For example, Hh is modified by palmitate at N-terminus and cholesterol at C-terminus. Hh (and mammalian homolog,sonicHh) is the only known cholesterol-modified protein. This modification regulates diffusion of Hh and thus facilitates long- and short-range Hh signaling during *Drosophila* development. Atg8 is another unique protein that ismodified by PE in ubiquitin-like manner. PE modification of Atg8 occurs during autophagosome formation. It regulates growth and maturation of autophagosomes (Resh 2013). Some lipid modifications are summarized in Table 3.

Table 5-3: Lipids as post-translational modifiers (Resh 2013). Several lipids attach to specific amino acid residues of specific target proteins to regulate different biological processes. The variety of functions associated lipid modifications emphasizes that each lipid modification has a own unique target protein and function.

Lipid Modification	Target protein	Function
Myristylation	Protein kinase K, ARF1, c-Src, Gα subunit	Membrane anchors, protein structural change for new interactions
Farnesylation	Ras proteins	Localization to membrane

Palmitoylation	Transferrin receptors, GPCRs	Cell surface delivery, stability and thereby signaling
Cholesterol + Palmitoylation	Hedgehog, sonic Hh	Only known cholesterol modified proteins; Helps Hh gradient formation
GPI anchor modification	NCAM, CD55, Thy1	Cell specific membrane anchoring of specific proteins

Lipids form very crucial structural and functional components of the cell. They regulate various important signaling pathways, thereby, regulating critical cellular processes. Thus, it is not surprising that genes involved in lipid metabolism are implicated in many pathological conditions as they directly affect lipid homeostasis. But very few genes which are not directly involved in lipid synthesis or breakdown are shown to cellular functioning through regulation of lipid homeostasis. In this chapter, I have identified Mt2 as novel player in controlling lipid homeostasis in age dependent manner in *Drosophila*.

5.4. RESULTS

5.4.1. Mt2 mutants show no significant changes in total proteome:

Mt2 mutant flies have unstable tRNA (Schaefer, Steringer, and Lyko 2008). This leads to errors in polypeptide synthesis during translation; these errors accumulate over time and as a result, visible phenotypes can be seen under stress conditions such as crowding, heat shock, and infection. Similar results are also observed in Mt2 mutant mice (Tuorto et al. 2015). Considering these findings, I analyzed global changes in the proteome of 15-day old Mt2 mutant flies in normal as well as stress conditions using 1D-SDS-PAGE (**Figure 5.3**). I did not observe any significant changes in proteomes of 15-day old *Mt2 mutant* flies, even after heat shock.

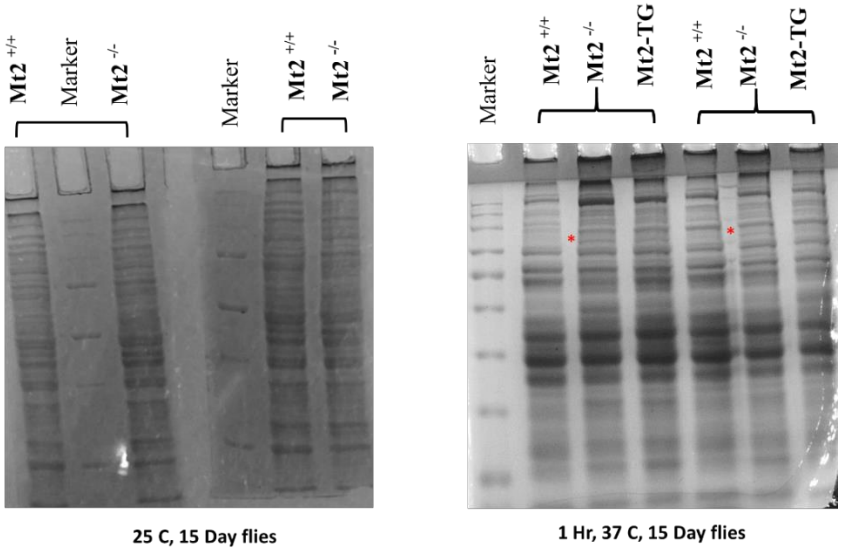

Figure 5-3: Protein profiles of Mt2-null flies at 25 °C and post 1 h heat shock at 37 °C. Each gel picture shows two biological replicates. The proteome analysis was performed using five 15-day old adult male flies. At 25 °C, no detectable change is observed in both replicates. However, heat shock for 1 h shows a novel protein band at 90 kDa in both replicates, as depicted by the red asterisks, although the identity of the proteins in the band needs further investigation.

5.4.2. Mt2 mutants have lower lipid content:

While extracting proteins from 15-day old Mt2 mutant flies, I observed that the thickness of the lipid layer is reduced in comparison with that from wild-type flies. To further explain this observation, I performed thin layer chromatography (TLC) of lipids extracted from 15-day old wild-type and mutant flies. Consistent with my previous observation, the TLC analysis showed reduced total cellular lipids in the Mt2 mutant flies (**Figure5.4**)

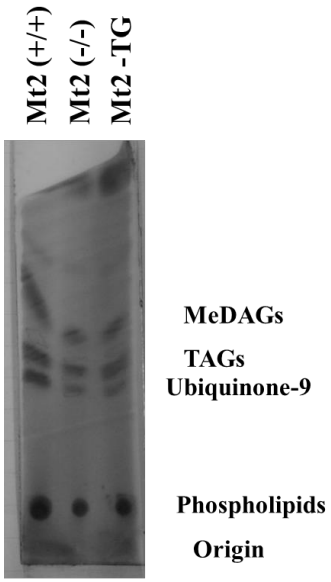

Figure 5-4: Decreased total cellular lipids in Mt2-null flies. Total cellular lipids were extracted from five 15-day old flies, both wild-type as well as mutants. The lipids were separated on silica TLC plate and visualized by 20% phosphomolybdic acid in ethanol followed by heat treatment. Different classes of lipids such as phospholipids, ubiquinone, TAGs, and MeDAGs were separated based on their mobility in the solvent used. Spots corresponding to all the classes were less intense in Mt2 mutants as compared to those in wild-type and the Mt2-TG rescue line.

5.4.3. Mt2 mutant flies show decrease in TAG content:

TAGs are the most abundant storage lipids in flies. They also act as carrier lipids for fat body. Reduction is TAG content has deleterious effects on organisms. Therefore, I decided to specifically investigate changes in TAG content in Mt2 mutant flies. Lipids extracted from five 15-day old flies were separated on TLC using a dual-solvent system and TAGs were specifically visualized. The mutant flies showed significant reduction in TAG content as compared to control flies (**Figure 5.5**).

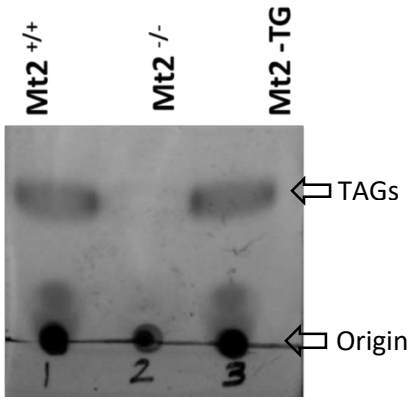

Figure 5-5: Reduction in TAGs in 15 day old Mt2-null flies: Lipids extracted from five 15-day old flies were separated on silica TLC plates using a dual-solvent system of n-hexane:ethylether:acetic acid (70:30:1) and hexane:ethylether (59:1). The separated lipids were visualized using 10% $CuSO_4$ in 8% H_3PO_4. Mt2 mutant flies showed significant reduction in TAG content as compared to control flies.

5.4.4. Mt2 mutant flies show age-dependent decrase in TAG content.

Mt2 null flies show reduced life span and altered immunity. The immunity is further compromised as the fly ages (Varada's thesis). I was curious to know if the change in TAG content is also age-dependent. I extracted lipids from 1-, 5-, 10- and 15-day old flies and performed TAG-specific TLC as described earlier. One-day old flies, whether wild-type or Mt2 mutant, showed comparable levels of TAGs. Mt2 mutants, however, exhibited age-associated reducing trend in TAG content by day 5, and this reduction was approximately 50% in 15-day old flies, as show in **Figure 5.6(A,B).** as compared to approximately 25% reduction seen in control flies.

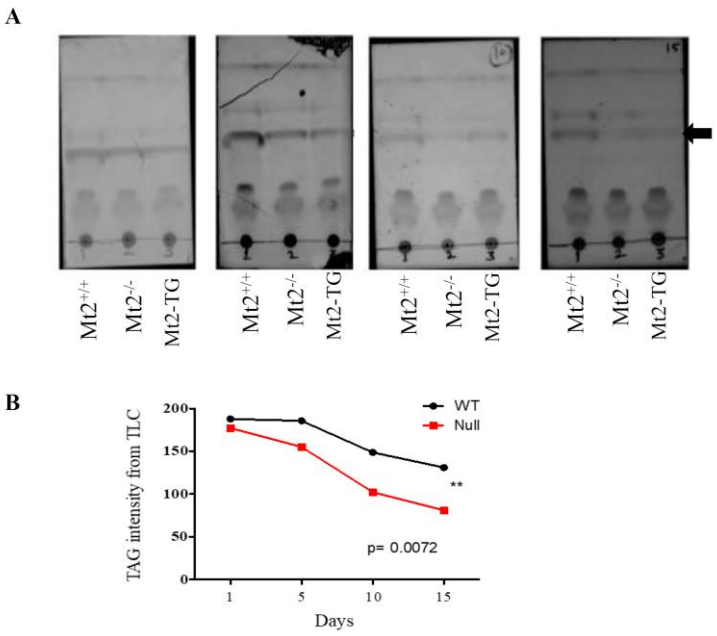

Figure 5-6: Age dependent decrease in TAGs in Mt2 mutant flies: TAG-specific TLC was performed for 1-, 5-, 10-, and 15-day old flies. The top panel shows TLC images, whereas the bottom panel shows TAG quantitation. The above data indicate that TAG contents in wild-type and mutants were comparable at day 1; however, the contents showed age-associated reducing trend in mutants at day 5 and onwards Graph plotted using GraphPad and Chi-Square test for trend was performed. ($p<0.05$).

The total cellular lipid TLC (**Figure 5.5**) and TAG-specific TLC (**Figure 5.6A**) together indicate that wild-type and Mt2 mutant lipid profiles are different and that the differences are highest for 15-day old flies (**Figure 5.6B**). For in-depth investigation of the differences observed in lipid profiles of 15-day old flies, I decided to quantitatively analyze the lipid profiles using mass spectrometry.

5.4.5. Accumulation of bioactive lipids in Mt2 mutant flies.

Lipids were extracted from 15 day old wild-type, Mt2 mutants, and transgenic rescue lines described in *Material and Methods*. The lipids were resuspended in chloroform and LC/MS analysis was performed. Each class of lipids was quantitatively assessed using internal standard for that class. The area under the peak corresponding to a lipid obtained from MS was calculated and normalized to the internal standard, thus quantitating that particular lipid. The data for some lipid classes are shown in **Figure 5.7**. The most significant change was observed in sphingosine-1-phosphate (S1P) levels. S1P levels are tightly regulated in a normal stress free wild type fly However, in Mt2 null flies, I observed about 3-fold accumulation as compared to control flies. I

also observed 2–3-fold increase in ceramides. Ceramides and S1P are potent bioactive lipids and accumulation of these are known for deleterious effects. On the contrary, TAGs, which function as important storage lipids, were decreased by approximately 30%, in comparision to control flies.as previously observed by TLC; whereas PE was reduced by 25%–30%. Most other lipids remained largely unchanged. This indicates that Mt2 is most likely involved in regulation of bioactive signaling lipids: S1P, ceramides, and TAGs.

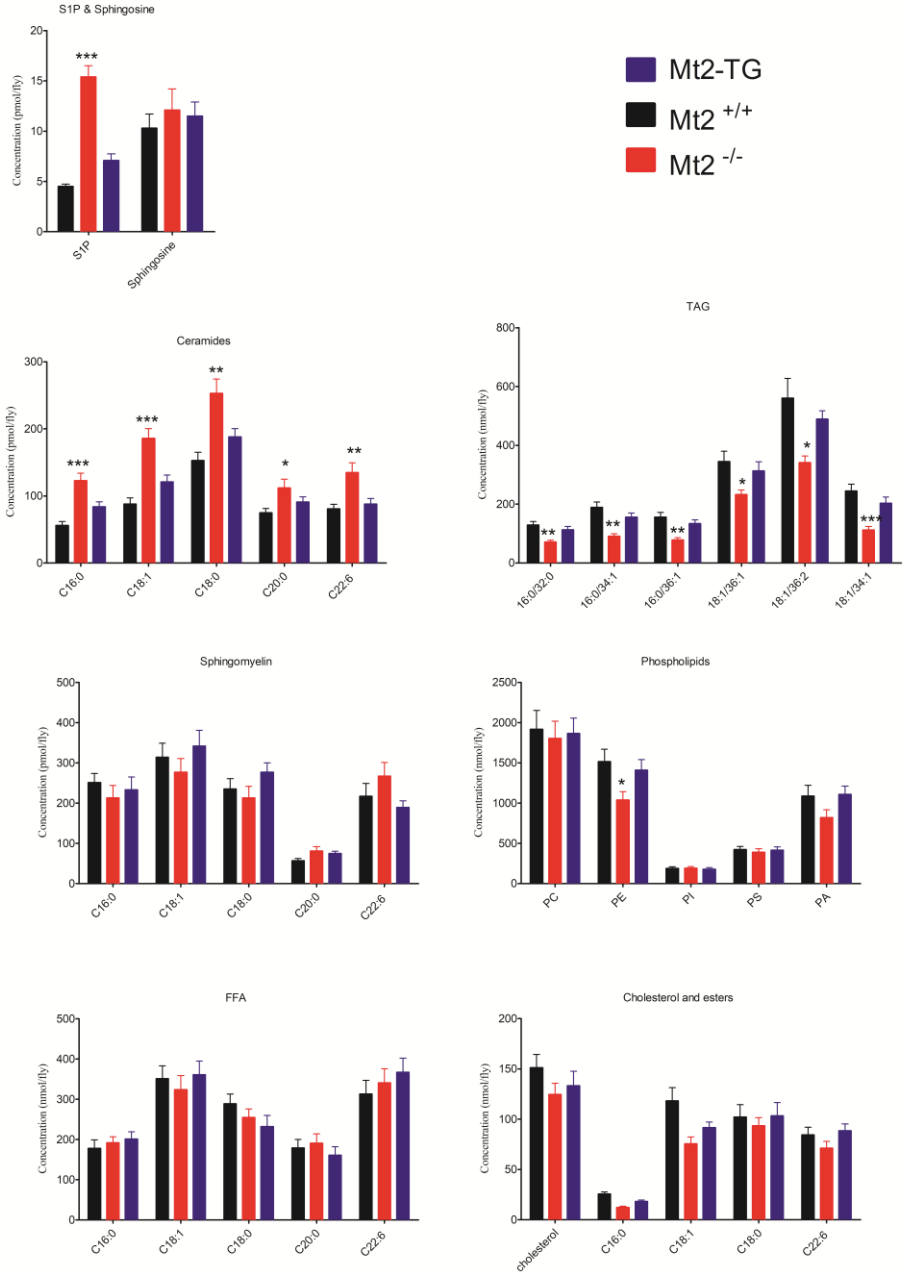

Figure 5-7: Quantitative lipidomics for Mt2 mutant and control lines. Quantitative lipid mass spectrometry was performed for wild-type, Mt2 mutants, and rescued mutants in five biological replicates. The data were pooled for each lipid class from all five replicates and were plotted as mean ± SEM. Mt2 mutant flies showed approximately 3-fold increase in S1P levels, whereas there was no change in sphingosine levels. Ceramides showed approximately 2–3-fold increase in levels. On the contrary, all kinds of TAGs and PE showed significant reduction in levels in the mutant as compared to the wild type and transgenic rescue line. Most other lipid classes such as FFA and sphingomyelin remained unchanged. The Graphs are plotted using GraphPad. 1-Way ANOVA followed by tukey's test were performed. * = $p<0.05$. ** = $p<0.01$, *** = $p<0.001$

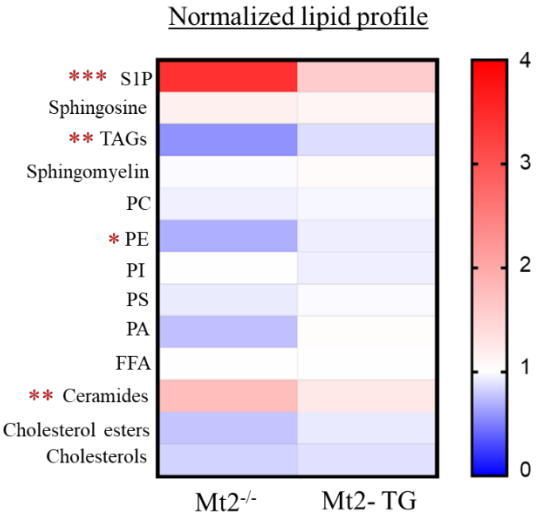

Figure 5-8: Heat map generated from the lipid LC/MS data. Levels of lipids from each class in Mt2 mutant and transgenic rescue line were normalized to the levels in the wild type. S1P and ceramides show significant increase in Mt2 mutants as compared to wild type, whereas TAGs, PE, and PA show reduction in the mutant. The close-to-one normalized levels for the rescued mutant confirm that the corresponding levels for the mutant are specifically due to the mutation in Mt2.

5.4.6. No significant change in *sply* and *midway* transcripts in Mt2 mutant flies.

Quantitative lipidomics showed accumulation of S1P in Mt2 mutant flies (**Figure 5.7**). Similar accumulation is observed in *sply* mutants. The gene *sply* encodes an enzyme having S1P lyase activity, which converts S1P to PE and hexadecenal. Mutations in *sply* result in developmental defects and embryonic lethality in flies. To understand if Mt2 alters the expression of *sply*, I performed quantitative real-time polymerase chain reaction (RT-PCR). When RT-PCR was performed on the whole animal, I did not observe any significant difference in transcript levels of *sply* in Mt2 mutants in comparison to those in control lines (**Figure 5.9A**). In some organisms, *sply* is known to be regulated in tissue-specific manner. To check if the same occurs in flies, I

performed RT-PCR only on hemocytes; however, I did not see any difference in *sply* transcript levels between wild type and Mt2 mutants (**Figure 5.9B**).

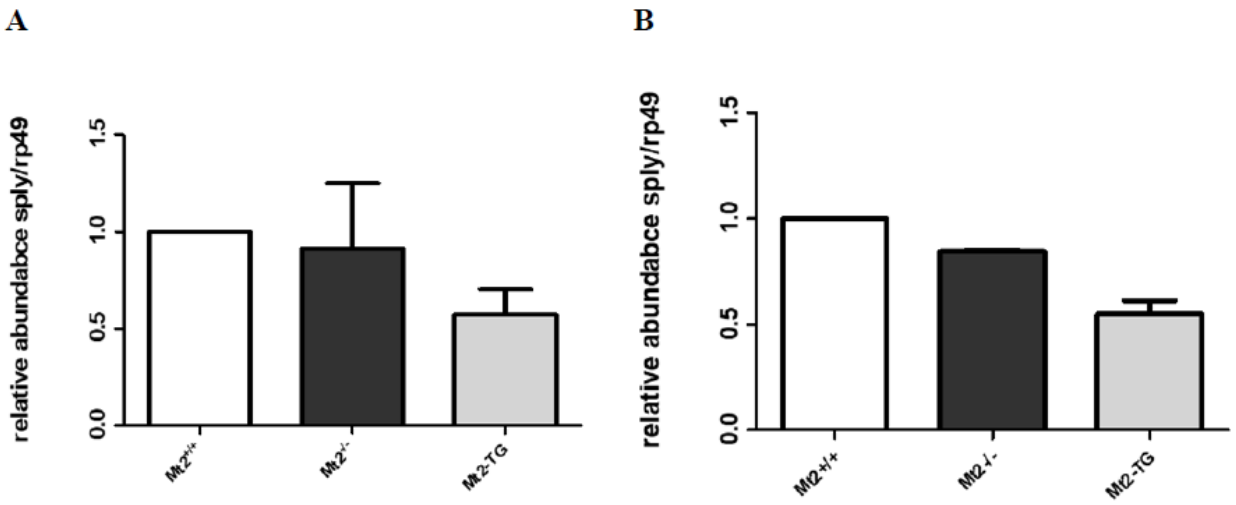

Figure 5-9: Quantitative RT-PCR for *sply* was performed on (A) whole animal and (B) hemocytes in biological triplicates. In both cases, no significant change in *sply* transcript levels was observed. Graphs were plotted using GraphPad. 1-Way ANOVA followed by tukey's test was performed.

5.4.7. Mt2 mutants showed significant decrease in Sply enzyme activity.

Although there was no significant difference in *sply* transcript levels in Mt2 mutant in comparison with the wild-type, S1P, a substrate of Sply, showed accumulation in Mt2 mutants. Mt2 has been reported to cause protein translation errors, thereby affecting functions of various proteins. Such translation errors probably result in defective Sply protein, which leads to accumulation of S1P. To test this hypothesis, I decided to estimate the activity of Sply in wild-type, Mt2 mutant, and rescued mutants. I performed an enzyme activity assay in which Sply-specific substrate conversion was measured. I noted an approximately 75% reduction in Sply enzyme activity in Mt2 mutants as compared to that in wild-type and rescued mutants (**Figure 5.10**).

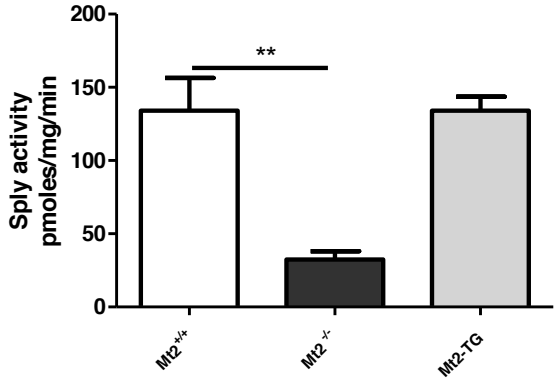

Figure 5-10: Sply activity assay in Mt2 mutant and control flies. Total protein was extracted from wild type, Mt2 mutant, and rescued mutant. The assay was performed in three biological replicates containing equal protein amounts. The activity was estimated as the amount of Sply-specific product formed per minute per mg of protein. Mt2 mutant flies showed about 75% reduction in Sply activity. Graphs plotted in GraphPad and assessed using 1-Way ANOVA followed by tukey's test. ** = $p<0.01$

5.5. DISCUSSION

Organisms have to manage energy in order to survive. Energy homeostasis is dependent on energy uptake, storage and expenditure. Since feeding is a discontinuous process, energy is usually stored in the form of carbohydrates, proteins or lipids to maintain a continuous supply in times of need. The *Drosophila* fat body, oenocytes, gut, malphigian tubules and special regions of the nervous system play key roles in metabolic regulation and energy homeostasis. Metabolic pathways are conserved between mammals and the fly allowing *Drosophila* to serve as a powerful model system to get a better understanding of functioning of complex metabolic networks (Owusu-Ansah and Perrimon 2014) including those of lipids. A finely tuned network of regulators and inter-organ communication is necessary to balance the energy intake, storage and expenditure of energy, whereby a deregulation of such networks can cause malfunction and disease.

TAG homeostasis is key link between nutrient uptake and metabolic needs of the organism. Any alteration in TAG levels leads to range of disorders like obesity and diabetes. In *Drosophila*, lower TAG levels are associated with lean, starvation sensitive flies with reduced life-span whereas accumulation of TAGs lead to increased life-span under starvation stress (Sieber and Thummel 2009). During immune response, TAGs act as only source of fatty acids that are incorporated into proliferating lymphoid cells, thus, making critical contribution to immune response (Pond and Mattacks 2003). In this study, I identify Mt2 as a novel player in regulation of TAGs. Mt2 mutants

show decrease in TAGs (Figure5) along impaired immune response and reduced life-span (Varada et al, submitted). In Mt2 mutant flies, TAG levels declines further with age (**Figure5.6**) and this also corresponds to decline in the ability fight infection (Varada et al, submitted). This suggest aging associated role for Mt2 in *Drosophila*.

Lipids, in addition to being storage molecules and playing structural roles in membranes, have increasingly been shown to have roles in signaling. Lipids, along with enzymes that modify and interconvert lipids constitute complex lipid signaling networks responsible for cellular and organismal homeostasis (Palm et al. 2012; Owusu-Ansah and Perrimon 2014). Sphingolipids or glycosylceramides constitute a class of lipids critical for metabolism (Saba and Hla 2004; Acharya and Acharya 2005). Levels of storage metabolites such as S1P, ceramides and TAG have to be maintained in a dynamic manner for cellular homeostasis. *Drosophila* mutants have contributed to insights into critical roles for sphingolipids in biological function. For example, mutants for sphingosine kinases (*Sphk*), which generate the important intra and intercellular signaling molecule S1P, and S1P-lyase (*Sply*) (Lovric et al. 2017), which breaks S1P down, have interesting developmental defects. *Sply* mutants show severe flight muscle defects as well as activation of apoptosis in reproductive organs (Herr et al. 2003; Phan et al. 2007), presumably by accumulating S1P. *Sphk* mutants should have reduced S1P and accumulate Sphingosine. *Sphk2* mutants, in fact, have flight defects and reduced fecundity (Herr et al. 2003). *Sply* phenotypes can be rescued by mutations in *lace*, which codes for a serine palmitoyl transferase that is a critical rate limiting step for Ceramide synthesis. Ceramides act as regulators of apoptosis and are also shown to directly affect phophorylation of retinoblastoma (Rb) in response to TNFα signaling (Lee, Hannun, and Obeid 1996). Ceramide, in turn, can be converted to Spingosine, by CDase's such as Slab and Brainwashing. S1P binds GPCRs and is suggested to regulate events such as cell shape change in PC12 cells (Edsall et al. 2001). In Mt2 mutants, I show accumulation S1P and Ceramides (Figure10) along with altered hemocyte shape (Varada et al., submitted) though, there is no direct evidence of altered hemocyte shape being result of S1P accumulation. S1P accumulation is known to alter cell shape in C. *elegans* and mammalian tissues through S1P-S1P receptor mediated signaling, but such S1P receptors are not yet reported in *Drosophila*. In flies, however, another gene, *serpent*, regulates hemocyte shape and function (Vouret-Craviari et al. 2002). *Serpent (srp)* is GATA-like transcription factor which regulates *alcholol dehydrogenase (adh)* in tissue-specific manner.(Abel, Michelson Am Fau - Maniatis, and Maniatis 1993). Interestingly, in *C*. *elegans*,

regulation of bioactive lipid, S1P is achieved through tissue-specific expression of GATA-like transcription factors which in turn leads to tissue-specific expression of S1P lyase (Oskouian et al. 2005). It is possible that Srp performs similar function in *Drosophila*. Consistent with this hypothesis, I observed a decrease in *srp* transcript levels in Mt2 mutant flies, which in turn may led to S1P accumulation and hemocyte shape change. Although, I did not observe significant decrease in *sply* trancripts in hemocytes (Figure12B), additional studies from tissues like fat body, oenocytes, gut, malphigian tubules are required.

It is worth exploring whether the changes in cell shape in *srp*-knockdown S2 cells occur due to S1P accumulation and whether knocking down *srp* or *sply* only in hemocytes or fat body is sufficient to mimic defects seen in Mt2 mutants.

5.6. MATERIALS AND MATHODS

Protein extraction and visualization: Five male flies of age fifteen days were used to make whole body lysates using 100 ul, 1X SDS-PAGE loading buffer as the lysing agent, the lysate was boiled at 95 degrees for 10 minutes and spun at 10000 g for 20 minutes. 30 ul supernatant was loaded in each well. Gels were stained Coomassie R250.

Lipid extraction for thin layer chromatography (TLC): Lipid isolation was done using a modified Folch extraction protocol (Kamat et al. 2015). Briefly, 5 whole adult males were crushed in 1ml DPBS in a glass vial and 1ml Methanol was added, and the mixture vortexed. Thereafter, 2ml of chloroform was added to these samples and vortexed vigorously. The sample was then centrifuged at 2800g for 5 minutes to separate the aqueous and organic phases. The organic phase (bottom) containing lipids was collected in clean glass vial. To enrich for phospholipids, the aqueous layer was acidified using 2.5% v/v formic acid, and re-extracted using 2 ml choloroform, and the two phases were separated by centrifugation at 2800g for 5 mins. The two organic phases were pooled and dried using N_2 gas. The extracted lipids were subjected to TLC analysis. TLC was performed using mobile phase of Hexane:Ethylacetate:Acetic acid in 80:20:1 ratio. The plate was developed using 20% phosphomolybdic acid (PMA) in ethanol by heating at 95 °C for 1-2 mins.

TLC for TAGs: Lipids were extracted as described earlier. The silica TLC plates (Merck) were pre-cleaned using chloroform followed by air drying and heating to 100ºC for 15 mins. The sample

was then spotted onto these plates using a glass capillary. The solvent system used was that of Wilfling *et. al*. (Wilfling et al. 2013) with minor modifications. The TLC was run using two different mobile phases sequentially. The first solvent was a mixture of n-hexane/diethyl ether/acetic acid (70:30:1). The first solvent was run halfway upto the top of the plate, after which the plate was air-dried. The plate was then run in solvent mixture of n-hexene:diethyl ether (59:1). The plate was dried and visualized by spraying with 10% (w/v) $CuSO_4$ in 8% (v/v) H_3PO_4 followed by baking in the oven above 150^oC for 20 mins. The plates were scanned and quantified using Image J-software.

Quantitative lipidomics: All lipid extractions were done as described above, with small modifications (Kamat et al. 2015). Briefly, the 5 whole adult males were washed with PBS (x 3 times), and transferred into a glass vial using 1 mL PBS. 3 mL of 2:1 (vol/vol) $CHCl_3$: MeOH with the internal standard mix (100 pmol of each internal standard listed in Suppl. Table 3) was added, and the mixture was vigorously vortexed. The two phases were separated by centrifugation at 2800g for 5 minutes. The organic phase (bottom) was removed, 50 µL of formic acid was added to acidify the aqueous homogenate (to enhance extraction of phospholipids), and $CHCl_3$ was added to make up 4 mL volume. The mixture was vortexed, and separated using centrifugation described above. Both the organic extracts were pooled, and dried under a stream of N_2. The lipidome was re-solubilized in 200 µL of 2:1 (vol/vol) $CHCl_3$: MeOH, and 20 µL was used for the targeted LC-MS analysis. All the lipid species analyzed in this study were quantified using the multiple reaction monitoring (MRM) method (see Suppl. Table 3) on an AbSciex QTrap 4500 LC-MS with a Shimadzu Exion-LC series quaternary pump. All data was collected using the Acquisition mode of the Analyst software, and analyzed using the Quantitate mode of the same software. The LC separation was achieved using a Gemini 5U C-18 column (Phenomenex, 5 µm, 50 x 4.6 mm) coupled to a Gemini guard column (Phenomenex, 4 x 3 mm, Phenomenex security cartridge). The LC solvents were: For positive mode: buffer A: 95:5 (vol/vol) H_2O: MeOH + 0.1% formic acid + 10mM ammonium formate; and buffer B: 60:35:5 (vol/vol) iPrOH: MeOH: H_2O + 0.1% formic acid + 10mM ammonium formate, For Negative mode: buffer A: 95:5 (vol/vol) H_2O: MeOH + 0.1% ammonium hydroxide; and buffer B: 60:35:5 (vol/vol) iPrOH: MeOH: H_2O + 0.1% ammonium hydroxide. All the MS based lipid estimations was performed using an electrospray ion source, using the following MS parameters: ion source = turbo spray, collision gas = medium, curtain gas = 20 L/min, ion spray voltage = 4500 V, temperature = 400 ^oC. A typical LC-run

consisted of 55 minutes, with the following solvent run sequence post injection: 0.3 ml/min 0% buffer B for 5 minutes, 0.5 ml/min 0% buffer B for 5 minutes, 0.5 ml/min linear gradient of buffer B from 0 – 100% over 25 minutes, 0.5 ml/min of 100% buffer B for 10 minutes, and re-equilibration with 0.5 ml/min of 0% buffer B for 10 minutes. A detailed list of all the species targeted in this MRM study, describing the precursor parent ion mass and adduct, the product ion targeted can be found in *Supp*. *Table 3B*. All the endogenous lipid species were quantified by measuring the area under the curve in comparison to the respective internal standard and then normalized to the number of flies. All the data is represented as mean ± s. e. m. of 5 biological replicates per group (*Suppl*. *Table 3*).

Hemocyte isolation: Hemolymph was extracted as described (Neyen et al. 2014). In brief, 15 flies from each genotype were placed on a 10 μM filter spin column (ThermoFisher, Cat. No. 69705), covered with 4 mm glass beads (Zymoresearch, Cat. No.S1001 Rattler™) and centrifuged for 20 min at 4 °C, 10 K rpm in a microcentrifuge. The extracted hemolymph was collected in 100ul Trizol® and stored.

Quantitative real time PCR: Total RNA was extracted from all the samples 6 hours of post infection (Direct-zol™ RNA MiniPrep Cat. No. R2050). cDNA was then synthesized from 1 ug total RNA using High capacity cDNA synthesis kit (Cat No. 4368814). Quantitative PCR experiments were accomplished with a Realplex^2 and using SYBR Green (KAPA CatNo.# KK4601). Relative gene expression was calculated after normalization to the control RpL32/rp49 mRNA.

Sply activity assay: Total protein was isolated from 5 flies per replicate per genotype. 15 μg of proteome was incubated with 100 μM S1P (S9666, Sigma) in a reaction volume of 100 μL in PBS at 37ºC with constant shaking. After 30 minutes the reaction was quenched with 350 μL of 2:1 (vol/vol) $CHCl_3$: MeOH, doped with 250 pmol internal standard, cis-10-heptadecenoic acid (C17:1 FFA). The mixture was vortexed, and centrifuged at 2800 *g* for 5 minutes to separate the aqueous (top) and organic (bottom) phase. The organic phase was collected and dried under a stream of N_2 gas, re-solubilized in 100 μL of 2:1 (vol/vol) $CHCl_3$: MeOH, and subjected to LC-MS analysis. A fraction of the organic extract (~ 20 μL) was injected onto an AbSciex QTrap 4500 LC-MS with a Shimadzu Exion-LC series quaternary pump. LC separation was achieved using a Gemini 5U C-18 column (Phenomenex, 5 μm, 50 x 4.6 mm) coupled to a Gemini guard column (Phenomenex,

4 x 3 mm, Phenomenex security cartridge). The LC solvents were: buffer A: 95:5 (vol/vol) H_2O: MeOH + 0.1% ammonium hydroxide, and buffer B: 60:35:5 (vol/vol) iPrOH: MeOH: H_2O + 0.1% ammonium hydroxide. A typical LC run consisted of 15 minutes post-injection: 0.1 mL/min 100% buffer A from for 1.5 minutes, 0.5 mL/min linear gradient to 100% buffer B over 5 minutes, 0.5 mL/min 100% buffer B for 5.5 minutes, and equilibration with 0.5 mL/min 100% buffer A for 3 minutes. All MS analysis was performed using an electrospray ionization source in a MS1 scan negative ion mode for product formation (free fatty acid from S1P). All MS parameters were the same as those described in the MS-based lipids profiling method described above. Measuring the area under the peak, and normalizing it to the internal standard quantified the product release for the lipid substrate hydrolysis assays. The substrate hydrolysis rate was corrected by subtracting the non-enzymatic rate of hydrolysis, which was obtained by using heat-denatured proteome (15 minutes at 95 $^{\circ}$C, followed by cooling at 4 $^{\circ}$C for 10 mins x 3 times) as a control. All the data is represented as mean ± s. e. m. of 3 biological replicates.

5.7. CONTRIBUTIONS.

We started this project in collaboration with Varada Abhyankar and Dr. Deepti Deobagkar from Zoology Dept., Pune University. During this collaboration, we identified the role of Mt2 in combating infections in age-dependent manner in flies. Considering the role of Mt2 in tRNA stability and protein translation, we wanted to check whether the age-dependent effects of Mt2 mutations on immune function were a result of global erroneous translation. While extracting total proteins from Mt2 mutant flies, I observed that they show a reduced fat layer in lysates. This led me to investigate further on lipid homeostasis in Mt2 mutants.

BIBLIOGRAPHY

Abel, T., T. Michelson Am Fau - Maniatis, and T. Maniatis. 1993. 'A *Drosophila* GATA family member that binds to Adh regulatory sequences is expressed in the developing fat body', *Development*, 119.

Acharya, U., and J. K. Acharya. 2005. 'Enzymes of sphingolipid metabolism in *Drosophila* melanogaster', *Cell Mol Life Sci*, 62: 128-42.

Adada, M., D. Canals, Y. A. Hannun, and L. M. Obeid. 2014. 'Sphingolipid regulation of ezrin, radixin, and moesin proteins family: implications for cell dynamics', *Biochim Biophys Acta*, 1841: 727-37.

Anand, P., S. Cermelli, Z. Li, A. Kassan, M. Bosch, R. Sigua, L. Huang, A. J. Ouellette, A. Pol, M. A. Welte, and S. P. Gross. 2012. 'A novel role for lipid droplets in the organismal antibacterial response', *Elife*, 1: e00003.

Baumann, Nikola A., and Anant K. Menon. 2002. 'Lipid modifications of proteins', *Biochemistry of Lipids, Lipoproteins and Membranes*.

Becker, M., S. Muller, W. Nellen, T. P. Jurkowski, A. Jeltsch, and A. E. Ehrenhofer-Murray. 2012. 'Pmt1, a Dnmt2 homolog in Schizosaccharomyces pombe, mediates tRNA methylation in response to nutrient signaling', *Nucleic Acids Res*, 40: 11648-58.

Chakrabarti, S., M. Poidevin, and B. Lemaitre. 2014. 'The *Drosophila* MAPK p38c regulates oxidative stress and lipid homeostasis in the intestine', *PLoS Genet*, 10: e1004659.

Durdevic, Z., K. Hanna, B. Gold, T. Pollex, S. Cherry, F. Lyko, and M. Schaefer. 2013. 'Efficient RNA virus control in *Drosophila* requires the RNA methyltransferase Dnmt2', *EMBO Rep*, 14: 269-75.

Edsall, L. C., O. Cuvillier, S. Twitty, S. Spiegel, and S. Milstien. 2001. 'Sphingosine kinase expression regulates apoptosis and caspase activation in PC12 cells', *J Neurochem*, 76: 1573-84.

Freymuth, P. S., and H. L. Fitzsimons. 2017. 'The ERM protein Moesin is essential for neuronal morphogenesis and long-term memory in *Drosophila*', *Mol Brain*, 10: 41.

Fujimoto, T., and R. G. Parton. 2011. 'Not just fat: the structure and function of the lipid droplet', *Cold Spring Harb Perspect Biol*, 3.

Goll, M. G., F. Kirpekar, K. A. Maggert, J. A. Yoder, C. L. Hsieh, X. Zhang, K. G. Golic, S. E. Jacobsen, and T. H. Bestor. 2006. 'Methylation of tRNAAsp by the DNA methyltransferase homolog Dnmt2', *Science*, 311: 395-8.

Goode, SCOTT, DAVID Wright, and ANTHONY P. Mahowald. 1992. 'The neurogenic locus brainiac cooperates with the *Drosophila* EGF receptor to establish the ovarian follicle and to determine its dorsal-ventral polarity', *Development*, 116: 177-92.

Hait, N. C., L. E. Wise, J. C. Allegood, M. O'Brien, D. Avni, T. M. Reeves, P. E. Knapp, J. Lu, C. Luo, M. F. Miles, S. Milstien, A. H. Lichtman, and S. Spiegel. 2014. 'Active, phosphorylated fingolimod inhibits histone deacetylases and facilitates fear extinction memory', *Nat Neurosci*, 17: 971-80.

Herr, D. R., H. Fyrst, V. Phan, K. Heinecke, R. Georges, G. L. Harris, and J. D. Saba. 2003. 'Sply regulation of sphingolipid signaling molecules is essential for *Drosophila* development', *Development*, 130: 2443-53.

Hinkovska-Galcheva, V., L. A. Boxer, A. Kindzelskii, M. Hiraoka, A. Abe, S. Goparju, S. Spiegel, H. R. Petty, and J. A. Shayman. 2005. 'Ceramide 1-phosphate, a mediator of phagocytosis', *J Biol Chem*, 280: 26612-21.

Hokin, Mabel, and Lowel Hokin. 1953. 'Enzyme secretion and the incorporation of 32P into phospholipids of pancreas slices', *J Biol Chem*, 203: 967-77.

Kamat, S. S., K. Camara, W. H. Parsons, D. H. Chen, M. M. Dix, T. D. Bird, A. R. Howell, and B. F. Cravatt. 2015. 'Immunomodulatory lysophosphatidylserines are regulated by ABHD16A and ABHD12 interplay', *Nat Chem Biol*, 11: 164-71.

KEITH, ALEC D. . 1966. 'Analysis of lipids in *Drosophila* melanogaster.', *Comp. Biochem. Physio*, 17: 1127-36.

Khan, Wasiuddin A., S. Wayne MASCARELLA, Anita H. Lewin, Chris D. WYRICK, F. Ivy CARROLLt, and Yusuf A. HANNUN. 1991. 'Use of D-erythro-sphingosine as a pharmacological inhibitor of protein kinase C in human platelet', *Biochem J*, 278: 387-92.

Kraut, R. 2011. 'Roles of sphingolipids in *Drosophila* development and disease', *J. Neurochem*, 116.
Kupperman, E., N. An S Fau - Osborne, S. Osborne N Fau - Waldron, D. Y. Waldron S Fau - Stainier, and D. Y. Stainier. 2000. 'A sphingosine-1-phosphate receptor regulates cell migration during vertebrate heart development', *Nature*, 406.
Lee, J. Y., Y. A. Hannun, and L. M. Obeid. 1996. 'Ceramide inactivates cellular protein kinase Calpha', *J Biol Chem*, 271: 13169-74.
Lee, M. J., J. H. Thangada S Fau - Paik, G. P. Paik Jh Fau - Sapkota, N. Sapkota Gp Fau - Ancellin, S. S. Ancellin N Fau - Chae, M. Chae Ss Fau - Wu, M. Wu M Fau - Morales-Ruiz, W. C. Morales-Ruiz M Fau - Sessa, D. R. Sessa Wc Fau - Alessi, T. Alessi Dr Fau - Hla, and T. Hla. 2001. 'Akt-mediated phosphorylation of the G protein-coupled receptor EDG-1 is required for endothelial cell chemotaxis', *Mol Cell*, 8.
Lin, M. J., L. Y. Tang, M. N. Reddy, and C. K. Shen. 2005. 'DNA methyltransferase gene dDnmt2 and longevity of *Drosophila*', *J Biol Chem*, 280: 861-4.
Liu, Z., and X. Huang. 2013. 'Lipid metabolism in *Drosophila*: development and disease', *Acta Biochim Biophys Sin (Shanghai)*, 45: 44-50.
Lovric, S., S. Goncalves, H. Y. Gee, B. Oskouian, H. Srinivas, ... , M. Simons, H. Riezman, C. Antignac, J. D. Saba, and F. Hildebrandt. 2017. 'Mutations in sphingosine-1-phosphate lyase cause nephrosis with ichthyosis and adrenal insufficiency', *J Clin Invest*, 127: 912-28.
Martin, S., K. Driessen, S. J. Nixon, M. Zerial, and R. G. Parton. 2005. 'Regulated localization of Rab18 to lipid droplets: effects of lipolytic stimulation and inhibition of lipid droplet catabolism', *J Biol Chem*, 280: 42325-35.
Mendel, J., K. Heinecke, H. Fyrst, and J. D. Saba. 2003. 'Sphingosine phosphate lyase expression is essential for normal development in Caenorhabditis elegans', *J Biol Chem*, 278: 22341-9.
Neyen, C., A. J. Bretscher, O. Binggeli, and B. Lemaitre. 2014. 'Methods to study *Drosophila* immunity', *Methods*, 68: 116-28.
Okano, M., S. Xie, and E. Li. 1998. 'Cloning and characterization of a family of novel mammalian DNA (cytosine-5) methyltransferases', *Nat Genet*, 19: 219-20.
Oskouian, B., Ellyn Mendel J Fau - Shocron, Michael A. Shocron E Fau - Lee, Jr., Henrik Lee Ma Jr Fau - Fyrst, Julie D. Fyrst H Fau - Saba, and J. D. Saba. 2005. 'Regulation of sphingosine-1-phosphate lyase gene expression by members of the GATA family of transcription factors', *J Biol Chem*, 280.
Owusu-Ansah, E., and N. Perrimon. 2014. 'Modeling metabolic homeostasis and nutrient sensing in *Drosophila*: implications for aging and metabolic diseases', *Dis Model Mech*, 7: 343-50.
Palm, W., J. L. Sampaio, M. Brankatschk, M. Carvalho, A. Mahmoud, A. Shevchenko, and S. Eaton. 2012. 'Lipoproteins in *Drosophila* melanogaster--assembly, function, and influence on tissue lipid composition', *PLoS Genet*, 8: e1002828.
Park, W. J., and J. W. Park. 2015. 'The effect of altered sphingolipid acyl chain length on various disease models', *Biol Chem*, 396: 693-705.
Phan, V. H., D. R. Herr, D. Panton, H. Fyrst, J. D. Saba, and G. L. Harris. 2007. 'Disruption of sphingolipid metabolism elicits apoptosis-associated reproductive defects in *Drosophila*', *Dev Biol*, 309: 329-41.
Pond, C. M., and C. A. Mattacks. 2003. 'The source of fatty acids incorporated into proliferating lymphoid cells in immune-stimulated lymph nodes', *Br J Nutr*, 89: 375-83.
Resh, M. D. 2013. 'Covalent lipid modifications of proteins', *Curr Biol*, 23: R431-5.
Saba, J. D., and T. Hla. 2004. 'Point-counterpoint of sphingosine 1-phosphate metabolism', *Circ Res*, 94: 724-34.
Schaefer, M., T. Pollex, K. Hanna, F. Tuorto, M. Meusburger, M. Helm, and F. Lyko. 2010. 'RNA methylation by Dnmt2 protects transfer RNAs against stress-induced cleavage', *Genes Dev*, 24: 1590-5.
Schaefer, Matthias, Julia P. Steringer, and Frank Lyko. 2008. 'The *Drosophila* Cytosine-5 Methyltransferase Dnmt2 Is Associated with the Nuclear Matrix and Can Access DNA during Mitosis', *PLoS One*, 3: e1414.

Shimoyama, M., J. De Pons, G. T. Hayman, S. J. Laulederkind, W. Liu, R. Nigam, V. Petri, J. R. Smith, M. Tutaj, S. J. Wang, E. Worthey, M. Dwinell, and H. Jacob. 2015. 'The Rat Genome Database 2015: genomic, phenotypic and environmental variations and disease', *Nucleic Acids Res*, 43: D743-50.

Sieber, M. H., and C. S. Thummel. 2009. 'The DHR96 nuclear receptor controls triacylglycerol homeostasis in *Drosophila*', *Cell Metab*, 10: 481-90.

Sivasubramanian, M., N. Kanagaraj, S. T. Dheen, and S. S. Tay. 2015. 'Sphingosine kinase 2 and sphingosine-1-phosphate promotes mitochondrial function in dopaminergic neurons of mouse model of Parkinson's disease and in MPP+ -treated MN9D cells in vitro', *Neuroscience*, 290.

Stratford, S., K. L. Hoehn, F. Liu, and S. A. Summers. 2004. 'Regulation of insulin action by ceramide: dual mechanisms linking ceramide accumulation to the inhibition of Akt/protein kinase B', *J Biol Chem*, 279: 36608-15.

Subramanian, M., S. K. Metya, S. Sadaf, S. Kumar, D. Schwudke, and G. Hasan. 2013. 'Altered lipid homeostasis in *Drosophila* InsP3 receptor mutants leads to obesity and hyperphagia', *Dis Model Mech*, 6: 734-44.

Suomalainen, Laura, Virve Pentika¨inen, and Leo Dunkel†. 2005. 'Sphingosine-1-Phosphate Inhibits Nuclear Factor □B Activation and Germ Cell Apoptosis in the Human Testis Independently of Its Receptors', *American Journal ofPathology*, 166.

Tang, L. Y., M. N. Reddy, V. Rasheva, T. L. Lee, M. J. Lin, M. S. Hung, and C. K. Shen. 2003. 'The eukaryotic DNMT2 genes encode a new class of cytosine-5 DNA methyltransferases', *J Biol Chem*, 278: 33613-6.

Thiagarajan, D., R. R. Dev, and S. Khosla. 2011. 'The DNA methyltranferase Dnmt2 participates in RNA processing during cellular stress', *Epigenetics*, 6: 103-13.

Tuorto, Francesca, Friederike Herbst, Nader Alerasool, Sebastian Bender, Oliver Popp, Giuseppina Federico, Sonja Reitter, Reinhard Liebers, Georg Stoecklin, Hermann-Josef Gröne, Gunnar Dittmar, Hanno Glimm, and Frank Lyko. 2015. 'The tRNA methyltransferase Dnmt2 is required for accurate polypeptide synthesis during haematopoiesis', *The EMBO Journal*, 34: 2350-62.

Tuorto, Francesca, Reinhard Liebers, Tanja Musch, Matthias Schaefer, Sarah Hofmann, Stefanie Kellner, Michaela Frye, Mark Helm, Georg Stoecklin, and Frank Lyko. 2012. 'RNA cytosine methylation by Dnmt2 and NSun2 promotes tRNA stability and protein synthesis', *Nature Structural &Amp; Molecular Biology*, 19: 900.

Van Brocklyn, J. R., L. C. Tu Z Fau - Edsall, R. R. Edsall Lc Fau - Schmidt, S. Schmidt Rr Fau - Spiegel, and S. Spiegel. 1999. 'Sphingosine 1-phosphate-induced cell rounding and neurite retraction are mediated by the G protein-coupled receptor H218', *J Biol Chem*, 274.

Vouret-Craviari, Valérie, Christine Bourcier, Etienne Boulter, and Obberghen-Schilling Ellen Van. 2002. 'Distinct signals via Rho GTPases and Src drive shape changes by thrombin and sphingosine-1-phosphate in endothelial cells', *J Cell Sci*, 115: 2475-84.

Watson, A. F., and E. Mellaby. 1930 'TAR CANCER IN MICE. II: THE CONDITION OF THE SKIN WHEN MODIFIED BY EXTERNAL. TREATMENT OR DIET, AS A FACTOR IN INFLUENCING THE CANCEROUS REACTION.', *Br J Exp Pathol*, 11: 311-22.

Welte, M. A. 2015. 'Expanding roles for lipid droplets', *Curr Biol*, 25: R470-81.

Wendler, C. C., and S. A. Rivkees. 2006. 'Sphingosine-1-phosphate inhibits cell migration and endothelial to mesenchymal cell transformation during cardiac development', *Dev Biol*.

Wren, J. J., and HERSCHEL Mitchell. 1959. 'Extraction methods and Investigation of *Drosophila* Lipids', *J Biol Chem*, 234.

Zhou, Z., S. Yon Toh, Z. Chen, K. Guo, C. P. Ng, S. Ponniah, S. C. Lin, W. Hong, and P. Li. 2003. 'Cidea-deficient mice have lean phenotype and are resistant to obesity', *Nat Genet*, 35: 49-56.

Appendix I

Reverse genetic screen to identify interactors of *hinge1*

SUMMARY

I have done a reverse genetic screen to identify novel interactors of *hinge1* using RNAi library available at National Institute of Genetics, Japan. I have identified 73 enhancers and 7 suppressors from 996 lines I screened.

INTRODUCTION

My lab had identified novel role for a few of 16 member MADF-BESS family proteins in *Drosophila melanogaster* wing-hinge development. Vallari had screened all 16 MADF-BESS protein RNAi lines using different tissue specific Gal4s. She showed that knockdown of *hinge1* (CG9437) using a wing specific Gal4, MS1096 gives a bend hinge phenotype with 100% penetrance. She had made a stable line, MS1096>UAS-CG9437i (Shukla et al. 2014). I used this line for my screen.

Strategy

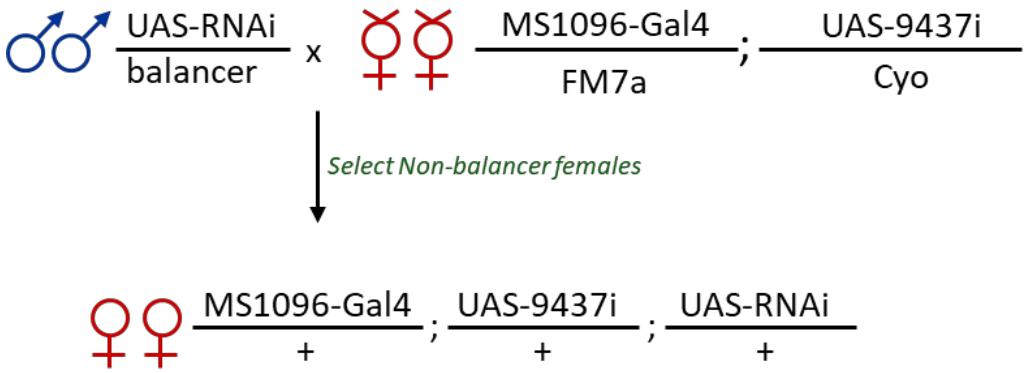

Figure A-1: The genetic scheme of crosses used for the screen. F1 females were observed for hinge and alula defects.

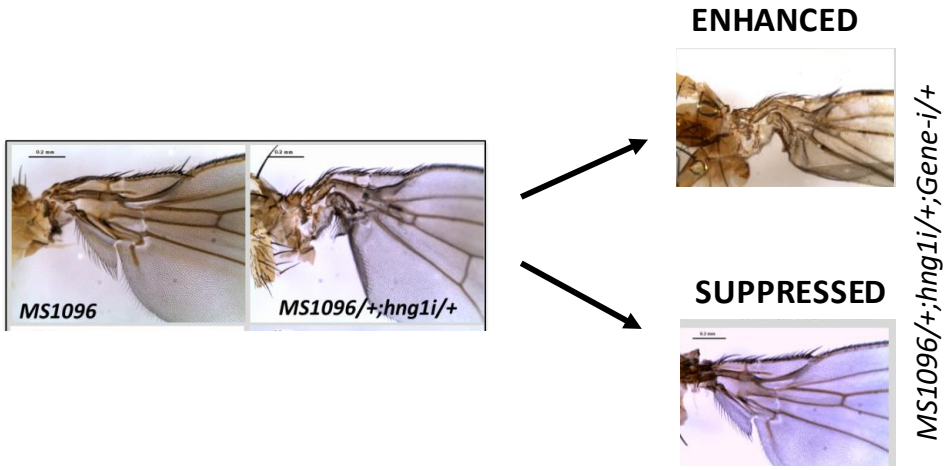

Figure A-2: Enhancement and suppression of the wing hinge phenotype (MS1096/+hng1i/+) was screened in F1 females. 5-10 animals were counted for each line in the experiment. Approximately 1000 genes and 2000 lines were screened for this experiment.

RESULTS

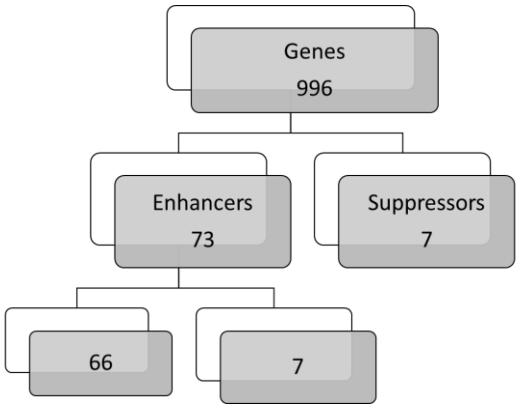

Figure A-3: The summary of the results obtained from the screen. Out of 73 enhancers of the phenotype, 7 genes did not have any reported wing phenotype on their own.

The list of enhancers was then compared to available data from Ueda's Lab to check if knockdown of the identified targets show wing defects independently.

Table AI.1: ***Comparative analysis of identified enhancers of hinge1 phenotype***

Gene	**Molecular Function**	**Act-Gal4 Phenotype**	**Apt-Gal4 Phenotype**
Nckx30c	Ca., Na/K antiporter	lethal	Not Listed
Insulin like receptor	insulin-activated receptor activity	lethal	2, very small wing @ 25C
nucleotide binding	nucleotide binding	lethal	Not Listed
mute	Unknown, muscle homeostasis	lethal	1, small wings, blistered, notch @25; Pupal Lethal @29
wing blister		lethal	2, small wing @ 25C; Blistered at @ 29C
neurogenesis	DNA binding	lethal	1, notching, very small wing, blistered @ 25 C; 1, notching, very small wing, blistered@29 C
Ephexin	Rho guanyl-nucleotide exchange factor activity; phospholipid binding.	lethal	3, curl, AP, blistered @25; 2, pupal lethal @29 C
thickveins	transforming growth factor beta receptor activity	lethal	Not Listed
taimin	steroid receptor binding	lethal	@25 1, semi-pupal lethal, no wing; @29 C Pupal Lethal
Ribosomal prt. S10 alpha	neurogenesis	lethal	Not Listed
arp11	structural constituent of cytoskeleton; actin binding.	lethal	@25 Pupal Lethal
ubiq. Thioesterase	protein deubiquitination	lethal	NONE?
cdc37	unfolded protein binding, neurogenesis	lethal	@25 & @29 Larval Lethal
Arm		lethal	@25 & @29 Larval Lethal
rasp	palmitoyltransferase activity; transferase activity, transferring acyl groups	lethal	NONE?
CG11417	neurogenesis, nucleotide binding	?	@25 & @29 Lethal
Rpb8	DNA-directed RNA polymerase activity	semi-lethal	Not listed
neurogenesis	binds DNA	lethal	Not listed
CG11107	neurogenesis, ATP-dependent helicase activity; ATP-dependent RNA helicase activity	lethal	Not listed
ORB	protein binding, oocyte anterior/posterior axis specification	lethal	Not listed
cdc2c, JAK-STAT	cyclin-dependent protein kinase activity	viable	Not listed
vn(EGFr)		lethal	@25 & @29 Larval Lethal
Rpn3	endopepetidase activity	lethal	Not Listed
foraging		lethal	@25 & @29 Lethal

TH1	negative regulator of Pol II binding	semi-lethal	Not Listed
skuld	RNA polymerase II transcription cofactor activity	lethal	3, larval or pupal lethal
huckebein	transcription factor binding; sequence-specific DNA binding	lethal	NONE?
rep. prt. A70	single-stranded DNA binding	larval lethal	3, very small wing, blistered? no vein?
ATP-dependent RNA helicase activity	ATP-dependent RNA helicase activity	larval lethal	Not Listed
sec61 alpha	negative regulator of autophagy	lethal	@25 & @29 Pupal Lethal
microtubule based movement	Unknown	viable	NONE?
RPA2	DNA binding, neurogenesis	lethal	@25 Larval or Pupal Lethal
found in a screen for wing phenotype	GTP binding	lethal	Not listed
Flap endonuclease1	neurogenesis	lethal	@25 pupal lethal @29 Small wings no bristles
clueless	translation initiation factor activity, mitochondria localization	lethal	@25 Pupal lethal and ?curled wing
lethal (2) K	neurogenesis	larval lethal	
pepple	Rho guanyl-nucleotide exchange factor activity	lethal	Semi-lethal very small wing
WD40 repeat	Unknown	lethal	Not Listed
dynein	microtubule motor activity; ATPase activity, coupled	lethal	Pupal Lethal
CG7269	helicase at 25e	lethal	Not listed
DNA pol alpha 50kDa		lethal	@25 1, very small wings, growth retarded, no bristles; @29 Pupal Lethal
TepIII	endopeptidase inhibitor,defense response to Gram-positive bacterium; phagocytosis, engulfment.	semi-lethal	@25 Small wing +
cct2	unfolded protein binding; ATP binding	lethal	Larval and pupal lethal
taranis	lateral inhibition; wing disc dorsal/ventral pattern formation; chromatin-mediated maintenance of transcription	lethal	Pupal Lethal or Small wing curl, veins lost
TAF2		lethal	Not Listed
Cbc	neurogenesis	lethal	Not Listed
CG5728	mRNA binding	lethal	Not Listed
pixie	ATP binding; ribosomal small subunit binding, negative regulation of neuron	lethal	Lethal or no wing

	apoptosis; translational initiation; cell growth		
mRpS28	structural constituent of ribosome	lethal	Larval or Pupal Lethal
sir2	histone deacetylase activity	lethal	Larva/pupal lethal or small wings with curl
Dachshund	protein binding,negative regulation of gene expression	lethal	NONE?
Nuclear pore protein	structural component of nuclear pore	lethal	Not Listed
bubblegum	long-chain fatty acid-CoA ligase activity	viable	Blistered, small abnormal margins
pcaf	H3 histone acetyltransferase activity; H4 histone acetyltransferase activity; chromatin binding.	lethal	Lethal
Pita	DNA binding, regulation of gene silencing; DNA replication; DNA endoreduplication	lethal	Not Listed
notch		lethal	
Gliatactin	carboxylesterase activity.	male semi-lethal	Not Listed
sec3	exocytosis, synaptic vessicle targeting	lethal	Not Listed
Nat1	translation initiation factor activity, lateral inhibition; autophagic cell death	lethal	Pupal Lethal, semi-lethal ; small wings
eIF2	eplison translation	lethal	Not listed
Shg	protein binding	lethal	No wing
U2 small nuclear prt. Aux. factor38	poly-pyrimidine tract binding.	melanotic aggregates	Not listed
spliceosome component	FH1 domain binding.	lethal	Not listed
Stromatin	neuron remodeling	lethal	Not listed
beta tubulin at 60D	structural constituent of cytoskeleto	lethal	Semi-Lethal (no wing); Blistered small wing
antimers, kinesin binding	kinesin bindin	lethal	Not Listed
RS1	ATP-dependent RNA helicase activity; RNA helicase activit	lethal	Not Listed
Pabp2	RNA binding; poly(A) RNA binding	lethal	Lethal
aralar1	calcium ion binding; transmembrane transporter activity	larval lethal	Not Listed
WD40 repeat	Unknown	viable	@25 Pupal Lethal
pavarotti	microtubule motor activity.	lethal	@25 & @29 Semi-Lethal, No Wing
Unknown	Armadillo-like helical; Armadillo-type fold; CCAAT-binding factor;	lethal	NONE?

AI.2: List of genes that suppressed the hinge1 phenotype

Gene	**Molecular Function**	**Act-Gal4 Phenotype**	**Apt-Gal4 Phenotype**
piefke	neurogenesis	lethal	Semi-pupal lethal at 25; Pupal Lethal @29. No phenotype.
Unknown	Unknown	viable	NONE?
olf186-M	Unknown	viable	NONE?
Unknown	Unknown	viable	NONE?
Glaikit (phosphodiesterase activity)	phosphoric diester hydrolase activity	viable	NONE?
SF2	protein binding	viable	Not Listed
MADF domain	Unknown	viable	3, EGFR?thickveins, ectopic veins at L2-3/4-5 @ 25C

CONTRIBUTIONS:

Vallari made the stable line (*MS1096/FM7a; UAS-9437i*). Vallari and Apurv helped in initial virgin collection. Prof. Ryu Ueda and his lab helped with setting up screen, providing RNAi lines and fly food at NIG, Japan.

BIBLIOGRAPHY

Shukla, V. et al., 2014. Sub-functionalization in the MADF-BESS Family patterns the *Drosophila* Wing Hinge. , 196(February), pp.481–496.

Appendix II

FlySUMObase, A confident dataset of proteins predicted to be SUMOylated in *Drosophila*.

The table lists the top 50 proteins, arranged on decreasing order confidence score, of the database that has been generated by collating and organizing information from the following datasets. *Drosophila* proteins that are validated *in-vivo* SUMO targets and their biological significance has been experimentally verified (EV). Proteins that are listed in more than one SUMO databases, namely MH (Handu et. al., 2015), NIE (Nie *et*. *al*., ,2009), S (iSUMO; Vodel *et*. *al*., 2016) and HN (Hendricks *et*. *al*., 2016). The Confidence Score ranges from 1-10, with higher confidence scores indicating that the possibility of SUMOylation of protein in Drosophila is high (See Chapter 2 for details).

Protein	Database	# of Databases	CS[1]	PSS[2]	VS[3]	S_m[4]
Bicoid	EV	NA	10	K79,308	K308	
Medea	EV	NA	10	K185	K113, K159, K222	
EcRB1	EV	NA	10	NA	K871	
EcR A	EV	NA	10	NA	K842	
Ecr B2	EV	NA	10	NA	K662	
STAT92E	EV	NA	10	K187,685		
p53	EV	NA	10	K82,302	K26, K302	
SU(VAR)3-7	EV	NA	10	K38, 269	K839	
dAda3/diskette	EV	NA	10	NA	unknown	
Sal and Salr	EV	NA	10	NA	Sal: 517-933 fragment; Salr: 803-1126 fragment	
soxNeuro	EV	NA	10	K439	K439	
USP	EV	NA	10	K16,20,37	K20 and 5 others	
RpL22e	EV	NA	10	NA	1to175	
Cp190	EV	NA	10	NA		
IRD5	EV	NA	10	K412,646,667, 713	K152	
Smo	EV	NA	10	NA		
NHP2	All 4 lists	4	7	K5,25,33,150		K5

tsu	All 4 lists	4	7	K159		K27
Top1	HN, Nie , S	3	6	K212,269,301, 368,373,385,61 6,668		K153,117,148,1 64,336
RnrS	MH, Nie, S	3	5	K289,369		
Gdh	MH, Nie, S	3	5	NO site		
Tpp II	MH, Nie, S	3	5	K105,917,1207		
Moe	MH, Nie, S	3	5	K134		
RpS10b	MH, Nie, S	3	5	NO site		
pont	MH, HN, S	3	4	K2 (low PS)		K2
Mcm3	MH, HN, S	3	4	NO site		K450.462
Gnf1	MH, HN, S	3	4	K146,183,320, 327,395		K568,498
Sym	MH, HN, S	3	4	K97,627,1122		K361, 483
Nup358	MH, HN, S	3	4	K889,1086,174 5,2380,2582,26 40		K1414,2571,253 1, 2592, 1605, 2181, 2594,
Hop	MH, HN, S	3	4	K839		K123, 210,
Spt5	MH, HN, S	3	4	K452,612,1034		K143, 453
Uba2	MH, HN, S	3	4	K570		K236
CG2807	MH, HN, S	3	4	K302,532,843		K413, 400
lwr	MH, HN, S	3	4	NO site		K49

Rrp6	MH, HN, S	3	4	K711,743,769		K583
Iswi	MH, HN, S	3	4	K262,355,359, 564,689,865		K944
eIF4AIII	MH, HN, S	3	4	K230,370		K19
dbe	MH, HN, S	3	4	K10,207,259		K340, 369
pUf68	MH, HN, S	3	4	NO site		K14, 43
CG4364	MH, HN, S	3	4	K60,218		K517
nop5	MH, HN, S	3	4	K67,133,234,391,455,467		K467, 540, 415, 497, 444, 422
Ctf4	MH, HN, S	3	4	No site		K1127
cher	MH, HN, S	3	4	K22		K299
Nop60B	MH, HN, S	3	4	K16,125		K413
Mi-2	MH, HN, S	3	4	K250,565,608, 1593,1608,1628,1637,1646,1650,1682		K1308
Top2	MH, HN, S	3	4	K138,420,723, 1235,1267,1269,1278,1311,1318		K1240, 1228, 662, 1385, 1196, 639
RpL18A	MH, HN, S	3	4	NO site		K2
dre4	MH, HN, S	3	4	K176,212,335, 653		K497
SmD2	MH, HN, S	3	4	K7		K8
Rack1	MH, HN, S	3	4	NO site		K271

Bx42	MH, HN, S	3	4	K100,249		K509, 193
mor	MH, HN, S	3	4	K610, 758,906,971		K704
RpS14b	MH, HN, S	3	4	K63		K106, 63
CG4747	MH, HN, S	3	4	NO site		K269
Rpn5	MH, HN, S	3	4	K135,446		K92
mod(mdg4)	MH, Nie	2	3	K97, 487		
Ugt	MH, Nie	2	3	K253,276,569, 960		
osa	MH, Nie	2	3	K134,1771,2062,2111,2544,2558		
Usp7	MH, Nie	2	3	K704		
exba	MH, Nie	2	3	No site		
swm	MH , HN	2	2	K139		K106
CG11583	MH , HN	2	2	K39,273,275		K322
Su(var)2-10	MH , HN	2	2	K406,493		K238, 315, 46, 137
Pgi	S, Nie	2	2	K501		
JhI-1	S, Nie	2	2	K241,752		
Spt6	S, Nie	2	2	No site		
Pgd	S, Nie	2	2	K52		

1: CS, Confidence; 2: PSS, Predicted SUMOylation site; 3: VS, Validated site of SUMOylation ; 4: S_m, site of SUMOylation identified in mammalian ortholog

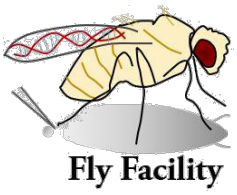

Appendix III

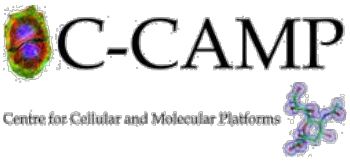

Scope document for generating single amino acid mutation in Caspar gene

User: Prof Girish Ratnaparkhi (IISER, Pune)

Organism: Drosophila melanogaster

Project summary: To generate single amino acid mutation in Caspar gene. This will be done in 2 parts. PART A- to be done by the fly facility, NCBS and PART B- to be done by the lab of Girish Ratnaparkhi, IISER-Pune.

PART A

I: Generation and testing of guide RNAs

1. Choosing the target genomic region for generating ds break using CRISPR/Cas9 and designing the gRNA in the region of interest
   a) Marked the genomic region around the required K551R mutation in the Caspar protein
   b) gRNAs were designed in the region of interest using the Drosophila specific online tools according to the following criteria:
      i) Minimal off-target effects
      ii) Best efficiency scores according to Doench et al (Doench et al., 2014) and Ren et al (Ren et al., 2014)

   We chose 2 gRNAs, both have one off target possibility each. Also chose another gRNA target further from this site to be able to do initial screen for gRNA efficiency by PCR.

   Sg1-Caspar: ATAGGATGGGGACTGGTCAGCGG
   Sg2-Caspar: TGATCAGGTGAAGGCAGAGCAGG

2. Sequencing the genomic region in the fly where the deletion will be made

   The region chosen as above is sequenced in the flies that will be used for the injection of the guide RNA- Deletion will be made in Attp40 flies. gRNAs will be tested in S2 cells.

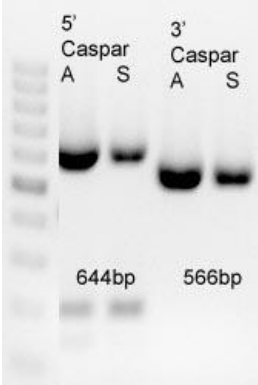

Primers used for 5' PCR:

Seq 5'-Caspar-F/ Seq 5' Caspar –R

Primers used for 3' PCR:

Seq 3'-Caspar-F/ Seq 3' Caspar –R

A = y1,v1; Attp40 flies
S = S2R+ cells

3. Synthesizing the guide RNAs

   Synthesized 2 guide RNA (sg1-Caspar and sg2-Caspar) within a plasmid vector pBFv-U6.2 and pBFv-U6.2B (ref the sequencing file)

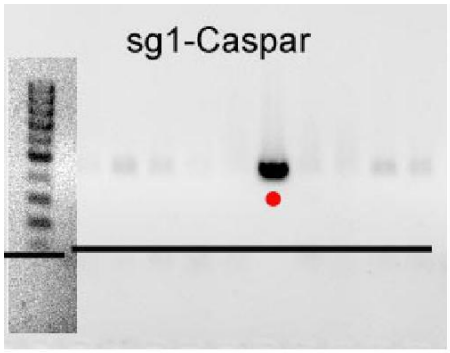

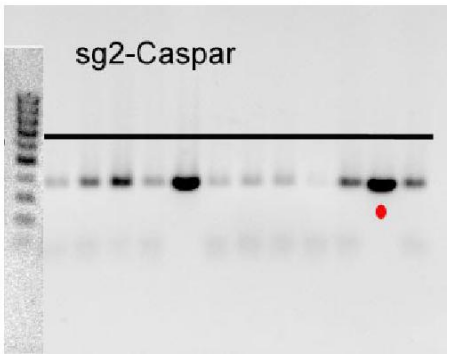

   Gel picture of colony PCR to screen for gRNA synthesis. The ones with red dot were sequenced and confirmed as correct clones.

4. Testing the guide RNA in S2 cell lines

   The gRNA pair was be tested in S2 cell lines by transiently transfecting sg1-Caspar (150ng), sg2-Caspar (150ng) and hsp70-Cas9 (300ng). Genomic DNA was extracted after 48-60 hours and PCRed to amplify the deleted genomic region.

Lane 1: S2 cells transfected with sg1/sg2/Cas9
Lane2: Untransfected S2 cells
Lane 3: Control PCR to show that there is DNA in untransfected control. 2 bands were seen, 1 at 500bp and another at 600bp, smaller than expected (620bp). The PCR was repeated and the bands were sequenced and found to delete the caspar gene.

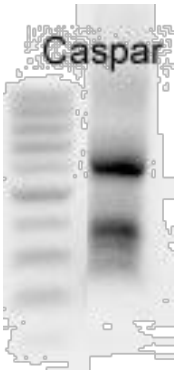

II: Generation of gRNA transgenic flies

Sg2-Caspar was injected in y1,v1, phiC1 integrase; attp40 embryos and the progeny was scored for v+ marker. The integrase was removed and the transgenics were made homozygous.

III: Generation of ssODN for homologous recombination

A 100 bases ssODN was synthesized to make the required K551R mutation and introduce a BssHII restriction site simultaneously.

ssODN sequence:
TTGCCGCATCCTTAGCCATGTCGGCTTGCAAAGTTTCCTGATAGGCCATGTCCTGCTCTGCGCG
CACCTGATCACGGGCAGCGCGTTCGTCCTCTTGCCG

IV: CRISPR/Cas9 based homologous recombination in flies

Act5c-Cas9 flies were crossed to sg2-Caspar(Attp40) flies. The embryos (Act5c-Cas9 /+; sg2-Caspar/+) were injected with Caspar-HR-ssODN. Approx 600 embryos were injected. These embryos, after transferring to the media vials are being sent to the PI.

PART B

I: Single line crosses

The flies emerging from the injected embryos should be crossed with second chromosome balancers.

Act5c-Cas9/+; sg2-Caspar/+ X Tft/CyO (G0 cross)

We suggest you keep some crosses at 25C and some at 18C.

The F1 progeny coming out of these crosses should again be crossed to second chromosome balancers. After you see some larvae in the vials, take out the F1 parent, make single fly preps and do the PCR using

Seq-3'-Caspar F CTGGGCAGCAATTGCGAAGT

Seq -3'-Caspar-R GTAGCACCTACCTGTAGGTTG

The PCR product (566bp) should be digested with BssHII enzyme and run on gel. You will see 350bp and 200bp products confirming the correct HR.

Deliverables

PART I

1. sgRNA constructs in pBFv-U6.2 vector with their sequencing data and protocol
2. Sequencing data on the genomic region of interest
3. gRNA test data in S2 cells
4. Transgenic flies expressing gRNA ubiquitously
5. Sequencing results to confirm the deletion
6. PCR primers as mentioned in the sequencing files.

Terms and conditions

1. Please acknowledge the Fly Facility, C-CAMP in any publication that arises from a reagent generated by the fly facility.
2. Kindly inform us of such a publication as we make a database for our records.
3. All the projects in which some intellectual input from a personnel of the fly facility is involved, a due credit to their input in form of authorship is expected.

References:

Doench, J.G., Hartenian, E., Graham, D.B., Tothova, Z., Hegde, M., Smith, I., Sullender, M., Ebert, B.L., Xavier, R.J., and Root, D.E. (2014). Rational design of highly active sgRNAs for CRISPR-Cas9-mediated gene inactivation. Nature biotechnology *32*, 1262-1267.

Ren, X., Yang, Z., Xu, J., Sun, J., Mao, D., Hu, Y., Yang, S.J., Qiao, H.H., Wang, X., Hu, Q.*, et al.* (2014). Enhanced Specificity and Efficiency of the CRISPR/Cas9 System with Optimized sgRNA Parameters in Drosophila. Cell reports *9*, 1151-1162.